N° d'ordre: 41523

Université de Lille 1 SCIENCES ET TECHNOLOGIES

Université Lille I

Ecole Doctorale des Sciences de la Matière, du Rayonnement et de l'Environnement

Thèse

pour obtenir le grade de

Docteur

Mention : « Molécules et Matières Condensée »

Par

Lei ZHANG

Catalyseurs à base de ruthénium pour la transformation des bio-alcools

12 décembre 2014

David J. Cole-Hamilton	Professeur	University of St. Andrews	Rapporteur
Rodolphe Jazzar	Chargé de Recherche	Université Lyon 1	Rapporteur
Jérôme Le Nôtre	Chef de Projet	SAS PIVERT	Examinateur
Franck Dumeignil	Professeur	Université Lille 1	Examinateur
Simon L. Desset	Maître de Conférences	Université Lille 1	Co-encadrant
Sébastien Paul	Professeur	Ecole Centrale de Lille	Directeur

I would like to express my sincere gratitude to my supervisors, Dr. Simon L. Desset and Prof. Sébastien Paul, for their guidance, patience, enthusiasm, kindness and understanding throughout last three years during my PhD research. It is my great honor to work with them for three years.

This work is performed in UCCS (Unité de Catalyse et Chimie du Solide-CNRS UMR8181) and Université Lille 1. I thank most deeply Prof. Franck Dumeignil for providing all the necessary resources. And I would like to thank CSC and PIVERT for financial support.

I would like to thank all members of the Valbio (Valorisation de la biomasse) group, for the very nice atmosphere here. Many thanks to Dr. Guillaume Raffa, for part of this work (organic synthesis) he carried out, and for many fruitful disscussions. I am most grateful to Dr. Régis M. Gauvin and Yohann Morin in C7, for their everyday help with the glovebox and for the music in their laboratory. I thank Dr. Jérémy Faye for the kindly help with the analysis system.

Special thanks to my friends, Mr. Wenhao Fang, Mr. Fangli Jing, Mr. Mengyang Liu, Ms. Elise Berrier, Ms. Asma Tougerti and Mr. Abdelali Zaki for their continuous support and for the pleasant time we shared. Finally I would like to thank my parents and sister for supporting me.

To all of you and those I forget, thank you. You've made a better world for me, this work would not have been made possible without your help.

Lei Zhang

Nov., 2014

Contents

Chapter 1 Introduction

1.1 From fossile to renewable carbon

Energy is one of the most important driving forces for human society. Nowadays, the economy of modern society relies almost entirely on fossil fuels. In 2011, fossil fuels accounted for 78.2 % of the global energy consumption[1]. In addition to be the primary energy source, fossil raw materials are also transformed into a large variety of chemicals, which have improved the quality of our everyday life.

However, on one hand, the fossil fuels are non-renewable, which means that with the consumption increase, resources are expected to be exhausted in short to mid-term; on the other hand, carbon dioxide together with atmospheric pollutants emissions arising from fossil fuels combustion are putting an important threat on the planet.

In this context, exploring alternative renewable and environmentally benign sources for energy, fuels, and chemicals has become an urgent issue in recent years.

Biomass represents the only abundant and renewable carbon source on the planet (except carbon dioxide but its activation remains problematic). Therefore, replacing fossil fuels with biomass has been suggested as a solution to overcome the abovementioned problems. Most of the present research focuses on the conversion of biomass into biofuels. Nevertheless, considering that, on a weight base, the energy content in biomass is only half of the one contained in crude oil, even if the conversion and selectivity of biomass transformation to fuels were 100 %, there will still need two times more biomass to obtain the energy equivalent of crude oil. Therefore, the limited availability of biomass appears to be the major bottleneck for replacing crude oil by biomass for energy application[2].

On the other hand, biomass molecules are highly functionalized (see 1.2) (mainly hydroxyl, carbonyl and carboxylic groups), making them more suitable than crude oil

to be used as starting materials for the production of high added-value chemicals. Moreover, the production volume of chemicals being less than a tenth of the fuels one, there would be enough biomass that could be sustainably harvestested to fully replace crude oil for chemicals production.

It therefore appears more realistic to dedicate biomass for the production of a large variety of high added-value chemicals, and to seek for non-carbon based energy source to replace crude oil for energy production.

1.2 Biomass composition and transformation

Biomass refers to biological material derived from living, or recently living organisms[3]. As a renewable organic carbon source, biomass exists in various forms, such as, for instance, virgin wood, crops, agriculture residues, food waste, industrial waste and co-products.

Among the different sources of biomass, the non-edible part of plants, the lignocellulosic biomass, has attracted the main attention as a renewable source of carbon. Lignocellulose is found in the secondary cell wall of higher plants ensuring protective and structural role. From a chemical point of view, lignocellulose is composed of two carbohydrate polymers, cellulose (45 %) and hemicellulose (30 %), and an aromatic polymer, lignin (25 %) (Fig. 1.1).

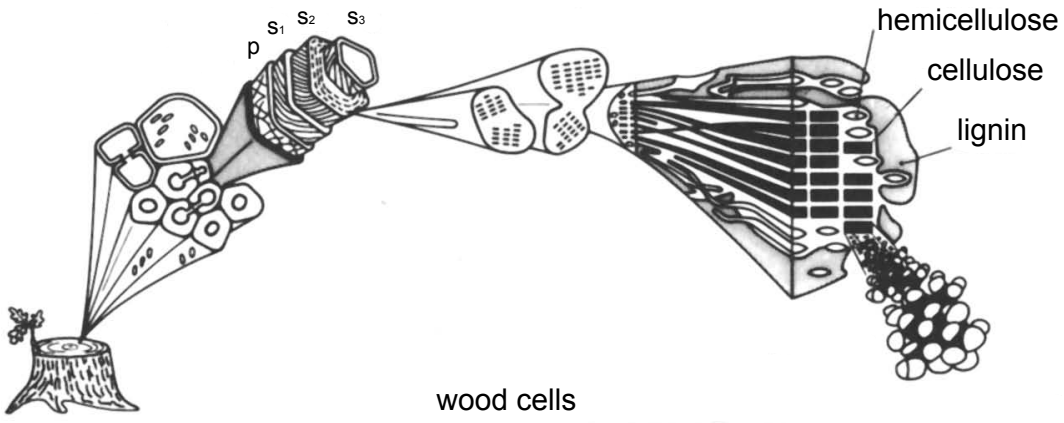

p, primary walls; s_1, s_2, s_3, outer, inner and terminal secondary walls, respectively.

Fig. 1.1 *Lignocellulose structure in wood cells*[4].

1.2.1 Structure of cellulose

Cellulose is the world's most abundant organic polymer[5]. It is the structural component of the plant cell walls, providing the plants its rigidity and mechanical resistance. It represents 15 % to 50 % of the dry weight of the plant biomass[6].

As a biodegradable, non-petroleum-based and carbon neutral resource, cellulose has versatile uses in biofuel production[7], pharmaceutical industries[8-9], bioelectronic devices[10], medical care[11] *etc*.

The historical developments, the chemistry and the structure of cellulose are well known[12]. With the formula $(C_6H_{10}O_5)_n$ (n = 7000 - 15000), cellulose is a linear polymer of glucose units covalently linked through β (1 - 4) glycosidic bonds[13] (Fig. 1.2).

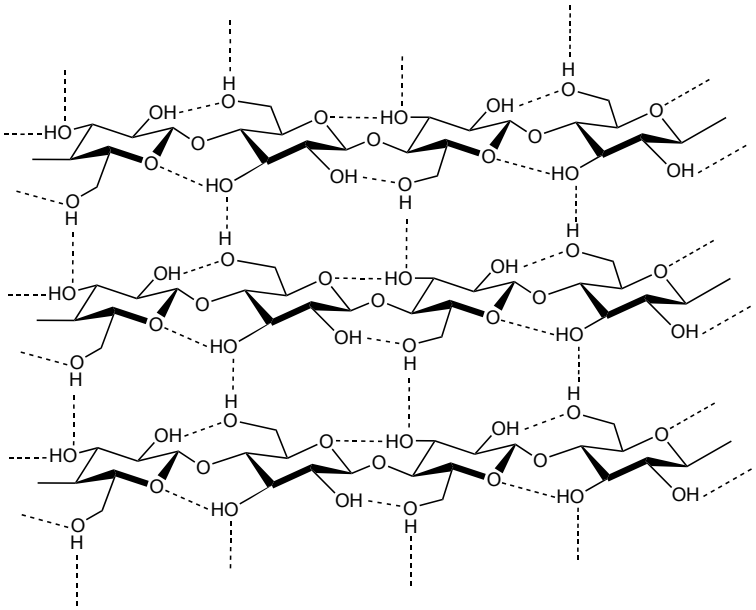

Fig. 1.2 *Structure of cellulose.*

1.2.2 Structure of hemicellulose

While cellulose is only constituted of glucose monomers units, hemicelluloses are composed of different C_5 and C_6 sugar monomers, such as glucose, xylose, mannose, galactose, rhamnose and arabinose. The hemicelluloses degree of polymerisation ranges from 500 to 3000 sugar units. While cellulose is a cristalline material made-up

of entirely linear polymer chains, hemicelluloses are branched polymers having an amorphous structure.

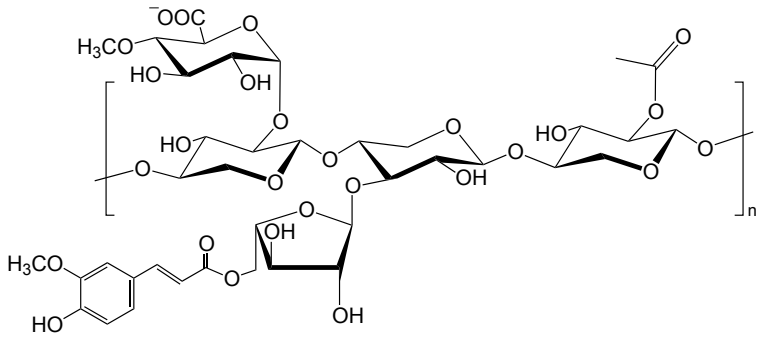

Fig. 1.3 *Example of one possible xylan structure.*

An example of one possible xylan (one type of hemicellulose made of xylose units) structure is shown in Fig. 1.3. Besides xylan, other polysaccharides such as glucuronoxylan, arabinoxylan, glucomannan, and xyloglucan are also part of the general hemicellulose family.

1.2.3 Structure of lignin

Lignin is another of the most abundant organic polymers on Earth. In woody biomass, the cell wall is reinforced by lignin which hold together the cellulose fibres and ensure protection against moisture and micro organism (5 - 30 % of the dry weight)[6].

From the structural viewpoint, lignin is a three dimensional polymer that is made up of *p*-coumaryl alcohol, coniferyl alcohol and sinapyl alcohol[14] (Fig. 1.4).

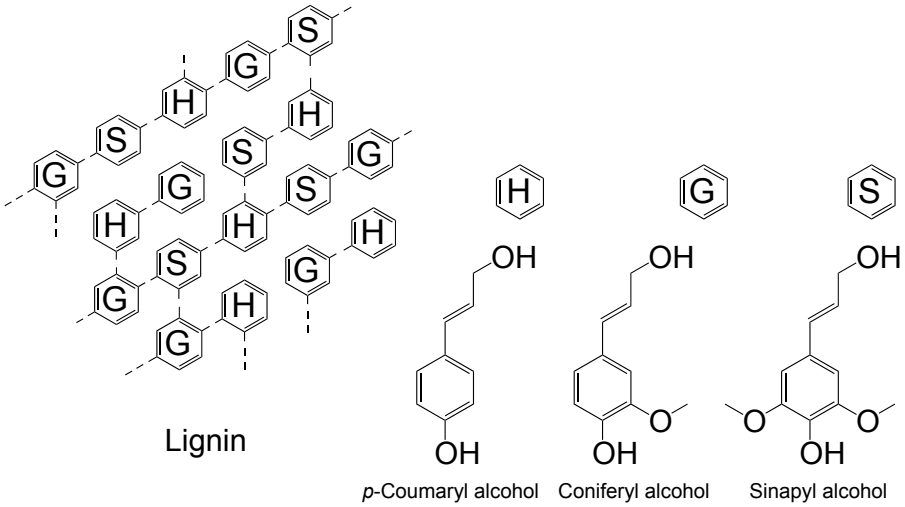

Fig. 1.4 *Example of one possible lignin structure.*

1.2.4 Basic transformation routes of lignocellulosic biomass

The transformation of lignocellulosic biomass into a wide range of products have been conceptualised into a process chain similar to oil refining and transformation (Fig. 1.5). The first stage (pretreatment) is the separation of the three main biopolymers, cellulose, hemicellulose and lignin that constitutes lignocellulose.These macromolecules are then depolymerized to recover their constituting monomers. Following such steps, pentose and hexoses are obtained from the hydrolysis of cellulose and hemicelluloses while lignin is anticipated to give access to mixtures of phenolic compounds. These primary platform molecules can then be converted to a wide range of chemicals using single or multi-step processes based on chemical or biochemical transformations. The US department of Energy, DOE, has carried an extensive study to evaluate the most desirable compounds one can obtain competitively and efficiently from lignocellulosic feedstock[15-16]. From this study, a group of chemical, usually referred as the «Top value added chemicals from biomass» or «Top 10», has emerged. This initial study, has been more recently refined to take into account recent market changes and technology advances[17] (Fig. 1.6).

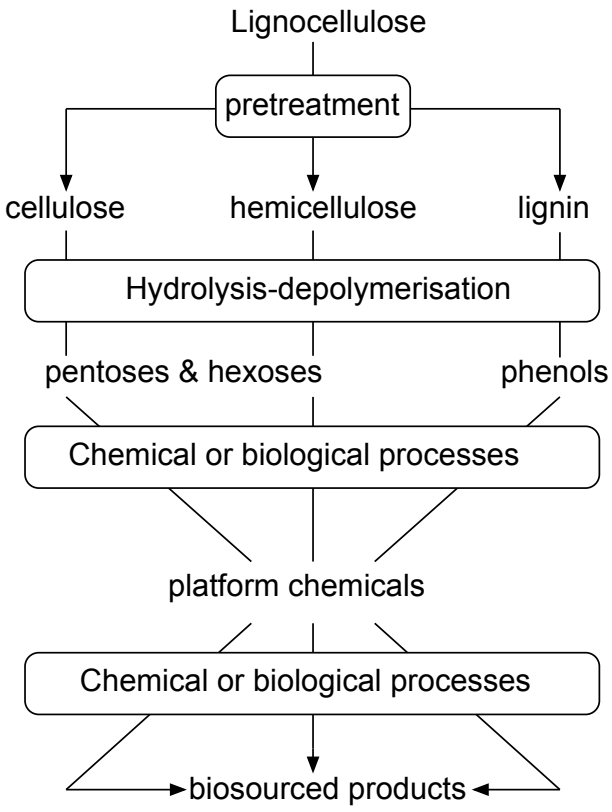

Fig. 1.5 *Basic transformation routes of lignocellulose*[18].

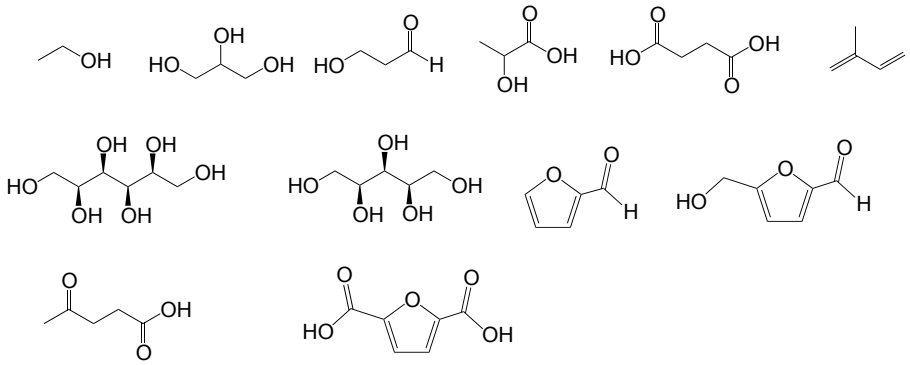

Fig. 1.6 *Structure of some top value added chemicals from biomass.*

In addition to these anticipated products, the current largest transformation of biomass is the production of simple alcohols such as ethanol and butanol by fermentation, which are used as biofuels.

Bioethanol can be produced from sugar and derivatives[19] or directly from lignocellulosics[20]. Bioethanol production has doubled from 2006 to 2011 reaching almost 89 billions litres of bioethanol produced in 2011 worldwide (Fig. 1.7).

Butanol can also be obtained by biomass fermentation[21]. Biobutanol provides numerous advantages over ethanol. First, the energy density of butanol is significantly higher than those of ethanol, leading to an increased mileage. Moreover, the air-fuel ratio of butanol is higher, resulting in richer mixtures in application and therefore to higher power delivery. The octane number of butanol is similar to that of gasoline, which is lower to the one of ethanol. The lower vapor pressure of butanol makes it safer to handle. Due to its corrosive and hygroscopic properties, ethanol can not be distributed in pipelines and must be transported by tanker trucks, rail car, or river barge, while butanol can be transported using the existing infrastructure[22]. Based on these facts, although nowadays in most cases bioalcohols refer to bioethanol, some researchers suggest biobutanol as a promising alternative for the future[22-23].

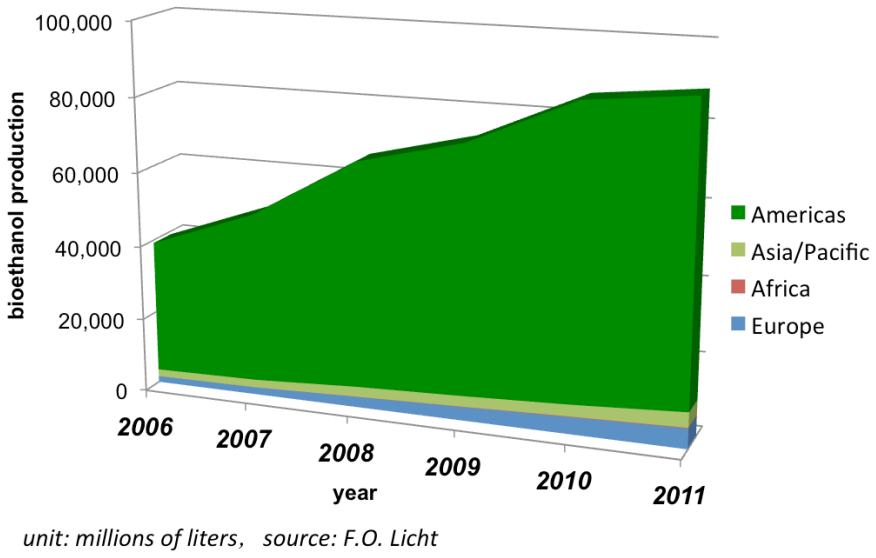

Fig. 1.7 *World bioethanol production.*

When considering the chemical structure of the main biopolymers (cellulose, hemicelluloses and lignin), the primary platform molecules (C_5 - C_6 sugars and phenols), the expected product arising from biorefineries (see Fig. 1.5) and the current production of bio-alcohols, it can be observed that there is an overwhelming abundance of hydroxyl groups among all these compounds. Therefore, developing

new chemical transformations of biomass, at any level of the process scheme, will rely on the transformations of the alcohol function.

1.3 Catalytic dehydrogenative activation of alcohols

1.3.1 Introduction

Alcohols are not very versatile platform molecules. They require base activation to form nucleophilic alkoxide or acid activation to turn the C_1 carbon into a reactive electrophile (see Fig. 1.8). On the other hand, carbonyl compounds such as aldehydes and ketones, are reactive O-nucleophile and C-electrophile requiring none to little activation. Moreover, transformation into enolates by base activation makes carbonyl compounds powerful C_2-nucleophile.

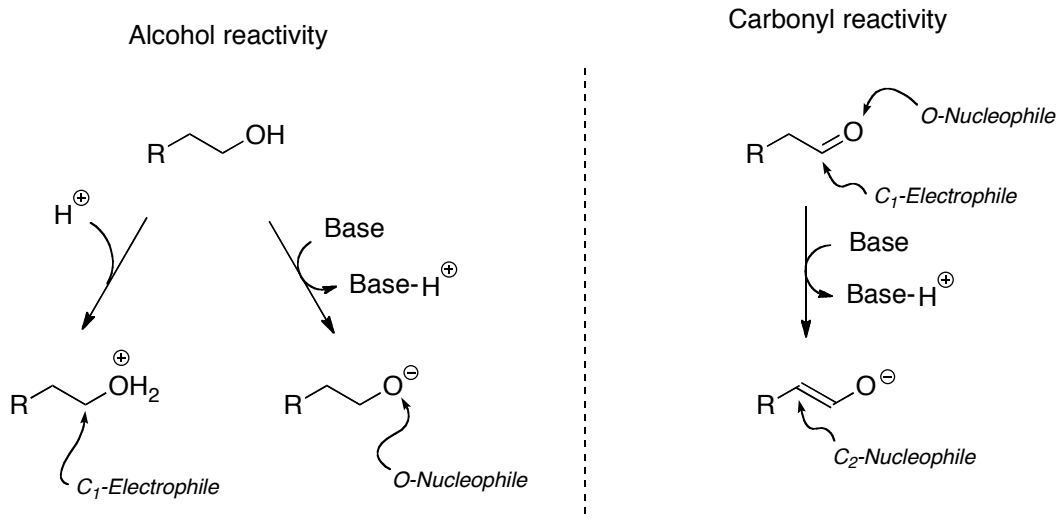

Fig. 1.8 *General reactivity of alcohols and carbonyls.*

This is reflected by the pivotal position of carbonyl compounds in the chemical industry were they are used as major intermediates in the manufacture of numerous products (see Table 1.1).

Table 1.1 *Applications of some important carbonyl compounds.*

carbonyl compounds	structure	major applications
formaldehyde		plastics[24]
acetaldehyde		synthetic intermediate
acrolein		biocide, chemical precursor
benzaldehyde	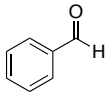	industrial flavour, synthetic intermediate
furfural	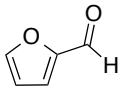	chemical feedstock, plastics, pharmaceuticals
acetone		solvent, chemical intermediate *etc.*
cyclohexanone	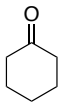	adipic acid, Nylon 6,6 and Nylon 6
acetophenone	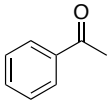	synthetic intermediate, pharmaceuticals *etc.*
cinnamaldehyde	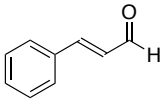	industrial flavour, pharmaceuticals *etc.*

Therefore, one way of considerably expending the versatility of hydroxyl group containing compounds, such as the bio-derived compounds described above, is to carry out the selective oxidation of their alcohol functionality into carbonyl.

The catalytic oxidation of alcohols can be performed using molecular oxygen or air as oxidant producing water as the sole by-product (Scheme 1.1). Both homogeneous and heterogeneous catalytic systems have been developed for this transformation[25]. For instance, in 2000 Kaneda's group developed a monomeric ruthenium species on the surface of an hydroxyapatite as an efficient heterogeneous catalyst[26]. In 2006, Sigman described a Pd(II)(-)-sparteine as an efficient homogeneous catalyst[27]. However, a common drawback for this catalytic

transformation is the non-desired overoxidation reactions of the carbonyl compounds yielding carboxylic acids and carbon dioxide.

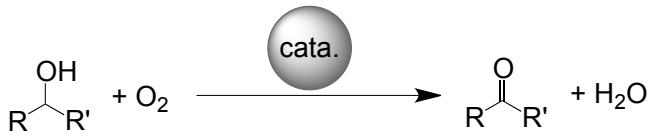

R = alkyl, aryl; R' = H, alkyl, aryl.

Scheme 1.1 *Aerobic oxidation of alcohols.*

A very elegant alternative technology is the acceptorless alcohols dehydrogenation (AAD). In this reaction, alcohols are dehydrogenated in the presence of a transition metal complex to yield the corresponding aldehydes or ketones together with molecular hydrogen (see Scheme 1.2).

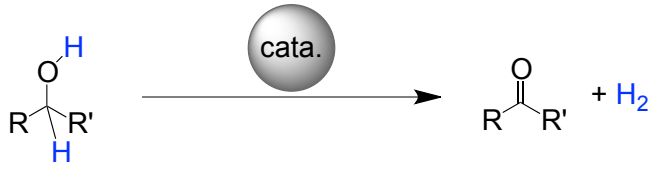

R = alkyl, aryl; R' = H, alkyl, aryl.

Scheme 1.2 *Acceptorless alcohols dehydrogenation.*

The intrinsic interest of such transformation is that it avoids overoxidation issues encountered in aerobic oxidation and produces one equivalent of molecular hydrogen that can be used for energy production or as reductant in other transformations. Moreover, depending on the reaction conditions and the nature of the catalyst, the produced carbonyl compounds can be further transformed *in situ* into a large variety of compounds such as esters, carboxylates, amines, amides or heavier alcohols.

For primary alcohols, the produced aldehyde can be attacked by a nucleophile to yield an addition compound such as an hemi-acetal, hemi-aminal or an hydrate. This compound can then be further dehydrogenated to yield carboxylic acid derivative such as esters or amides. Alternatively, the addition compound can be dehydrated to yield

an insaturated intermediate such as an imine that can be hydrogenated yielding a substitution product, *i.e.* an amine (borrowing hydrogen mechanism) (Scheme 1.3).

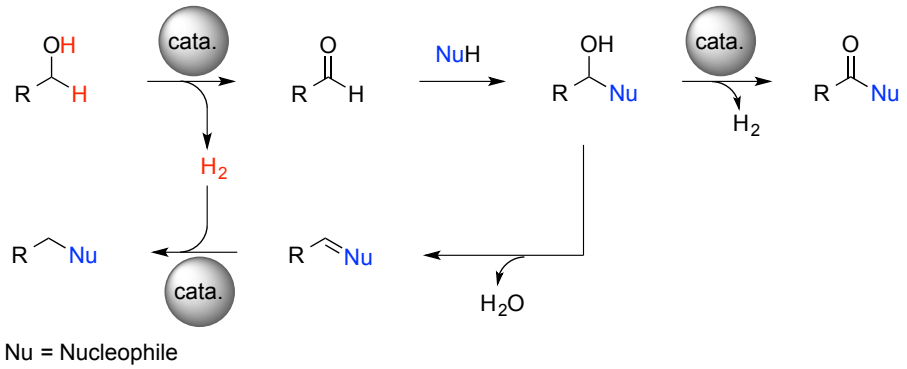

Scheme 1.3 *Dehydrogenation strategies in organic synthesis.*

For secondary alcohols, the dehydrogenation would yield a ketone. The ketone can be attacked by a nucleophile to give an addition product, however since this adduct does not possess β-hydrogen relative to the oxygen, it cannot undergo further dehydrogenation reaction.

In the present thesis we will limit our discussions to alcohol dehydrogenation, and dehydrogenative coupling to ester and carboxylate. For the interested reader, informations about general borrowing hydrogen and amine alkylation with alcohol can be found in several reviews[28-30].

1.3.2 Acceptorless alcohols dehydrogenation

Catalytic systems for dehydrogenation of alcohols can be divided in two different categories corresponding to two concepts. In the first category, the organometallic complex has ligands that do not play a role in the catalytic cycle and that we refer as innocent ligands. The ligand ensures complex stability, appropriate electronic configuration and steric bulk to the complex. In the second category, the ligand plays an active role in the catalytic cycle and directely interacts with the substrate during different steps of the catalytic cycle. Such ligands are referred to as “non-innocent” ligands.

1.3.2.1 Metal complexes with innocent ligands

In 1987, Morton and Cole-Hamilton reported one of the earliest examples of alcohol dehydrogenation catalyst already targeting at the time the production of hydrogen from biomass[31]. The authors pointed out that the dehydrogenation of ethanol is a thermodynamically uphill process ($\Delta G° = + 41.2$ kJ.mol^{-1}) and that working in an open system at high temperature is required to drive the reaction. In addition they noted that the transformation becomes thermodynamically favourable if the alcohol is converted to a mixture of methane, hydrogen and carbon dioxide ($\Delta G° = - 33.3$ kJ.mol^{-1}) via dehydrogenation, decarbonylation and water-gas shift reaction. Their first reported catalyst, [Rh(bipy)$_2$]Cl, **1**, was able to catalyse all the reaction steps in the presence of a base for ethanol, isopropanol and butane-2,3-diol with a TOF of hydrogen production in the range of 100 h^{-1}. The authors proposed that the dehydrogenation reaction proceeds via the attack of an ethoxide ion onto the rhodium ion **A**, to give the alkoxyrhodium complex **B** followed by a β-H elimination that releases acetaldehyde and a rhodium hydride species **C**. The rhodium hydride species **C** is then protonated by an alcohol molecule to give a dihydride complex **D** that release molecular hydrogen by reductive elimination (see Scheme 1.4).

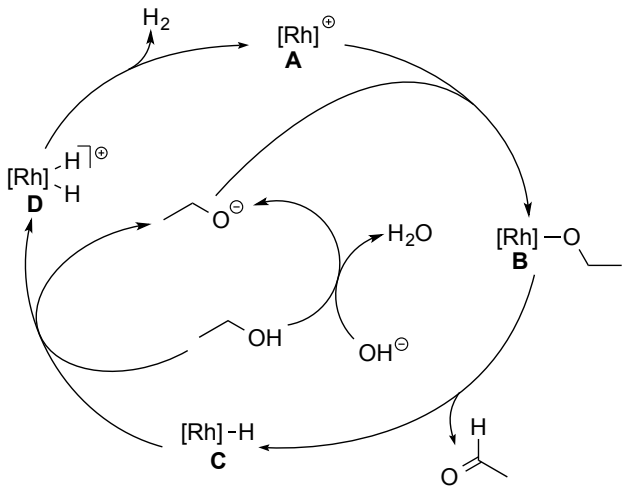

Scheme 1.4 *Proposed catalytic cycle for ethanol dehydrogenation by [Rh(bipy)$_2$]Cl **1**.*

Following this study, the same team showed that ruthenium dihydride complexes could also be used to catalyse the dehydrogenation of primary alcohol and diols[32-33]. In the presence of a base, NaOH, the catalyst $[RuH_2(N_2)(PPh_3)_3]$, **2a**, showed a TOF of 148.1 h^{-1} (210.2 h^{-1} upon illumination) for ethanol dehydrogenation while catalyst $[RuH_2(PPh_3)_4]$, **2b**, showed a TOF of 23.8 h^{-1} (138.7 h^{-1} under illumination). The proposed mechanism is similar to the one described for the $[Rh(bipy)_2]Cl$, **1**, system. Hydrogen is believed to be released from the tetrahydride complex $[RuH_4(PPh_3)_3]$, **D**, generated from protonation of $[RuH_3(PPh_3)]$, **C**, (Scheme 1.5).

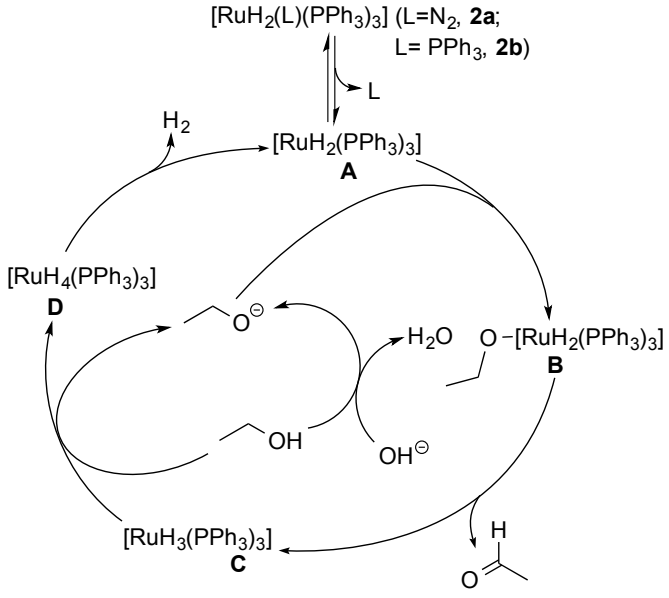

Scheme 1.5 *Proposed catalytic cycle for the dehydrogenation of ethanol catalysed by* $[RuH_2L(PPh_3)_3]$ ***2***.

Recently, it was shown that addition of free PPh_3 inhibits the reaction indicating that ligand dissociation is involved in the reaction mechanism[34]. This was more recently supported by DFT study evidencing reaction pathways where decoordination of one phosphine ligand from intermediate **B** lead to similar activation energies for the dehydrogenation of alcohol involving ruthenium bis-phosphine $16e^-$ complexes[35-36].

Illumination is proposed to improve the activity by increasing the rate of hydrogen release from $[RuH_4(PPh_3)_3]$, **D**, and/or the removal of carbon monoxide

from less active carbonyl complexes such as $[RuH_2CO(PPh_3)_3]$, **2c**, formed by decarbonylation of the produced aldehyde. Decarbonylation and dehydrogenation were shown by DFT to have similar activation energy[37]. This is especially problematic for lower primary alcohols such as methanol and ethanol whereas secondary alcohols preferentially lead to clean dehydrogenation. For ruthenium and rhodium complexes, base was found to be crucial to ensure high activity. Base acts primarily to generate the alkoxide that reacts with the complex. The base is also believed to assist CO realease from the carbonyl complexes, formed by decarbonylation of the aldehyde, by nucleophilic attack at the carbonyl followed by the release of carbon dioxide. Rhodium-phosphine complexes such as $[RhCl(PPh_3)_3]$, **3a**, and $[RhH(P\textit{i}Pr_3)_3]$, **4**, were also investigated for ethanol dehydrogenation[32]. However, these catalysts showed very little activity for ethanol dehydrogenation ($5\ h^{-1} < TOF < 10\ h^{-1}$). The use of light irradiation or the addition of $[Rh(dppp)_2]Cl$, a decarbonylation catalyst, improved the activity of the system allowing to obtain a TOF of about $20\ h^{-1}$.Wilkinson catalyst, $[RhCl(PPh_3)_3]$, **3a**, and its hydride analog $[RhH(PPh_3)_3]$, **3b**, have also been tested for the dehydrogenation of *i*-propanol to acetone[38]. Wilkinson catalyst was found to be inactive for this transformation but catalytic activity can be induced by addition of triethylamine. The low TOF observed, *c.a.* $2\ h^{-1}$, is similar to those described for the same catalyst in the presence of NaOH and for the hydride analog $[RhH(PPh_3)_3]$, **3b**, suggesting that NEt_3 or NaOH promotes the transformation of the chloride to the hydride complex.

Dehydrogenation of methanol was studied in the presence of a series of ruthenium-phosphine complexes[34]. It was found that in the presence of ruthenium (II) complexes $(RuCl_2(P(p\text{-}C_6H_4X)_3)_3$, **5a**, X=H; **5b**, X= Me; **5c**, X=F; **5d**, X=OMe and $RuCl_2(PMePh_2)_3$, **5e**) the produced formaldehyde further transformed into acetals and esters (Scheme 1.6). For these complexes, addition of free phosphine was also found to retard the reaction suggesting that ligand dissociation takes place during the catalytic cycle.

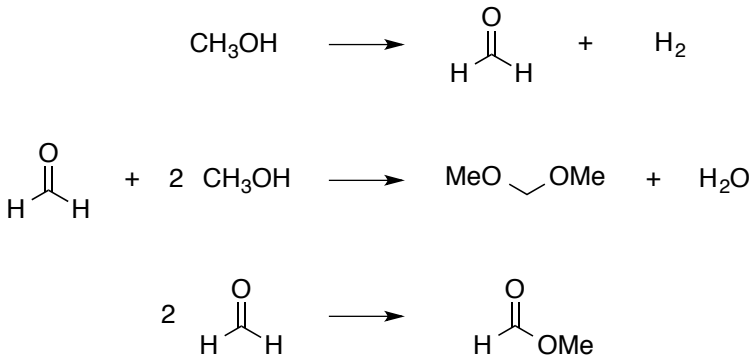

Scheme 1.6 *Dehydrogenation of methanol by complex **5**.*

Adair and Williams investigated the use of several commercially available ruthenium complexes for the dehydrogenation of 1-phenylethanol to acetophenone in the presence of a base[39] (Scheme 1.7).

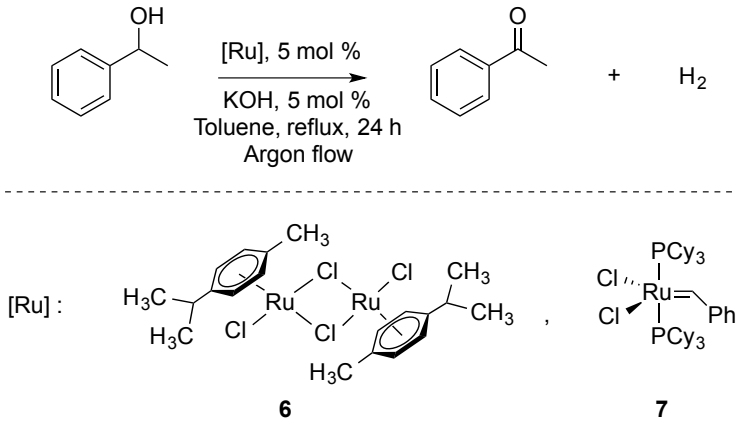

Scheme 1.7 *Dehydrogenation of 1-phenylethanol by ruthenium complexes **6** and 7.*

Among the different complexes, ruthenium dimer $[(p\text{-cymene})RuCl_2]_2$, **6**, and Grubbs first generation catalyst, $[PhCH{=}Ru(PCy_3)_2Cl_2]$, **7**, were found to be the more active, albeit with relatively low TOFs in the range of 6 h^{-1}. Both catalysts were found to be inactive for the dehydrogenation of benzyl alcohol, a primary alcohol. The author suggested that the produced benzaldehyde deactivates the catalyst by formation of inactive ruthenium carbonyl complexes. However, it was found that in the presence of both phenylethanol and benzyl alcohol, both ruthenium complexes led to the formation of condensation products arising from consecutive dehydrogenation, aldol

condensation and hydrogenation following cross Guerbet type reaction sequence (Scheme 1.8).

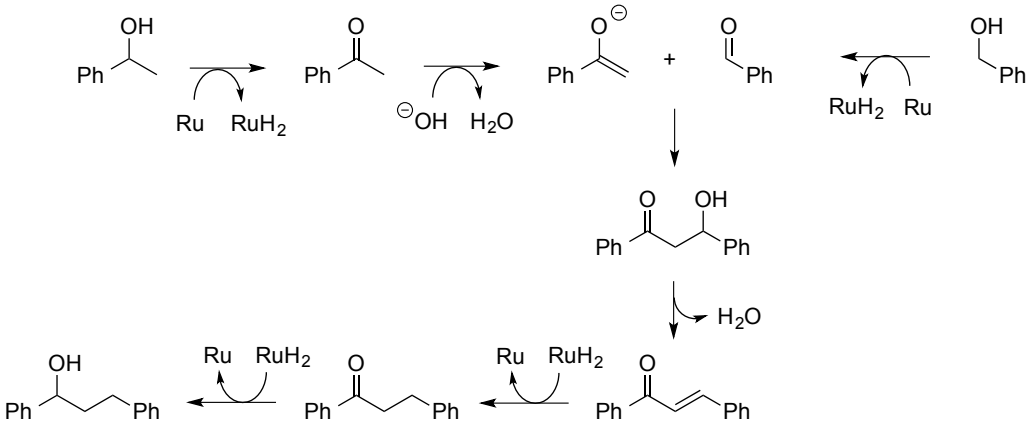

Scheme 1.8 *A cross Guerbet reaction sequence.*

Beller and Junge investigated the use of *in situ* formed ruthenium catalysts for the dehydrogenation of *iso*-propanol at 90°C[40-41]. Among the different ruthenium precursors screened, [$RuCl_3$•xH_2O], **8**, and [$RuCl_2$(*p*-cymene)]$_2$, **6**, showed to be the most active in the presence of two equivalents of tricyclohexylphosphine, PCy_3, **9**. Using 315 ppm of ruthenium precursor, two equivalents of PCy_3, **9** and 0.8 mol L^{-1} of NaOH at 90 ^oC, dehydrogenation of *i*-propanol proceeded with TOFs of 78 h^{-1} and 94 h^{-1} after 2 h (54 h^{-1} and 43 h^{-1} after 6 h) for [$RuCl_3$•xH_2O], **8**, and [$RuCl_2$(*p*-cymene)]$_2$, **6**, respectively (Table 1.2, entries 2 and 3). The performances of the system could be further improve by using [$RuCl_3$•xH_2O], **8** with PCy_3, **9**, (1:2) in the presence of metallic sodium as a base instead of NaOH (TOF = 101 h^{-1} after 2 h and 57 h^{-1} after 6 h) (Table 1.2, entry 4). Switching from PCy_3, **9** to more bulky phosphine ligand **10**-**13** (Fig. 1.9) and using sodium as a base allowed to reach TOF > to 100 h^{-1} after 2 h (Table 1.2, entries 7, 9 and 10).

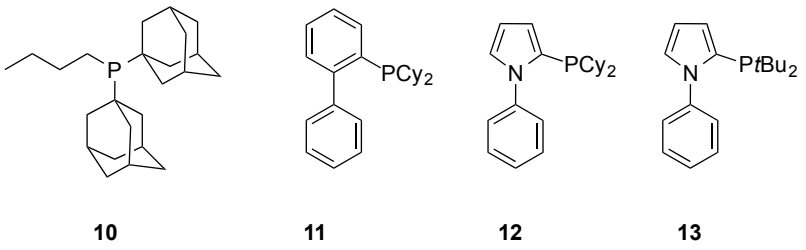

10 **11** **12** **13**

Fig. 1.9 *Structures of four bulky phosphine ligands.*

Table 1.2 *Catalytic performance for dehydrogenation of iso-propanol by **6** or **8** in the presence of phosphine ligands*[‡].

entry	Ru precursor	ligand	P: Ru ratio	base	reaction time (h)	TOF (h^{-1})
1	$[RuCl_3.xH_2O]$, **8**	/	/	NaOH	2	24
					6	20
2	$[RuCl_3.xH_2O]$, **8**	PCy_3, **9**	2	NaOH	2	78
					6	54
3	$[RuCl_2(p\text{-cymene})]_2$, **6**	PCy_3, **9**	2	NaOH	2	94
					6	43
4	$[RuCl_3.xH_2O]$, **8**	PCy_3, **9**	2	Na	2	101
					6	57
5	$[RuCl_3.xH_2O]$, **8**	**10**	2	NaOH	2	104
					6	55
6	$[RuCl_3.xH_2O]$, **8**	**11**	2	NaOH	6	7
7	$[RuCl_3.xH_2O]$, **8**	**11**	2	Na	2	114
					6	61
8	$[RuCl_3.xH_2O]$, **8**	**12**	2	NaOH	2	30
9	$[RuCl_3.xH_2O]$, **8**	**12**	2	Na	2	120
					6	64
10	$[RuCl_3.xH_2O]$, **8**	**13**	2	Na	2	155
					6	78

[‡]reaction conditions: [Ru] = 315 ppm, *V* (*iso*-propanol) = 5.0 mL, [base] = 0.8 mol L^{-1}, 90 °C.

The same group extended the use of ruthenium complexes for the dehydrogenation of *iso*-propanol using amines instead of phosphine as ligands[41]. A broad screening of various mono-, bi- and tridentate nitrogen ligands in the presence of $[RuCl_2(p\text{-cymene})]_2$, **6**, and NaO*i*Pr as a base ([Ru] = 16 ppm, [NaO*i*Pr] = 0.8 mol L^{-1}) was carried for the dehydrogenation of *iso*-propanol. Without additional ligand, $[RuCl_2(p\text{-cymene})]_2$, **6**, showed TOFs of 192 h^{-1} after 2 h and 120 h^{-1} (Table 1.3, entry 1). In the presence of most of the tested nitrogen ligands, TOFs higher than 200 h^{-1}

after 2 h and higher than 100 h^{-1} after 6 h were obtained. TOFs higher than 300 h^{-1} were obtained using tetramethylethylenediamine, TMEDA, **14**, tetramethyl propane-1,3-diamine, **15**, tridentate TMEDA derivative, **16**, dimethylaniline, **17** and 2-dimethylaminoethanol, **18**, as ligands (see the structures in Fig. 1.10 and catalytic performance in Table 1.3).

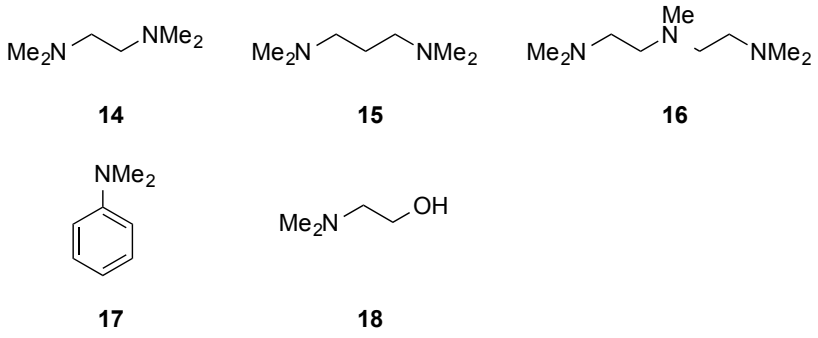

Fig. 1.10 *Structures of five nitrogen ligands.*

Table 1.3 *Catalytic performance for dehydrogenation of iso-propanol by* ***6*** *in the presence of nitrogen ligands*[‡].

entry	ligand	TOF (2 h) (h^{-1})	TOF (6 h) (h^{-1})
1	/	192	120
2	**14**	309	190
3	**15**	314	194
4	**16**	322	203
5	**17**	348	211
6	**18**	373	236

[‡]reaction conditions: cata. = $[RuCl_2(p\text{-cymene})]_2$, **6**, [Ru] = 16 ppm, Ru: N = 1: 2 for bidentate ligand, 1: 3 for tridentate ligand, *V* (iso-propanol) = 10 mL, [NaO*i*Pr] = 0.8 mol L^{-1}, 90 °C.

When the catalyst loading was decreased to 4 ppm and the ligand: catalyst ratio was increased to 10:1, using TMEDA, **14**, as ligand, TOFs of 519 h^{-1}, 317 h^{-1} and 189 h^{-1} after 2 h, 6 h and 24 h could be obtained. This system was still active after 11 days (TOF = 64 h^{-1} after 268 h) with a total TON of 17215. Under the same conditions, using ligand **18**, TOFs of 313 h^{-1}, 233 h^{-1} and 137 h^{-1} were obtained after 2 h, 6 h and 24 h, respectively. $[RuCl_2(p\text{-cymene})]_2$, **6**, with ligand **18** proved to be less efficient for the dehydrogenation of ethanol and 1-phenylethanol with TOFs of 7.6 h^{-1} and 3.0 h^{-1} obtained after 2 h, respectively.

1.3.2.2 Metal complexes with non-innocent ligands

A. Early systems

In 1977, Dobson and Robinson developed one of the earliest homogeneous catalysts for acceptorless alcohols dehydrogenation[42-43]. Using an excess of a fluorinated carboxylic acid, they found that the complex $[Ru(OCOCF_3)_2(CO)(PPh_3)_2]$, **19** was active for the dehydrogenation of various primary and secondary alcohols. TOFs of 2952 h^{-1} and 1620 h^{-1} were reported for 1-heptanol and cyclooctanol dehydrogenation, respectively, with a catalyst loading of 0.03 %. TOFs for lighter primary and secondary alcohols were found to be lower presumably because of the lower reaction temperature (TOFs lower than 100 h^{-1} for ethanol, 1-propanol and 2-propanol). Even if not generally recognized as such, this catalytic system constitutes an early example of non-innocent ligand application. The proposed catalytic cycle starts by the addition of the alcohol onto the $[Ru(OCOCF_3)_2(CO)(PPh_3)_2]$, **19** which changes the coordination of the trifluoro acetate ligand from η_3 to η_1. The coordinated alcohol is believed to be hydrogen bonded to one of the η_1 trifluoroacetate ligand in analogy to isolated $[Ru(OCOCF_3)_2(CO)(PPh_3)_2(RR'CHOH)]$, **A**, complex[43]. Dissociation of trifluoroacetic acid lead to the formation of an alkoxide complex $[Ru(RR'CHO)(OCOCF_3)(CO)(PPh_3)_2]$, **B**. In this process, the ligand plays an active role and is directely involved in the steps leading to the alkoxide complex. In the following step, the alkoxide is transformed into the corresponding carbonyl by β-H elimination leading to the hydride complex $[RuH(RR'CO)(OCOCF_3)(CO)(PPh_3)_2]$ **C**. Attack of trifluoroacetic acid onto the hydride complex liberates the carbonyl product together with molecular hydrogen and closes the catalytic cycle by forming the starting ditrifluoroacetate complex $[Ru(OCOCF_3)_2(CO)(PPh_3)_2]$, **19** (see Scheme 1.9).

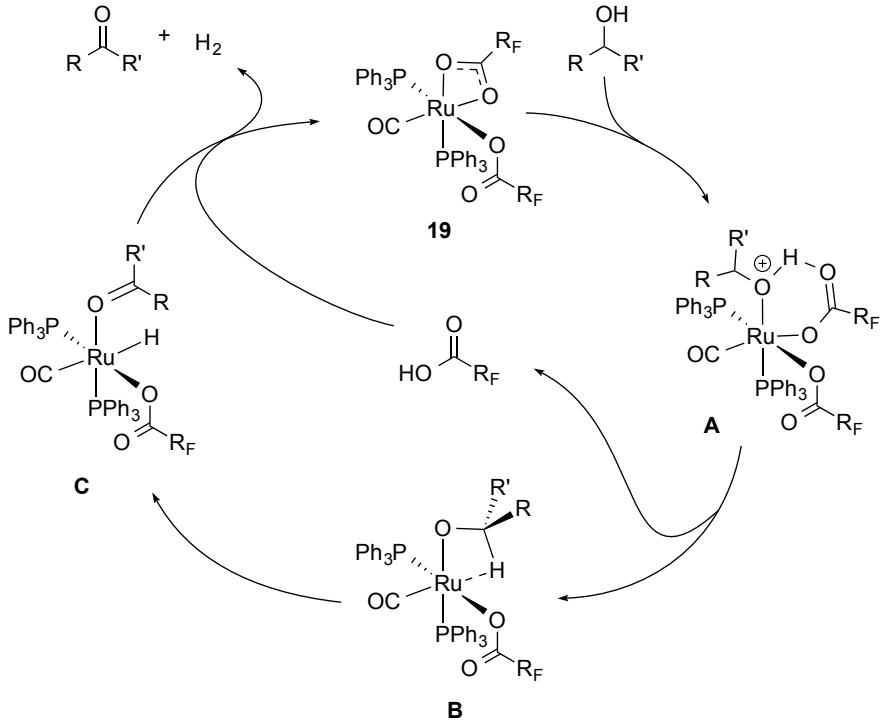

Scheme 1.9 *Proposed catalytic cycle for alcohol dehydrogenation catalysed by [Ru(OCOCF$_3$)$_2$(CO)(PPh$_3$)$_2$] **19**.*

In an independent study aiming at replacing triphenylphosphine by diphosphine ligand in [Ru(OCOCF$_3$)$_2$(CO)(PPh$_3$)$_2$], **19** complex, Jung and Garrou were unable to reproduce the results disclosed by Dobson and Robinson[44]. They argued that decarbonylation of the aldehyde led to the formation of inactive carbonyl complexes which, together with the evaporation of trifluoroacetic acid under reaction conditions were responsible for catalyst deactivation. Under their reaction conditions, diphosphine complexes [Ru(OCOCF$_3$)$_2$(CO)(P-P)], **20** (with P-P = dppe, 1,2-(Ph$_2$P)$_2$C$_6$H$_4$) were found to be slightly more active than [Ru(OCOCF$_3$)$_2$(CO)(PPh$_3$)$_2$], **19** complex, for the dehydrogenation of cyclohexanol. Further studies on the dehydrogenation of secondary alcohols using [Ru(OCOCF$_3$)$_2$(CO)(PPh$_3$)$_2$], **19**, or *in-situ* formed catalysts from [RuH$_2$(CO)(PPh$_3$)$_3$], **2c**, and acids (PTSA, TFA, trichloroacetic acid, AcOH) were carried out[45]. It was found out that high boiling secondary aliphatic alcohol such as 2-octanol and 2-decanol could be efficiently dehydrogenated to the corresponding ketones using

Robinson catalyst. However, upon increase of the acidity and amount of added acid, selectivity was found to decrease due to acid catalysed aldol condensation and dehydration. Primary alcohol dehydrogenation was complicated by decarbonylation (leading to catalyst deactivation) and aldol condensations.

In 2006, Hulshof *et al.* extended this catalytic system to a series of complexes that contain bidentate derivatives of the fluorinated acids as ligands and various bidentate phoshine ligands (Fig. 1.11)[46]. For 1-phenylethanol dehydrogenation, a TON of 651 could be obtained with a TOF of 27 h^{-1} using catalyst containing dppf (1,1′-Bis(diphenylphosphino)ferrocene) as bidentate phosphine. Interestingly, these catalytic systems did not require any additional acid allowing to obtain selectivies up to 100%.

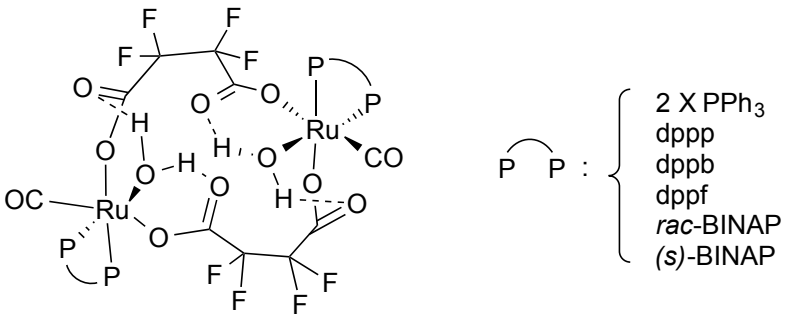

Fig. 1.11 *Structures of Hulshof's catalysts.*

Shvo's dinuclear ruthenium complex is a well-known bifunctional catalyst which finds numerous applications in oxidation and reduction reactions[47-48]. In solution, the ruthenium dimer **21** dissociate into an unsaturated **21a** and a saturated ruthenium complex **21b** (Scheme 1.10).

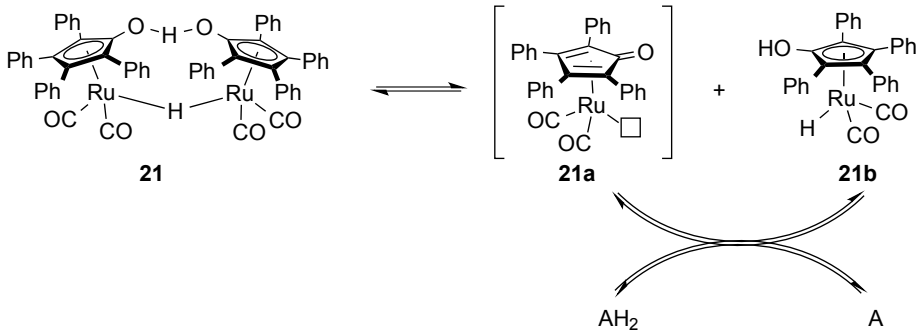

Scheme 1.10 *Shvo's catalyst.*

Both complexes can interconvert into one another by hydrogenation of a hydrogen acceptor (A) or dehydrogenation of a hydrogen donor (AH_2). Shortly before the isolation and structural determination of the ruthenium dimer, Shvo reported the acceptorless dehydrogenation of 2-octanol and cyclohexanol at 145°C using a ruthenium dimer described as $[(\eta_4\text{-}Ph_4C_4CO)Ru(CO)_2]_2$ **22**[49]. More recently, Shvo's catalyst was used for the dehydrogenation of 1-phenylethanol leading to up to 98% of acetophenone[50]. The catalyst was heterogenized by entrapment of a hydroxymethyl analog of **21**, using a sol-gel process. The heterogeneous catalyst was found to be slightly more active than the homogeneous complex **21** and could be recycled up to 5 times maintaining 87 % of its initial activity.

B. Metal complexes with active OH groups

In 2006, Fujita *et al.* developed the Cp*Ir catalyst **23** bearing a functional 2-hydroxypyridine ligand[51]. This catalyst is active for the acceptorless dehydrogenation of a great variety of aromatic and aliphatic secondary alcohols under base-free conditions. For 1-phenylethanol, a model substrate, 70 % yield of acetophenone is obtained after 20 h refluxing in toluene with a catalyst loading of 0.1 mol %. TONs up to 2120 were obtained by decreasing the catalyst loading to 0.025 mol %. Interestingly, the authors demonstrated that the 2-hydroxypyridine ligand is crucial to ensure high catalytic activity. In comparison, iridium complexes bearing pyridine or isomer 3- and 4-hydroxypyridine displayed very little activity in alcohol dehydrogenation. Based on this observation, the authors proposed that the

2-hydroxypyridine ligand is directly involved in the catalytic cycle acting as an acid-base site. Under reaction conditions, the alcohol adds to the iridium to form an alkoxy complex **A** which undergo β-H elimination to form a hydridoiridium complex **B** and release the ketone product. Hydrogen is released from the hydrido complex **B** by interaction between the hydride and the hydroxy proton from the ligand forming a 2-hydroxypyridinate chelated complex **C**. Addition of an alcohol molecule regenerates the alkoxy iridium complex **A**, the proton being transferred to the oxygen atom of the ligand. Supporting this mechanism, 2-hydroxypyridinate chelated complex **24** was prepared and displayed similar activity to the catalyst **23** (Table 1.4, entries 2 and 3).

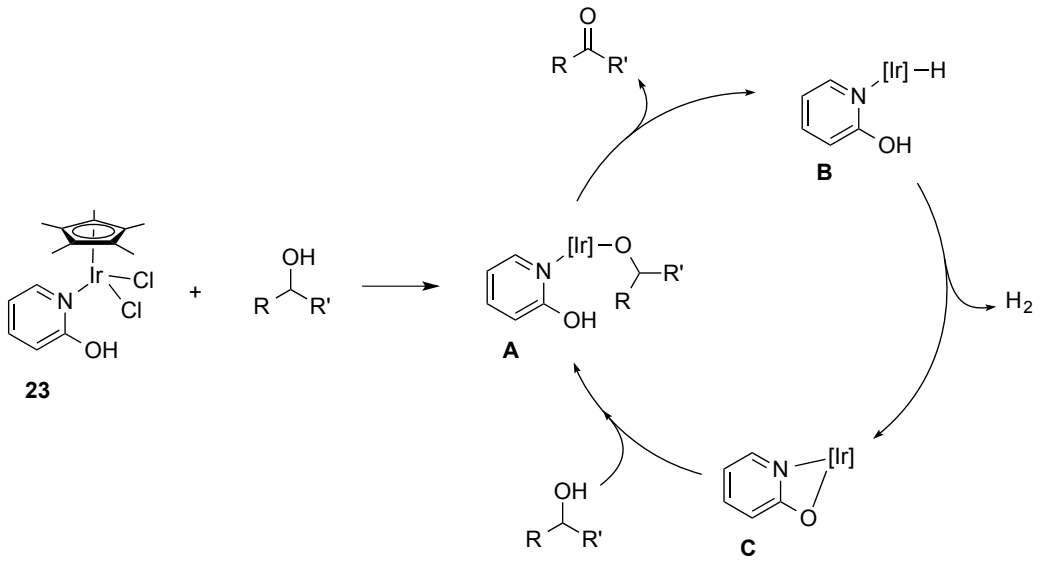

Scheme 1.11 *Proposed catalytic cycle for alcohol dehydrogenation catalysed by **23**.*

Yamaguchi further developed related catalysts based on the 2-hydroxypyridine structure. Iridium catalyst **25** bearing a C,N-coordinated 6-phenyl-2-hydroxypyridine was synthesised and used for the dehydrogenation of primary and secondary alcohols[52].

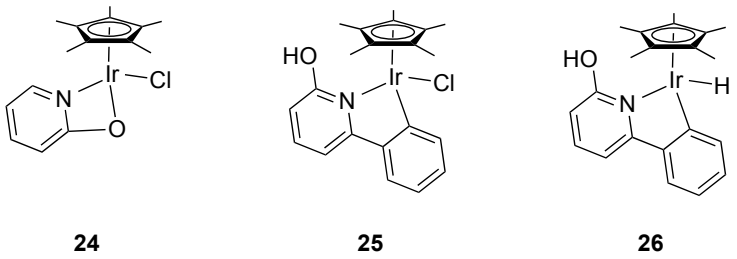

24 **25** **26**

Fig. 1.12 *Structures of Yamaguchi's catalysts* ***24-26****.*

Catalyst **25** displays similar activity to 2-hydroxypyridine complex **23** for the dehydrogenation of benzyl alcohol under base-free conditions yielding *c.a.* 60 % benzaldehyde after 20 h in refluxing toluene with 2.0 mol % of catalyst (TON = 35) (Table 1.4, entries 1 and 2). The analog hydridoiridium complex **26** allows obtaining higher yields than catalyst **25** under base-free conditions (78 % vs. 59 %), but is less active than catalyst **25** in the presence of NaOMe (90 %) or $NaHCO_3$ (88 %) (Table 1.4, entries 4, 1, 6 and 7). In the presence of 5.0 mol % of NaOMe, 90 % benzaldehyde is obtained under the same reaction conditions with catalyst **25** while only 30 % is obtained with catalyst **23** (Table 1.4, entries 5 and 6). In addition to benzyl alcohol, other primary alcohols and secondary alcohols were also used as substrates with catalyst **25**. For aliphatic primary alcohols, lower yields of the corresponding aldehydes were observed (Table 1.4, entries 8-11), while for aliphatic secondary alcohols, higher yields were obtained (Table 1.4, entries 12-14).

Table 1.4 *Dehydrogenation of alcohols with Yamaguchi's catalysts* ***23-26***[‡][51-52].

entry	substrate	cat. (mol %)	base (5.0 mol %)	solvent	conv. (%)	yield (%)
1	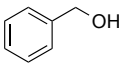	**25** (2.0)	/	toluene	59	59
2		**23** (2.0)	/	toluene	63	63
3		**24** (2.0)	/	toluene	52	50
4		**26** (2.0)	/	toluene	n.d.	78
5		**23** (2.0)	NaOMe	toluene	31	30
6		**25** (2.0)	NaOMe	toluene	91	90
7		**25** (2.0)	$NaHCO_3$	*p*-xylene	91	88
8	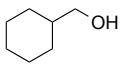	**25** (2.0)	NaOMe	toluene	26	18
9		**25** (5.0)	$NaHCO_3$	*p*-xylene	74	62
10	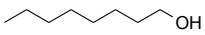	**25** (2.0)	NaOMe	toluene	40	34
11		**25** (5.0)	$NaHCO_3$	*p*-xylene	65	46
12	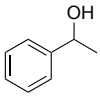	**25** (0.1)	/	*p*-xylene	96	96
13	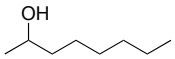	**25** (0.2)	/	*p*-xylene	93	92
14	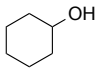	**25** (0.5)	/	*p*-xylene	100	100

[‡]reaction conditions: substrate: 1.0 mmol, solvent: 18 mL, reflux, 20 h.

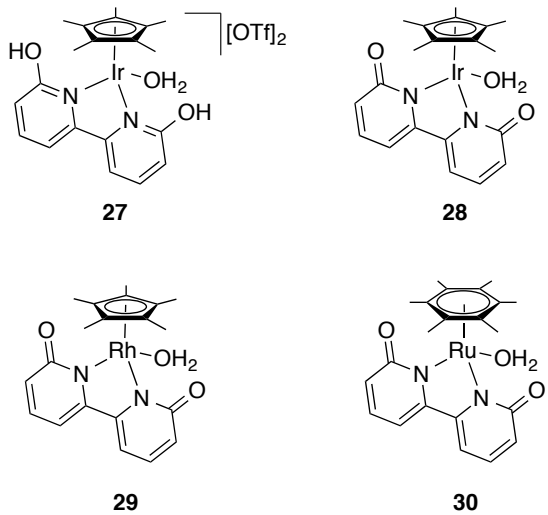

Fig. 1.13 *Structures of Yamaguchi's catalysts* ***27-30***.

The same group developed the water-soluble and reusable iridium catalyst **27** bearing a bipyridine-based functional ligand (see Fig. 1.13)[53]. According to the author, this represents the first example of the dehydrogenative oxidation of alcohols in aqueous media. Dehydrogenation of both primary and secondary alcohols was

investigated. Using benzyl alcohol as substrate, with a catalyst loading of 1.5 mol % in water, benzaldehyde is obtained with 92 % yield after 20 h of reaction (Table 1.5, entry 2). Similar yield was obtained when the reaction was conducted under air, evidencing the catalyst stability (Table 1.5, entry 3). High yields could be achieved for other primary alcohols and secondary aromatic alcohols (Table 1.5, entries 6-8 and 12). Lower catalyst loading could be used, leading to turnover number of *ca.* 2500 for the dehydrogenation of *p*-methoxybenzaldehyde using 0.02 mol % of complex **27** (Table 1.5, entry 13). Since catalyst **27** is water-soluble, the catalyst and the organic product could be easily separated by product extraction using hexane after the desired reaction time, allowing for catalyst recycling. Using such an approach, catalyst **27** was used for 8 consecutive runs for 1-(*p*-methoxyphenyl)ethanol dehydrogenation with only slight decrease of the product yields (Fig. 1.14).

The authors proposed the following catalytic cycle for alcohol dehydrogenation with complex **27** (Scheme 1.12). In the first step, a monocationic unsaturated species **A** is formed as a result of the elimination of HOTf and release of the aqua ligand from catalyst **27**. Then an alkoxy iridium species **B** is generated from the activation of an alcohol by **A**. Hydrido iridium complex **C** is then generated by a β-hydrogen elimination of the alkoxide that releases the carbonyl product. Finally, the catalytic cycle is closed by a ligand-promoted release of hydrogen from **C** to give back the unsaturated complex **A**.

Table 1.5 *Dehydrogenation of alcohols using Yamaguchi's catalysts **27-30**.*

entry	Substrate	cata. (mol %)	solvent (bp)	time (h)	conv. (%)	yield (%) (TON)	ref.
1	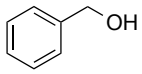	**27** (1.5)	water (100 °C)	6	60	60	[53]
2		**27** (1.5)	water (100 °C)	20	92	92	[53]
3‡		**27** (1.5)	water (100 °C)	20	92	91	[53]
4		**28** (1.5)	benzene (80 °C)	20	n.d.	96	[54]
5		**28** (1.5)	THF (66 °C)	20	n.d.	54	[54]
6	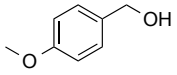	**27** (1.5)	water (100 °C)	20	n.d.	93	[53]
7	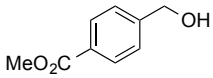	**27** (3.0)	water (100 °C)	20	n.d.	77	[53]
8	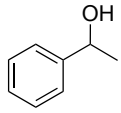	**27** (1.0)	water (100 °C)	20	n.d.	92	[53]
9		**28** (0.5)	benzene (80 °C)	20	100	100	[55]
10		**28** (0.5)	pentane (36 °C)	5	n.d.	100	[54]
11		**28** (0.01)	pentane (36 °C)	48	n.d.	95 (9500)	[54]
12		**28** (0.0002)	*p*-xylene (138 °C)	48	n.d.	55 (275000)	[54]
13		**29** (0.5)	benzene (80 °C)	20	95	95	[55]
14		**30** (0.5)	benzene (80 °C)	20	97	97	[55]
15	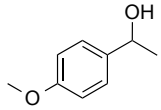	**27** (1.0)	water (100 °C)	20	n.d.	98	[53]
16		**27** (0.02)	water (100 °C)	100	n.d.	51 (2550)	[53]
17	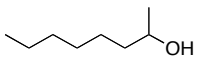	**27** (3.0)	water (100 °C) 4.5 mL, *t*-butyl alcohol (82 °C) 0.5 mL	20	n.d.	85	[53]
18		**28** (3.0)	pentane (36 °C)	20	n.d.	80	[54]
19	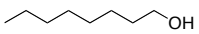	**27** (3.0)	water (100 °C)	20	17	16	[53]
20		**28** (5.0)	toluene (110 °C)	20	n.d.	87	[54]

‡under air

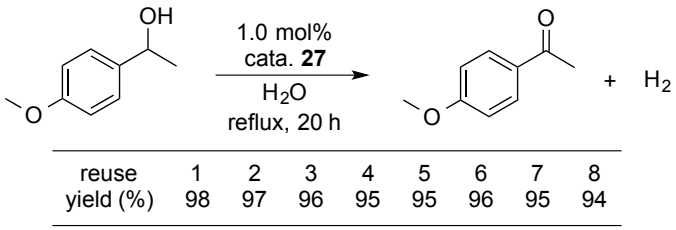

reuse	1	2	3	4	5	6	7	8
yield (%)	98	97	96	95	95	96	95	94

Fig. 1.14 *Reuse of catalyst **27**.*

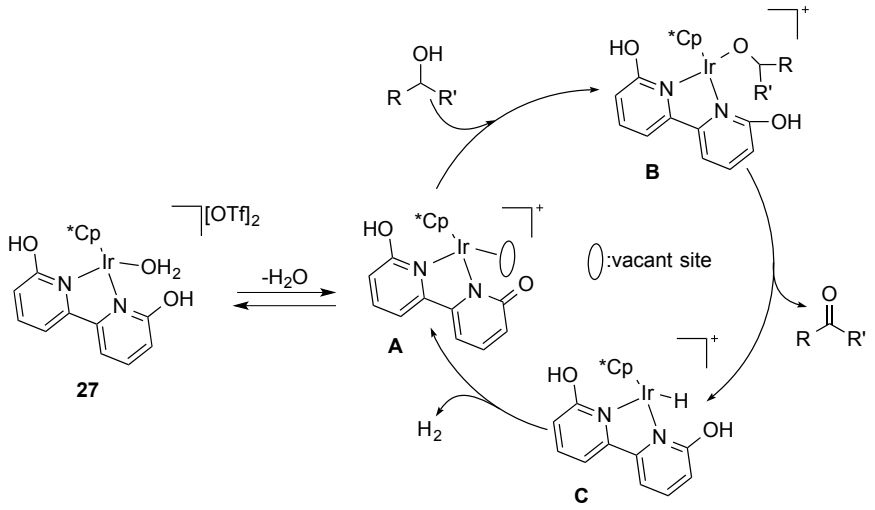

Scheme 1.12 *Proposed catalytic cycle for catalyst 27.*

Related iridium complex **28**, bearing a bipyridonate ligand showed activity at temperature as low as 36 °C for the dehydrogenation of 1-phenylethanol (Table 1.5 entry 10). Catalyst loading could be decreased from 0.01 down to 0.0002 leading to turnover number of 9500 and 275000, respectively (Table 1.5, entries 11 and 12). Catalysts **27** and **28** were both active for the oxidation of aliphatic secondary alcohols such as 2-octanol, (Table 1.5, entries 17 and 18). Interestingly, while complex **27** proved to be inefficient for the oxidation of primary alcohol, complex **28** efficiently catalysed the oxidation of 1-octanol leading to 87 % yield of octanal (Table 1.5, entries 19 and 20). The superior activity of complex **28** compare to **27** could be explained by the fact that complex **28** is already in the active form and do not require initial deprotonation (see step **27** to **A** in Scheme 1.12). Using density functional theory, the authors proposed that the dehydrogenation of alcohol by complex **28** proceed by an outer sphere mechanism involving both the metal and the pyridonate ligand[55].

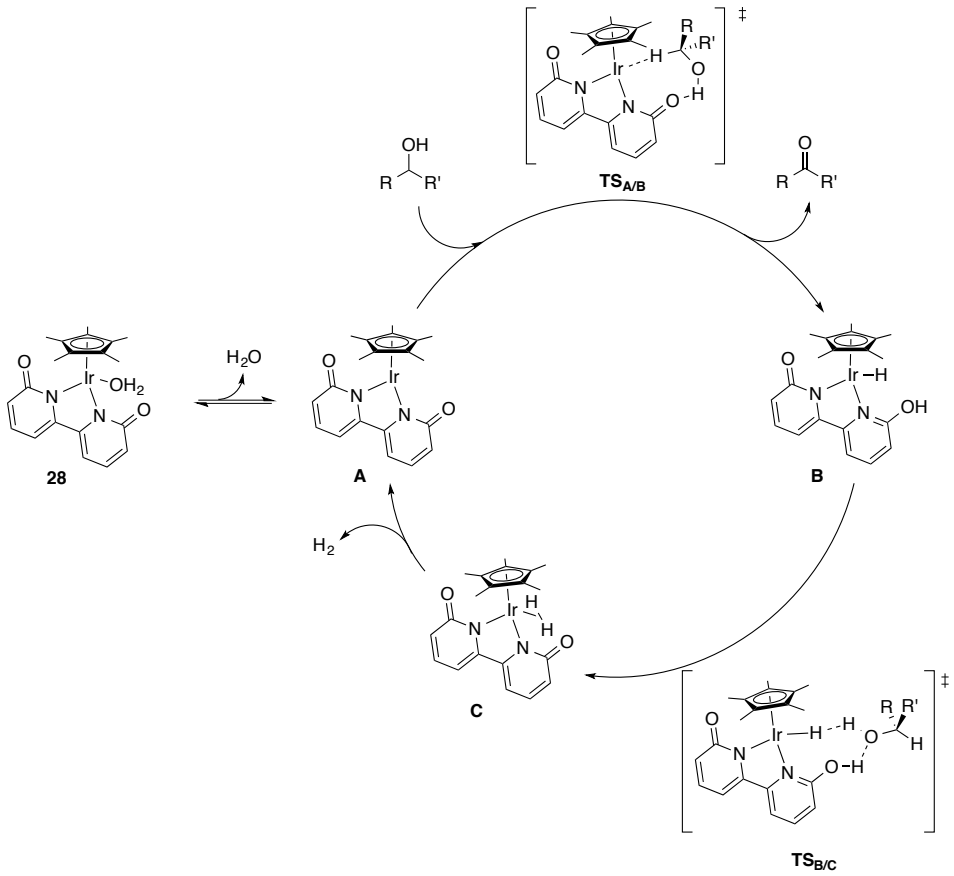

Scheme 1.13 *Outer-sphere mechanism for the alcohol dehydrogenation catalysed by complex **28**.*

Initial loss of the aqua ligand from complex **28**, generates complex **A** that dehydrogenates the alcohol in a single concerted step where the hydroxy proton is transfered from the alcohol to the pyridonate ligand and the hydridic C-H hydrogen is transfered to the iridium (**TS$_{A/B}$**, Scheme 1.13). During this step, the pyridonate ligand is aromatised leading to an hydroxypyrine ligand. Formation of the dihydrogen complex **C** from the iridium-hydride **B** is facilitated by an alcohol molecule that assists the proton transfer from the hydroxypyridine to the hydride (**TS$_{B/C}$**, Scheme 1.13). Decoordination of hydrogen from complex **C** closes the catalytic cycle. Calculated activation energies suggests that the formation of the hydrogen complex **C** is the rate determining step with an energy barrier of 23.9 kcal mol^{-1} for benzyl alcohol dehydrogenation. Based on this mechanism, the author calculated the energy profile for 1-phenylethanol dehydrogenation using analog d^6 metal complexes bearing

bis-pyridonate ligand. For rhodium (III) complex **29** and ruthenium (II) complex **30,** bearing hexamethylbenzene instead of Cp*, calculated activation energy were similar to those obtained for iridium complex **28** (see structure in Fig. 1.13**)**. Therefore, complexes **29** and **30** were synthesised and tested for 1-phenylethanol dehydrogenation. In agreement with the calculated activation energies, complexes **29** and **30** showed similar activity to complex **28** producing acetophenone with yield over 95 % under identical reaction conditions (Table 1.5, entries 8, 13 and 14). This opens the possibility of further development of new metal-pyridonate complexes replacing iridium by more abundant and cheaper ruthenium.

Gelman and co-workers developed the bifunctional iridium PCP pincer complex **31**[56] **(**Scheme 1.14**)**. This complex reversibly extrudes molecular hydrogen by interaction between the hydride and the pendant hydroxy proton of the ligand to form the "closed arm" iridium complex **32 (**Scheme 1.14**)**.

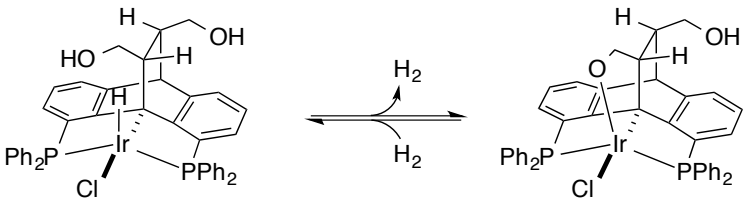

31 **32**

Scheme 1.14 *Reversible hydrogen extrusion from Gelman iridium PCP pincer complex **31**.*

Complexes **31** and **32** were shown to be active for the acceptorless dehydrogenation of various secondary alcohols (Table 1.6). Dehydrogenation of both aromatic and aliphatic secondary alcohol could be carried out with almost quantitative yield to the corresponding ketones with 0.01 mol % of **31** or **32** after 10 h in refluxing *p*-xylene (Table 1.6, entries 1, 2 and 5). Addition of 5.0 mol % of Cs_2CO_3 allowed to reduce reaction time to 6 h while maintaining yields of *ca.* 90 % in the corresponding ketones (Table 1.6, entries 3 and 6). The reaction is proposed to proceed by initial extrusion of hydrogen from **31** to form complex **32** (Scheme 1.15). Interaction of the

alcohol with **32** leads to the formation of an open arm alkoxy complex **A**. Finally, β-hydride elimination leads to the formation of the ketones product and regeneration of the open arm hydride complex **31**. Base addition is proposed to accelerate the formation of **A** by addition of nucleophilic cesium alkoxide instead of free alcohol to complex **32**.

Catalyst **31** was heterogenised by entrapment into a silica matrix by sol-gel process[57]. The solid catalyst containing 3 mol % of **31** relative to the substrate was active for the dehydrogenation of 1-phenylethanol in the presence of 3 mol % of Cs_2CO_3 giving 93 % of acetophenone after 24 h in refluxing mesitylene (Table 1.6, entry 4). Altough the heterogenised catalyst showed lower activity than its homogeneous analog, it could be recycled by simple filtration allowing to be used for 5 consecutive runs without noticeable deactivation.

Table 1.6 *Dehydrogenation of alcohols using Gelman's catalysts*[‡].

entry	substrate	catalyst (mol %)	additive (mol %)	time (h)	yield (%)
1	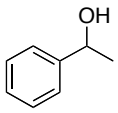	**31** (0.01)	/	10	94
2		**32** (0.01)	/	10	91
3		**31** (0.01)	Cs_2CO_3 (5.0)	6	94
4[†]		**31**@SiO_2 (3.0)	Cs_2CO_3 (3.0)	24	93
5	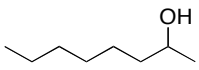	**31** (0.01)	/	10	92
6		**31** (0.01)	Cs_2CO_3 (5.0)	6	87

[‡]reaction conditions: solvent: *p*-xylene, reflux.

[†]solvent: mesitylene, reflux.

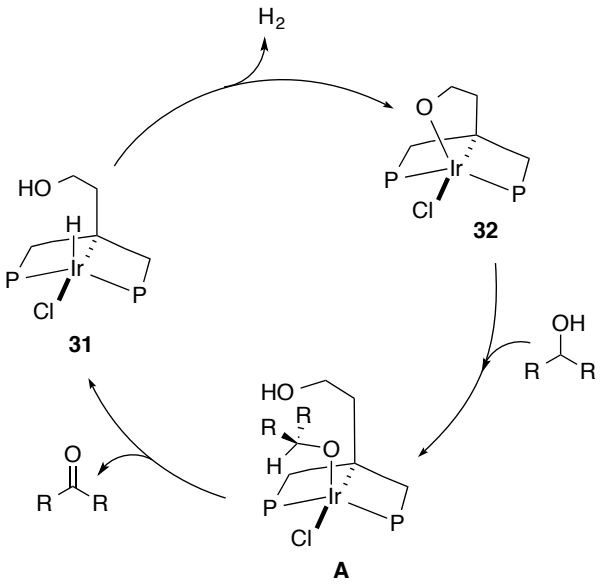

Scheme 1.15 *Proposed reaction mechanism for the dehydrogenation of alcohols catalysed by complex **31** or **32**.*

C. Metal with non-innocent PNP and PNN pincer ligand.

Milstein *et al.* carried out pioneering work onto the use of aromatic PNP and PNN pincer ligands in cooperative metal-ligand catalysis[28-29, 58-59]. Reactivity of such complexes relies on the cooperation between the metal and the dearomatized-aromatized ligand for the reversible activation of chemical bonds (Scheme 1.16). In this process, there is no change in the formal oxidation state of the metal while the nitrogen atom of the pyridine ring switches from a two electron donor amino ligand to a one electron (en)amido ligand donor.

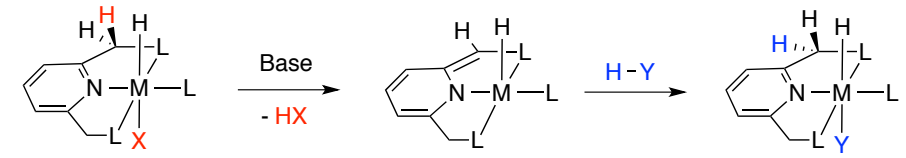

Scheme 1.16 *Activation of Milstein's catalyst.*

Ruthenium PNP complexes **33** and **34a** were used for the acceptorless dehydrogenation of secondary alcohols[60] (Fig. 1.15). In the presence of one

equivalent of base per Ru-Cl bond, complexes **33** and **34a** catalyse the conversion of secondary alcohol to the corresponding ketone in refluxing dioxane (Table 1.7)

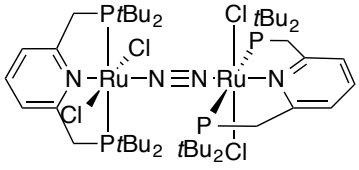

33

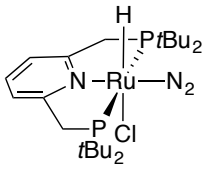

34a

Fig. 1.15 *Structures of Milstein's catalysts **33** and **34a**.*

Table 1.7 *Dehydrogenation of secondary alcohols catalysed by complexes **33** and **34a**‡.*

entry	substrate	catalyst	base/ cata.	time (h)	conv. (%)	yield (%)	TON
1		**33**	4	70	60.0	57.4	144
2		**34a**	1	70	94.0	91.0	228
3		**34a**	1	100	64.4	64.4	161

‡reaction conditions: [Ru] = 0.4 mol %, base = NaO*i*Pr, 100 °C, under argon, open system.

More recently Beller and co-workers studied the use of ruthenium aromatic and aliphatic PNP pincer complexes for the dehydrogenation of alcohols targeting hydrogen production[61]. Similar to aromatic PNP pincer complexes, aliphatic PNP pincer complexes are able to activate chemical bonds by metal-ligand cooperation. In this process, the formal oxidation state of the metal does not change during the transformation but the nitrogen donor atom switches from a two electrons donor amino ligand to a one electron amido ligand donor (Scheme 1.17).

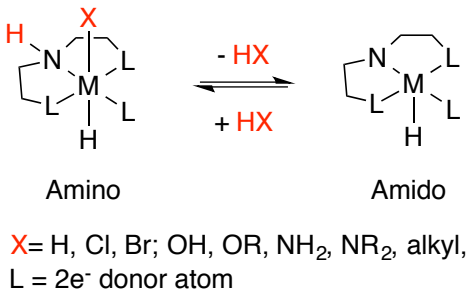

Scheme 1.17 *Activation of LNL-Ru catalysts.*

Isolated ruthenium de-aromatized PNN complex **35a** and aliphatic complex **36** together with *in situ* formed aliphatic ruthenium PNP catalysts (ruthenium source: **37a-b**; aliphatic PNP ligand: **38a-c**; equimolar) were tested for the dehydrogenation of *i*-propanol at extremely low catalyst loading, 32 ppm, without solvent (Fig. 1.16).

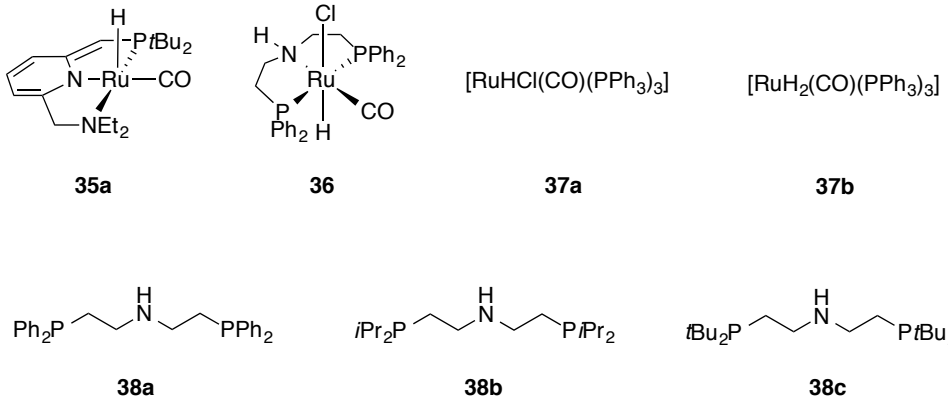

Fig. 1.16 *Structures of complexes **35a-38c**.*

Catalyst were evaluated by monitoring the volume of evolved hydrogen over time (Table 1.8). In the presence of a 100 fold excess of base relative to the catalyst, de-aromatized PNN ruthenium complex **35a** and aliphatic PNP ruthenium complex **36** showed similar activity (Table 1.8, entry 1 and 5). However the activity of complex **36** could be improved by reducing the amount of base down to an almost equimolar ratio to the catalyst (Table 1.8, entry 4 and 5). In the absence of base catalyst **36** was found to be almost inactive presumably because elimination of HCl from the complex is necessary to give the active catalyst (Table 1.8, entry 3). *In situ* formed complexes from equimolar mixture of hydrido chloro ruthenium complex **37a** and aliphatic PNP ligands **38a** and **38b** were found to be active in the presence of 1.3 equivalent of NaO*i*Pr (Table 1.8, entries 6 and 7). Interestingly, the nature of the substituents on the phosphorus atoms of the PNP ligand had a significant influence on the catalyst activity (Table 1.8, entries 6 and 7). A two-fold rate increase is obsverved when going from phenyl substituent to more electrons donating *i*-propyl substituent with TOF after 2h of 460 h^{-1} and 1187 h^{-1}, respectively. As for isolated complex **36**, *in situ* catalyst made from hydrido chloro ruthenium complex **37a** was found to be inactive

in the absence of additionnal base (Table 1.8, entry 8). Using dihydride complex **37b** as ruthenium source with PNP ligand **38b** led to more active catalyst (Table 1.8, entry 9). In addition, it could be used in the absence of base showing improved activity (Table 1.8, entry 10). Decrease of the catalyst loading from 32 ppm to 4 ppm led to an impressive reaction rate wih a TOF of 8382 h^{-1} (Table 1.8, entry 11). The use of more bulky and electron donating ligand **38c** together with ruthenium dihydride **37b** did not give an active catalytic system (Table 1.8, entry 12).

Table 1.8 *Dehydrogenation of i-propanol with ruthenium PNN and PNP catalysts*[‡].

entry	cata.	NaO*i*Pr (equiv)	TOF 2h (h^{-1})	TOF 6h (h^{-1})	conv. 6h (%)
1	**35a**	100	855	379	7.3
2	**35a**	2000	826	407	7.8
3	**36**	/	< 100	/	/
4	**36**	1.3	1231	644	12.4
5	**36**	100	929	346	6.6
6	**37a/38a**	1.3	460	384	7.4
7	**37a/38b**	1.3	1187	851	16.3
8	**37a/38b**	/	<100	/	/
9	**37b/38b**	1.3	1834	1009	19.4
10	**37b/38b**	/	2048	1109	21.3
11[†]	**37b/38b**	/	8382	4835	6.7
12	**37b/38c**	/	< 100	/	/

[‡]reaction conditions: [Ru] = 32 ppm (4.2 μmol), *V* (*i*-propanol) = 10 mL, reflux (90°C).

[†][Ru] = 4.0 ppm, *V* (*i*-propanol) = 40 mL.

Compared to the previousely described catalytic systems, the ruthenium aromatic and aliphatic PNP and PNN pincer system shows the higest activity in terms of reaction rate, expressed by the TOFs, for the dehydrogenation of secondary alcohol. Moreover, this system is active at relatively low reaction temperature (90°C) and is active without additional base or acid providing that dihydride precursor is used. However, it should be noted that this system are prone to deactivation as the TOF decreases over reaction time well before the reaction reaches completion (TOF (6h) < TOF (2h) with conversions ≤ 20 %). Regarding the reaction mechanism for the catalytic system **37b/38b**, the author proposed that after initial formation of the $[RuH_2(CO)(PNP)]$ complex **A**, this complex extrudes molecular hydrogen to form the

unsaturated 16 e^- complex **B**. The alcohol is dehydrogenated via an outer-sphere mechanism involving both the ruthenium center and the PNP ligand nitrogen atom of complex **B** which give back complex **A** and the carbonyl product.

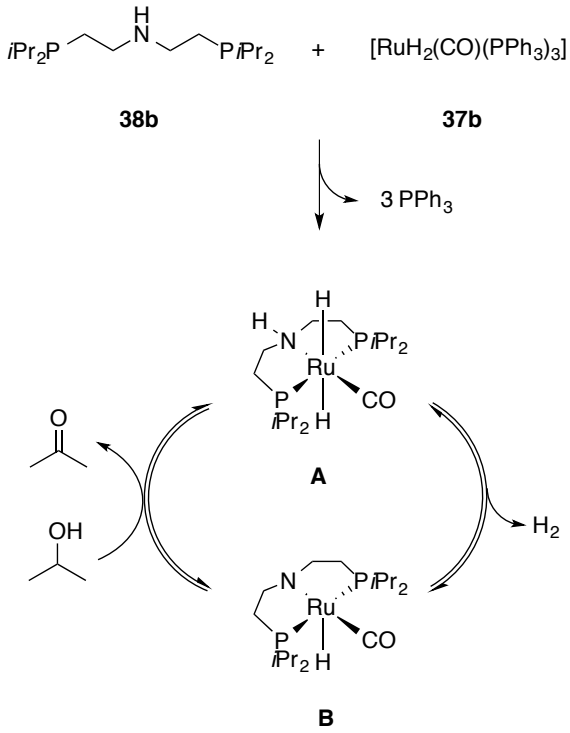

Scheme 1.18 *Proposed mechanism for the dehydrogenation of alcohol by aliphatic ruthenium pincer complex.*

1.4 Acceptorless dehydrogenative coupling of alcohols

1.4.1 Introduction

While dehydrogenation of secondary alcohols leads to the formation of ketones, transformation of primary alcohols usually proceeds toward the formation of esters. Only in few cases, aldehydes are the obtained products as for example in the case of Yamaguchi's catalysts (*vide supra*). For most catalytic systems the produced aldehydes further react to give an ester either by i) Tischenko reaction with another aldehyde or ii) by reaction with another alcohol molecule to give a hemiacetal that is dehydrogenated to form an ester.

Considering that there are significant differences in substrate reactivity and reaction conditions, a meaningful comparison of the efficiency for all the reported

catalysts are problematic. Therefore, it is important to introduce some "guidelines" regarding this reaction.

I. Due to thermodynamics and kinetics, the substrate reactivity toward dehydrogenation usually increases following: aliphatic primary alcohol < benzyl alcohol < aliphatic secondary alcohol < aromatic secondary alcohol.

II. In most reported cases, a base and an organic solvent are required for the transformation. From the viewpoint of green chemistry and atom economy, a base-free and solvent-free condition would be preferable.

III. Regarding catalyst performance evaluation, both turnover frequency and product yield are very important. A highly efficient catalyst should give at the same time a high turnover frequency (*i.e.* high reaction rate) and a high product yield (*i.e.* high selectivity and high catalyst stability).

Based on these guidelines, the most challenging transformation appears to be the acceptorless dehydrogenative coupling of primary alcohols under neutral and neat conditions. Among all the primary alcohols, ethanol represents the most challenging substrate due to its low boiling point, setting the reaction temperature at 78 °C (ethanol boiling point).

In the present thesis, due to their availability from biomass and the challenges of their transformation, the most unreactive substrates, namely primary alcohols are investigated. More specifically, two bioalcohols—butanol and ethanol—are studied as substrates, under the ideal base-free and solvent-free conditions for acceptorless dehydrogenation.

One of the earliest example of dehydrogenative coupling of alcohols to esters was reported by Shvo in the early eighties[62-63]. Following reports on the activity of $Ru_3(CO)_{12}$ in the presence of 1,2-diphenylacetylene for dehydrogenative coupling of alcohol, it was established that in the presence of Shvo's catalyst **21,** this

transformation could be carrried in the absence of acceptor[49]. $[RuH_2(PPh_3)_4]$ complex **2b** has been reported to catalyse the acceptorless transformation of aliphatic alcohols to esters in the abscence of base at high temperature (180 °C)[64].

Beside these early reports most of the development on the catalytic acceptorless dehydrogenative coupling of alcohols stems from the ruthenium aromatic PNP and PNN pincer complex developed by the team of Milstein in the mid 2000s[65]. Following this pionnering work, aliphatic PNP and PNN pincer complexes have been simultaneousely developed by the teams of Beller, Gusev and us.

1.4.2 Milstein's group work

In the last ten years, Milstein and co-workers have developed a large variety of ruthenium complexes bearing aromatic pincer PNP, PNN and PNNP ligands for the dehydrogenation and dehydrogenative coupling of alcohols (Fig. 1.17)[60, 65-71]. A large part of their work has recently been reviewed[28-29]. Herin we focus on the activity of the different complexes for the dehydrogenative coupling of primary alcohol to esters (Table 1.9). As previousely shown for alcohol dehydrogenation, reactivity of such complexes arises from the cooperation between the metal and the dearomatized-aromatized ligand for the reversible activation of chemical bonds (1.3.2.2.C and Scheme 1.16). This is illustrated by comparison of complexes **35b** and **35a** catalytic activity for the dehydrogenative coupling of 1-hexanol. In the absence of base, catalyst **35b** do not catalyse the dehydrogenative coupling of 1-hexanol (Table 1.9, entry 2). Upon addition of one equivalent of base relative to **35b**, 90.4 % of hexyl hexanoate is obtained after 24 h reflux (Table 1.9, entry 3). The base eliminates HCl from the inactive aromatic PNN ruthenium complex **35b** to give the active dearomatized PNN complex **35a**. Supporting this, when isolated **35a** is used for the dehydrogenative coupling of 1-hexanol in the absence of base, 91.4 % of the corresponding ester is obtained after 2.5 h (Table 1.9, entry 1). Instead of hydridochloro aromatic PNN ruthenium complex, corresponding dichloride such as

35c can also be used in the presence of base to catalyse the dehydrogenative coupling of primary alcohols (Table 1.9, entry 4). Aromatic PNP and PNN pincer ruthenium complexes bearing borohydride ligands instead of chlorides are active for the dehydrogenative coupling of primary alcohols in the absence of base (Table 1.9, entries 5, 7 and 8). Presumably, these complexes, where borohydrides are "masked" hydrides, eliminate H_2 upon thermal activation to give active dearomatized complexes. Regarding the ligand structure, PNN pincers usually give more active complexes than the corresponding PNP (Table 1.9, entry 3 vs. 6 and entry 5 vs. 8). According to the authors, such a difference arises from the ease of decoordination of the "hemilabile" amine arm of the PNN ligand. Decoordination of one of the ligand is necessary to create a vacant site at the metal for the β-elimination step (see steps A→ B→ C in Scheme 1.19). Hence, this step is facilitated when more labile nitrogen ligand is used instead of strongly coordinating phosphine ligand. Taking into account all the previous observations, an inner-sphere cooperative ligand-metal mechanism is proposed by the authors where complex **35a** plays a pivotal role (Scheme 1.19)[65]. Regarding substrates of interest for the present thesis, Milstein's catalysts have been tested for 1-butanol dehydrogenative coupling (Table 1.9, entries 9-10). The best performances are obtained using 0.1 mol % of complex **35a** under neat and base-free conditions. Butyl butyrate is obtained in 90 % yield after 5 h reflux which corresponds to a TON of 900 and a TOF of 180 h^{-1}.

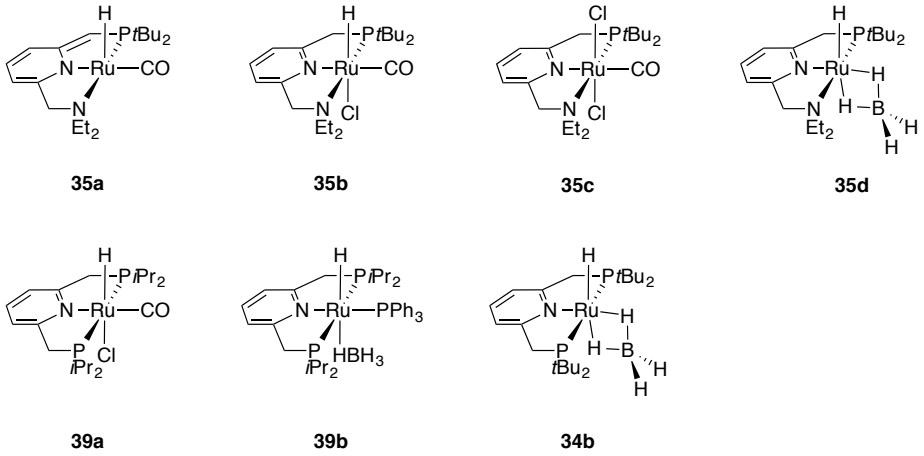

Fig. 1.17 *Selected examples* of *Milstein's catalysts.*

Table 1.9 *Dehydrogenative coupling of primary alcohols by Milstein's catalysts.*

entry	cata. (mol %)	substrate	base (mol%)	solvent	temp. (°C)	time (h)	yield (%) ester	yield (%) aldehyde	ref.
1	**35a** (0.1)	1-hexanol	/	/	157	2.5	91.4	0.5	[65]
2	**35b** (0.1)	1-hexanol	/	/	157	24	0	0	[65]
3	**35b** (0.1)	1-hexanol	KOH (0.1)	/	157	24	90.4	0.3	[65]
4	**35c** (0.1)	1-hexanol	NaO*i*Pr (0.2)	dioxane	100	24	91	0.5	[66]
5	**35d** (0.1)	1-hexanol	/	toluene	115	24	94	0	[68]
6	**39a** (0.1)	1-hexanol	KOH (0.1)	/	157	24	67.2	2.8	[65]
7	**39b** (0.1)	1-hexanol	/	/	157	24	47	10	[68]
8	**34b** (0.1)	1-hexanol	/	toluene	115	24	69	3	[68]
9	**35a** (0.1)	1-butanol	/	/	117	5	90	0.5	[65]
10	**35d** (0.1)	1-butanol	/	toluene	110	24	96	0	[68]

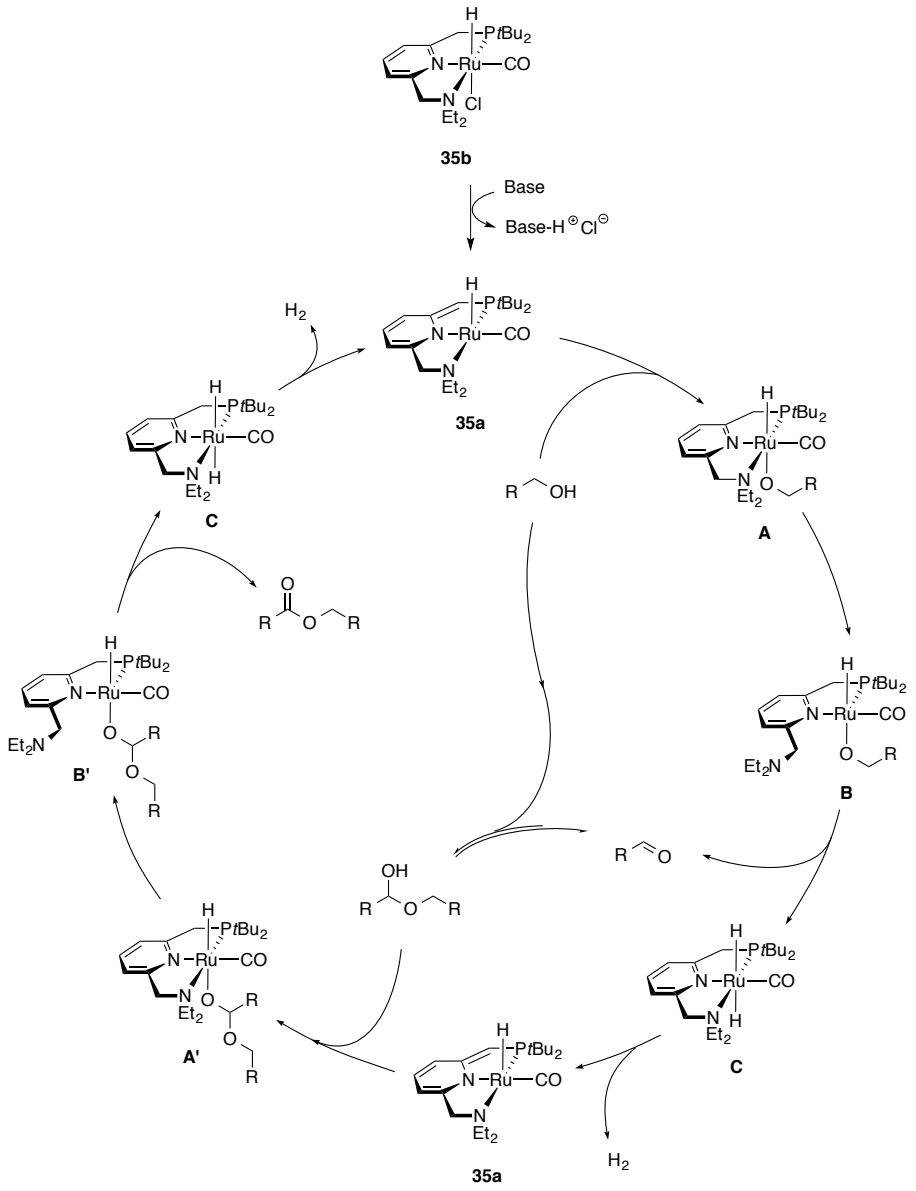

Scheme 1.19 *Proposed mechanism for the acceptorless dehydrogenative coupling of alcohol by Milstein's catalyst **35b**.*

Although Milstein's catalysts show high efficiency for acceptorless dehydrogenative coupling of many different primary alcohols such as 1-hexanol and 1-butanol, for one of the most challenging substrates among all primary alcohols—ethanol, none of these catalysts were tested.

1.4.3 Gusev's group work

Gusev *et al* developed several ruthenium (complex **40** - **45**) and osmium (complex **46** - **51**) complexes for the dehydrogenative coupling of primary alcohols

(Fig. 1.18)[72-76]. For most of the complexes, the metal (Ru or Os) is coordinated by a tridentate pincer ligand having a functional NH group spaced by two carbon atoms from the phosphorus, nitrogen or sulfur donor atoms. These complexes were used for the acceptorless dehydrogenative coupling of various primary alcohols in the presence of base or under base-free conditions (Table 1.10).

The ruthenium dihydride PNP complex **40a** was able to catalyse the dehydrogenative coupling of primary alcohols under base-free conditions but required temperature above 120 °C to become efficient (Table 1.10, entries 1 and 2). Hydridochloro and dichloro ruthenium PNP complexes **40b**, **41** and **36** were found to be active for the formation of ethyl acetate from ethanol at relatively low temperature and low catalyst loading (Table 1.10, entries 3 to 7). For hydridochlororuthenium PNP complexes, the nature of the substituents at the phosphorus seems not to affect the activity of the catalysts (Table 1.10, entries 4 vs. 5). The same ethyl acetate yields are obtained under the same reaction conditions with catalyst **36** having phenyl substituent and with catalyst **40b** having more electron-donating iso-propyl substituents. On the other hand, the dichlororuthenium complex **41** proved to be less efficient that the hydridochloro complexes, albeit with different substituents at the phosphorus (Table 1.10, entries 7 vs. 3). Analog hydridochlororuthenium complexes, having PNN ligand instead of PNP were studied for the dehydrogenative coupling of primary alcohols in the presence of base (Table 1.10, entries 8 to 13). All three related complexes **42a**, **42b** and **42c** were found to be active for the production of ethyl acetate from ethanol. Due to differences in testing conditions, structure activity relationship cannot clearly be established. However, one can note that complex **42b** bearing a bulky PNN ligand is far less active than the less hindered complexes **42a** and **42c**. Interestingly, when comparing the activities of complex **36** and **42c** (Table 1.10, entries 5 vs. 13) it appears that substitution of one diphenylphosphine moiety by a more labile pyridine do not affect significally the activity of the complex. On the contrary, for PNN complexes, substitution of the carbonyl ligand trans to the active

NH group by a triphenylphosphine greatly improves the activity of the catalyst (comparing complexes **42c** and **43,** Table 1.10 entries 12 vs 14 and 13 vs. 15). With complex **43**, TON as high as 17 000 can be obtained for the dehydrogenative coupling of ethanol with a catalyst loading of 0.05 mol %. For these dichlorotriphenylphosphino ruthenium complexes, replacement of the PNN ligand by an NNN analog having two pyridine moieties lead to completely inactive catalyst **44** (Table 1.10, entry 17). Impressively, when switching to a SNS pincer ligand, the resulting complex **45** displays a catalytic activity almost identical to its PNN analog (Table 1.10, entries 14 vs. 18 and 15 vs. 19). When examining the variation of the catalytic activity with the catalyst loading, the authors noted an improvement of the reaction rate with lower catalyst loading[73]. For instance, for complex **43**, the TOF changed as follows: 135 h^{-1} (0.05 mol %, 4 h), 117 h^{-1} (0.05 mol%, 16 h), 375 h^{-1} (0.01 mol %, 24 h) and 567 h^{-1} (0.005 mol %, 24 h). Even if it regards single point averaged TOFs, one observe a 3.2 fold increase of the TOF (from 117 to 375) when decreasing five times the catalyst concentration (from 0.05 to 0.01). No clear reason is found for such a behaviour which has been observed for other catalytic systems and by other research groups (*vide infra*).

In addition to ruthenium, several osmium pincer complexes were tested for the dehydrogenation of primary alcohols. Poly hydrido osmium complexes **46a** and **46b** were found to be active for the dehydrogenation of primary alcohol but required reaction temperatures higher than 120°C to become efficient (Table 1.10, entries 20 to 22). In comparison, hydridocarbonylosmium complexes bearing pincer PNP ligand **47a**, **47b** and **48** showed improved activity (Table 1.10, entries 24 to 27). However, the osmium complexes displayed lower activity than their ruthenium analogs (Table 1.10, entries 1 vs. 24 and 3 vs. 26). Interestingly, when substituting the active NH group from the PNP ligand by an oxygen atom, the resulting complex, **49**, lost completely its activity, evidencing the crucial role played by the NH group of the ligand (Table 1.10, entry 25 vs. 28). In addition to PNP pincer ligands, Gusev's team

developed hydridochloro carbonyl osmium complexes bearing PNN ligands. However, as observed with ruthenium complexes, replacing one phosphine arm of the pincer by a pyridine moiety did not greatly affect the activity of the resulting osmium complexes (Table 1.10, entry 26 vs. 29). When looking at the influence of the substituents at the phosphorus for the hydridochlorocarbonylosmium PNN complexes, the activity increase following *t*Bu < *i*Pr < Ph (Table 1.10, entries 29, 30 and 31). The hydridocarbonylosmium PNN dimer **51** was found to be the most active among all the tested osmium complexes (Table 1.10, entry 32). The hydridorochlorocarbonylosmium PNN pincer complexes **50b** and **50c** displayed similar activities with their ruthenium analogs **42b** and **42c** showing the very small influence on the nature of the metal for this type of complexes (Table 1.10, entry 11 vs. 30 and 12 vs. 31). As previousely observed for ruthenium complexes, the authors found that reaction rate also increased with lower catalyst loading for the osmium dimer **51**. A five fold increase of the TOF, from 56 h^{-1} to 275 h^{-1}, was obtained when decreasing the catalyst loading from 0.05 to 0.01 mol %. Lower catalyst loading might favor the dissociation of the osmium dimer **51** to active mononuclear unsaturated $16e^-$ amido complex [OsH(CO)(PNN)] and thus enhance the reaction rate.

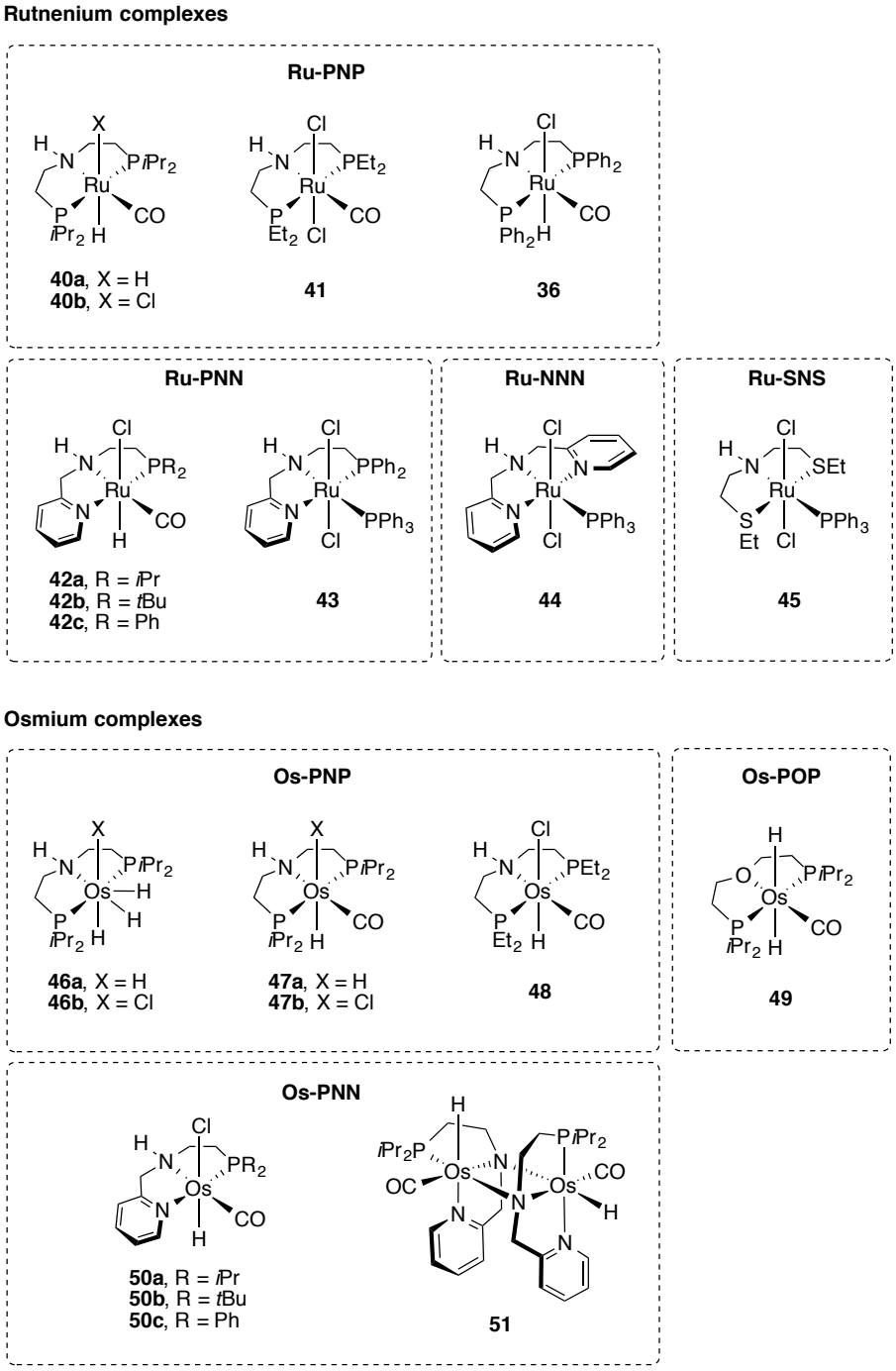

Fig. 1.18 *Structures of Gusev's catalysts.*

Table 1.10 *Catalytic performance of Gusev's catalysts.*

entry	cata. (mol %)	base (mol %)	substrate	temp. (°C)	time (h)	yield (%)	ref
1	**40a** (0.1)	/	1-butanol	118	6	21	[72]
2	**40a** (0.1)	/	isoamylalcohol	130	4	91	[72]
3	**40b** (0.05)	NaOEt (1.0)	ethanol	78	16	57	[73]
4	**40b** (0.01)	NaOEt (1.0)	ethanol	78	24	47	[73]
5	**36** (0.01)	NaOEt (1.0)	ethanol	78	24	47	[73]
6	**36** (0.005)	NaOEt (1.0)	ethanol	78	40	42	[73]
7	**41** (0.05)	NaOEt (1.0)	ethanol	78	16	17	[73]
8	**42a** (0.1)	*t*BuOK (0.5)	ethanol	78	7.5	30	[74]
9	**42a** (0.1)	*t*BuOK (0.5)	butanol	118	3	78	[74]
10	**42a** (0.1)	*t*BuOK (0.5)	isoamylalcohol	131	2.5	92	[74]
11	**42b** (0.05)	NaOEt (1.0)	ethanol	78	16	12	[73]
12	**42c** (0.05)	NaOEt (1.0)	ethanol	78	16	41	[73]
13	**42c** (0.01)	NaOEt (1.0)	ethanol	78	24	42	[73]
14	**43** (0.05)	NaOEt (1.0)	ethanol	78	16	95	[73]
15	**43** (0.01)	NaOEt (1.0)	ethanol	78	24	91	[73]
16	**43** (0.005)	NaOEt (1.0)	ethanol	78	40	85	[73]
17	**44** (0.05)	NaOEt (1.0)	ethanol	78	16	0	[73]
18	**45** (0.05)	NaOEt (1.0)	ethanol	78	16	97	[75]
19	**45** (0.01)	NaOEt (1.0)	ethanol	78	24	89	[75]
20	**46a** (0.1)	/	ethanol	78	5	3	[76]
21	**46a** (0.1)	/	1-butanol	118	8	3	[76]
22	**46a** (0.1)	/	isoamylalcohol	131	22	79	[76]
23	**46b** (0.05)	NaOEt (1.0)	ethanol	78	16	2	[73]
24	**47a** (0.1)	/	1-butanol	118	7	6	[72]
25	**47a** (0.1)	/	isoamylalcohol	131	8	93	[72]
26	**47b** (0.05)	NaOEt (1.0)	ethanol	78	16	23	[73]
27	**48** (0.05)	NaOEt (1.0)	ethanol	78	16	30	[73]
28	**49** (0.1)	/	isoamylalcohol	131	5	0	[72]
29	**50a** (0.05)	NaOEt (1.0)	ethanol	78	16	27	[73]
30	**50b** (0.05)	NaOEt (1.0)	ethanol	78	16	20	[73]
31	**50c** (0.05)	NaOEt (1.0)	ethanol	78	16	40	[73]
32	**51** (0.05)	NaOEt (1.0)	ethanol	78	16	45	[73]

Based on computational and experimental results, Gusev and co-workers proposed an outer-sphere reaction mechanism involving a $16e^-$ amido metal complex **A** for the dehydrogenative coupling of primary alcohols in the presence of ruthenium

and osmium PNP complexes (Ru: **40a-b**, **41** and **36**; Os: **46a-b**, **47a-b** and **48**) (Scheme 1.20)[72-74, 76]. Upon reaction with a base, the hydridochloro metal complexes (M = Ru: **40b**, **36**; M = Os: **47b**, **48**) release HCl to give the insaturated amido metal complex **A**. Complex **A** is then protonated by an alcohol molecule at the nitrogen atom of the ligand to give a cationic complex $[MH(CO)(PNHP)]^+$ **B** connected to an alkoxide ion RO^- via an O···H-N hydrogen bond and an agnostic C-H···M interaction. For ruthenium, this species is in equilibrium with an alkoxyruthenium complex **B'**. Such complex was isolated and fully characterised from the reaction of **40b** with *t*BuOK and iso-propanol (Scheme 1.21)[72]. In solution, **B'** exists in equilibrium with the dehydrogenation product, *i.e.* acetone, and the dihydride metal complex **40a**. From complex **B**, the hydride is transferred to the metal to give the aldehyde product and the metal dihydride $\mathbf{MH_2}$ (M = Ru: **40a**; M = Os: **47a**). Hydrogen is extruded from the dihydride complex following two steps involving an intermediate dihydrogen complex **C.** The highest activation energy was found for the formation of the dihydrogen complex **C** via $\mathbf{TS_{MH2/C}}$, $\Delta G^{\neq}$ = 30.9 and 29.2 kcal mol^{-1} for osmium and ruthenium respectively. DFT study on the dehydrogenation of ethanol with complex **40a** carried by Yang also found this step being rate determining with a calculated activation energy $\Delta G^{\neq}$ = 29.4 kcal mol^{-1}[77]. However, assistance of an alcohol molecule for the formation of the dihydrogen complex **C** was found to decrease the energy barrier to $\Delta G^{\neq}$ = 22.8 kcal mol^{-1} (Scheme 1.22). Similar observations have been made by Schneider both experimentally and theoretically for the dehydrogenation of the related complex $[RuH_2(PMe_3)(iPr_2PCH_2CH_2)_2NH)]$ to the unsaturated amido complex $[RuH(PMe_3)(iPr_2PCH_2CH_2)_2N)]$ assisted by a water molecule[78].

For PNN ruthenium and osmium complexes, no reaction mechanism was suggested by the team of Gusev. However, for the reverse reaction, the hydrogenation of esters, they suggested that both outer-sphere and inner-sphere mechanism, with amine arm decoordination, could be operative[74].

For SNS ruthenium complex, two complexes could be isolated following conditions similar to ethanol dehydrogenation reaction (Scheme 1.23)[75]. When complex **45** was refluxed in ethanol in the presence of EtONa, a hydridoethoxy ruthenium SNS complex **45-H-OEt** hydrogen-bonded to an ethanol molecule was isolated after 1 h of reaction. Upon heating, complex **45-H-OEt** transformed into the dihydride ruthenium complex **45-*fac*-H_2** and ethyl acetate. Such reactivity suggests an inner-sphere mechanism involving the dihydride ruthenium complex **45-*fac*-H_2** similar to the dihydride ruthenium and osmium complexes **40a** and **47a** involved in the dehydrogenative coupling of alcohols (Scheme 1.20).

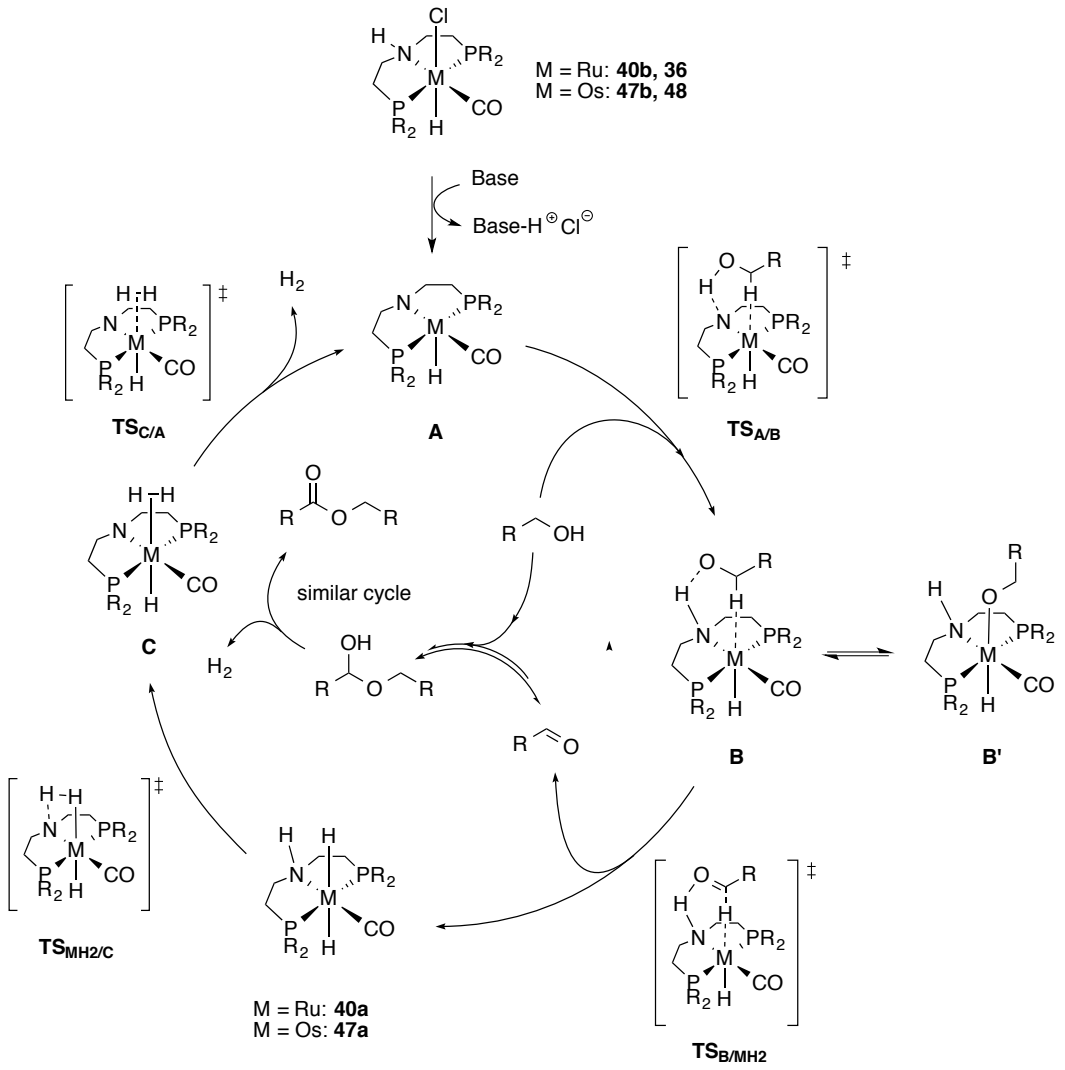

Scheme 1.20 *Catalytic cycle for Gusev's catalysts.*

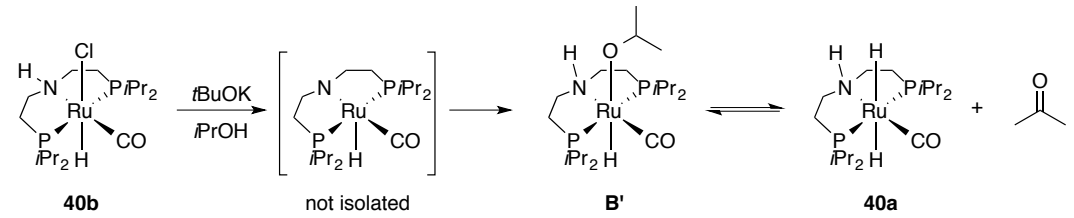

Scheme 1.21 *Isolation of complex **40a/B'**.*

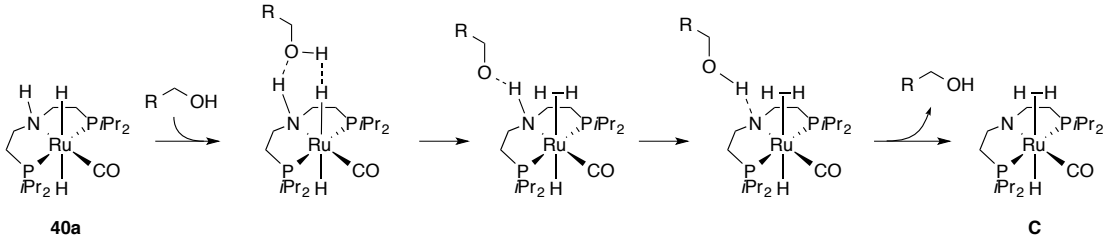

Scheme 1.22 *Alcohol assistance for hydrogen extrusion from **40a**.*

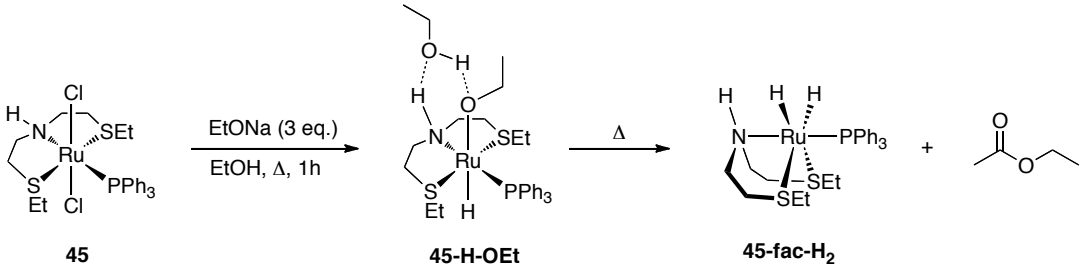

Scheme 1.23 *Reactivity of Gusev's Ru-SNS catalyst **45**.*

1.4.4 Beller's group work

Beller *et al* reported the use of a series of *in situ* formed catalysts[61] and commercially available ruthenium complexes for the dehydrogenative coupling of ethanol[79].

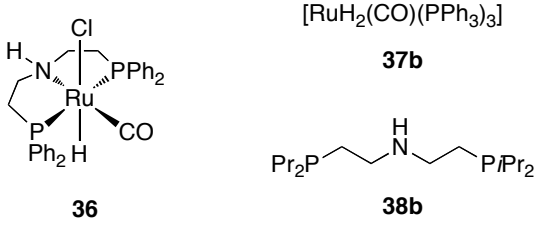

Fig. 1.19 *Structures of catalysts used by Beller et al.*

Table 1.11 *Dehydrogenative coupling of ethanol by Beller.*

entry	cata. (ppm)	base (mol %)	time (h) yield (%)			time (h) TOF (h^{-1})			TON max (time)	ref
1	**37b/38b** (3.1)	/	2 0.9	6 1.3		2 1483	6 690		4140 (6h)	[61]
2	**36** (500)	EtONa (1.3)	2 49.8	6 81		2 498	6 270		1620 (6h)	[79]
3	**36** (50)	EtONa (0.6)	2 9.3	10 36.5	46 77	2 934	10 730	46 335	15400 (46 h)	[79]

For the *in situ* formed catalyst (catalyst **37b** + **38b** in Fig. 1.19), the catalytic tests were performed under base-free and solvent-free conditions using ethanol as substrate with an extremely low catalyst loading, *i.e.* 3.1 ppm (Table 1.11, entry 1). A turnover frequency as high as 1483 h^{-1} is observed after 2 hours of reaction time, but it decreases to 690 h^{-1} after 6 h, indicating that catalyst deactivation is occuring. It should be noted that while the reaction rates are relatively high, the corresponding yields are extremely low with 0.9 % after 2 h and 1.3 % after 6 h. The isolated complex **36** was used in the presence of a base at two different catalyst loading, 50 and 500 ppm (Table 1.11, entries 2 and 3). Thus, using 1.3 mol % NaOEt, ethyl acetate is obtained in 81 % yield after 6 hours in the presence of 500 ppm catalyst making this system a productive catalyst. When decreasing the catalyst loading to 50 ppm, 77 % of ethyl acetate was obtained after 46 h of reaction that corresponds to a total TON of 15400. As already pointed out by Gusev (see 1.4.3), one can note that upon decrease of the catalyst loading from 500 to 50 ppm, the TOF increases from 498 to 934 h^{-1} (Table 1.11, entries 2 and 3). Both Beller and Gusev's teams used catalyst **36** for the dehydrogenative coupling of ethanol in the presence of EtONa as a base. Using almost identical reaction conditions, *i.e.* 50 ppm catalyst and EtONa 0.6 and 1 mol %, both teams report rather different results, with 77 % yield after 46 h for Beller and 42 % yield after 40 h for Gusev (Table 1.11, entry 3 and Table 1.10, entry 6). Such discrepancy in the reported catalyst performances raises the question of the catalyst robustness and test reproducibility.

The authors proposed a catalytic cycle similar to the one described for the dehydrogenation of alcohol (Scheme 1.18). For *in situ* formed catalyst **37b+38b**, first the dihydride complex **A** is formed by ligands exchange (Scheme 1.24). Upon heating, the unsaturated 16 e^- amido complex **B** is formed as a result of a hydrogen molecule released from **A**. Complex **B** can also be formed by release of HCl from complex **36** by reaction with a base. Next, the dehydrogenation of alcohol takes place to give the aldehyde product and regenerate the dihydride complex **A**. The author suggested that the dehydrogenation step occurs through an outer-sphere mechanism. Condensation of the aldehyde with the alcohol yields a hemiacetal that is dehydrogenated following the same mechanism to produce the final ester product.

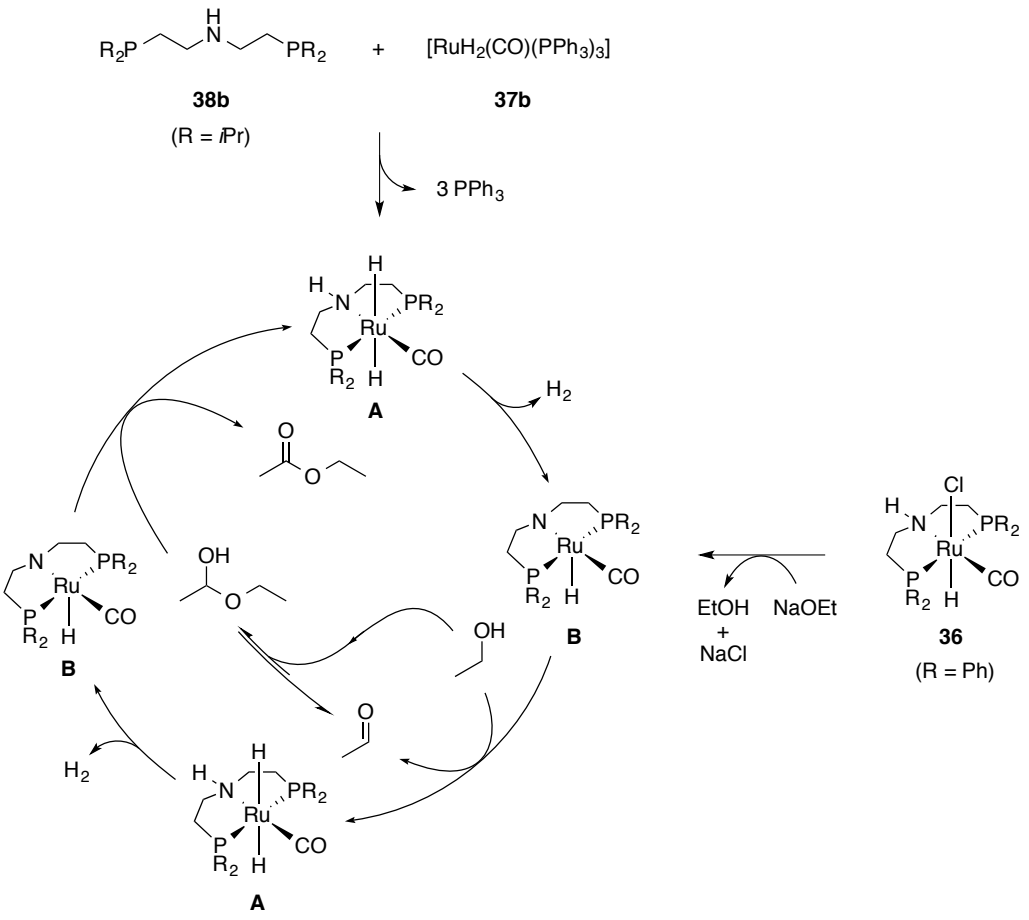

Scheme 1.24 *Proposed catalytic cycle for the dehydrogenative coupling of ethanol catalysed by **37b/38b** and **36**.*

1.4.5 Conclusion: unsolved challenges in this process

Ethanol is largely produced from biomass fermentation but until now most of it is directly used as biofuel. As a promising valorization route, catalytic transformation of ethanol has attracted more and more attention in the past decades. Among all transformation routes, several reactions share the dehydrogenation of alcohol to aldehyde as the activation step, as for instance the acceptorless dehydrogenative coupling of alcohols.

However, primary alcohols are much more difficult substrates for dehydrogenation than other types of alcohols (such as benzyl alcohol and secondary alcohols). Moreover, due to its low boiling point, ethanol represents one of the most challenging substrates among all the primary alcohols. Bases and organic solvents are largely used to assist the catalytic system in this transformation, which leads to waste and separation problems between the solvent and the desired product.

Although many catalytic systems for primary alcohols dehydrogenation have been established in last decade. In a few cases high yields to ethyl acetate have been obtained[73-75, 79], nevertheless, in many cases an organic solvent is used and in all these cases the base is an essential factor. The ideal catalyst should work in a base-free and solvent-free condition, in which no waste would be produced.

Based on these analyses, it can be seen that a well-defined catalytic system that can be used for high yield ethanol dehydrogenation under ideally base-free and solvent-free conditions is then still highly expected. Up to now, this remains an unsolved and challenging area.

1.5 Acceptorless dehydrogenation of alcohols to corresponding acid salts

1.5.1 State-of-the-art catalysts

Another way of transforming primary alcohol to high value added products is to oxidize them to the corresponding carboxylic acids. Traditionally, the transformation of alcohols to corresponding acids is performed using stoichiometric oxidants and chlorinated solvents[80]. Nowadays, 40 % of all catalytic oxidations to carboxylic

acids are carried out by a two-step procedure via the aldehyde. This made Fernandez and Tojo come to the conclusion that "the transformation of primary alcohols to carboxylic acids is undoubtedly not a mature technology"[81].

Lately, Grützmacher presented a rhodium catalyst system for alcohol oxidation to the corresponding acid salt under mild conditions using a sacrificial hydrogen acceptor in high pH conditions[82-84]. Nevertheless, the use of sacrificial substrates may limit the applications of this catalytic system.

In 2013, Milstein *et al* reported a new catalytic transformation route for the oxidation of primary alcohols to carboxylic acid salts[85]. In this system, water is used as the oxygen source and it constitutes "the first example of homogeneously catalysed transformation of alcohols to carboxylic acids using no oxidant or hydrogen acceptor, with liberation of hydrogen gas." (Scheme 1.25)

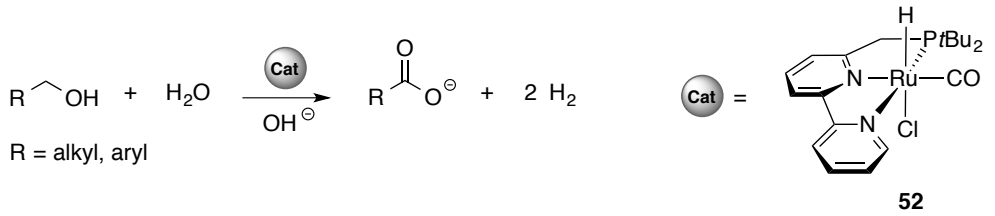

Scheme 1.25 *Milstein's catalyst **52**.*

For this system, the reaction network is believed to follow a dehydrogenative coupling sequence. The alcohol is dehydrogenated to give an aldehyde that reacts with water to give a hydrate that is finally dehydrogenated to give the carboxylic acid product, which is deprotonated in the basic reaction media (Scheme 1.26).

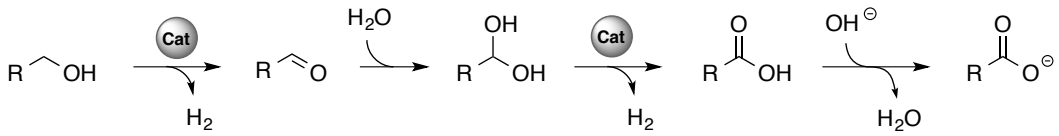

Scheme 1.26 *Proposed mechanism for Milstein's catalyst **52**.*

For this transformation, Milstein reported the high activity of the ruthenium aromatic PNN pincer complex **52**. Using this complex at moderate loading (0.2

mol %) with a slight excess of sodium hydroxide (1.1 equivalent) in water, butanol could be oxidised to the corresponding carboxylic acid salt and hydrogen with 84 % yield after 18 h of reflux. Using complex **52**, the scope of this transformation was extended to a wide variety of functionalize primary alcohols.

Based on reaction intermediate characterization and DFT calculations, the authors proposed an inner-sphere mechanism relying on aromatisation – dearomatisation of the ruthenium PNN pincer complex (Scheme 1.27). In the basic reaction media, complex **52** is transformed into the dearomatized amido complex **53** by HCl elimination. Complex **53** is rearomatized upon addition of water to give the hydroxycomplex **A**. Alkoxy complex **B** is then formed by alcohol exchange with the hydroxy ligand. Alternatively, complex **B** may arise from direct addition of the alcohol onto **53**, albeit alcohol concentration is lower than water concentration in the media. An hydrogen transfer from the ligand arm leads to the dearomatized dihydrogen complex **C,** which releases hydrogen to give the unsaturated dearomatized alkoxy complex **D**. β-hydride elimination from the alkoxy ligand in complex **D** leads to dearomatized complex **E** with an associated aldehyde. Addition of water to complex **E** leads to complex rearomatization and turn the aldehyde into a hydrate bonded to the metal in complex **F**. The carboxylic acid product is generated by loss of H_2 from **F** which regenerates complex **53**. According to the authors, the base is believed to trap the carboxylic acid and hence avoid its addition onto complex **53** which produce inactive ruthenium carboxylate complexes.

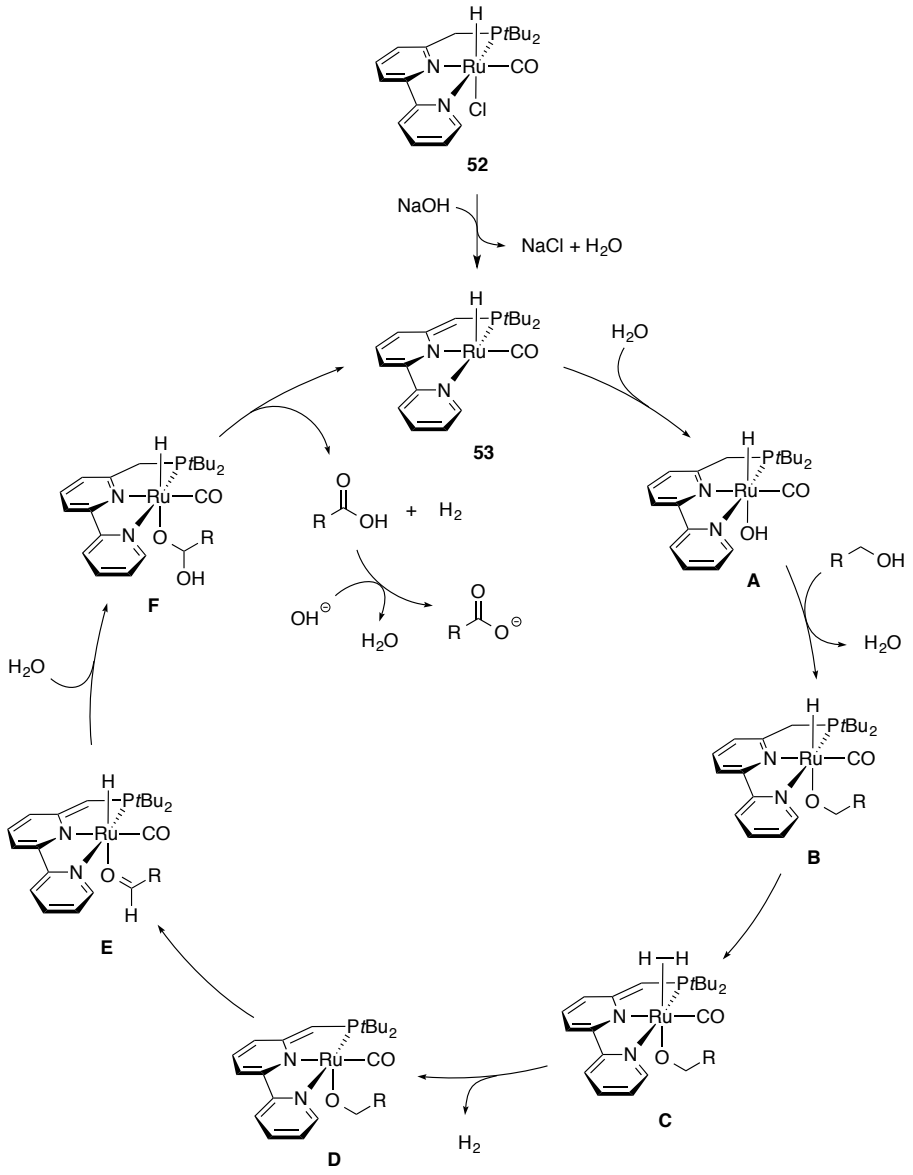

Scheme 1.27 *Proposed mechanism for formation of carboxylate from alcohol.*

1.5.2 Conclusion: unsolved challenges in this process

Compared with the traditional oxidation reactions, the acceptorless dehydrogenative transformation of primary alcohols to corresponding acid salts represents an attractive new technology. The sole byproduct, hydrogen gas, is a valuable in itself and the reaction can be conducted in water avoiding the need for organic solvents.

Today, Milstein's complex **52** is the only reported catalyst for this transformation. While high yield can be obtained with this complex, the reaction rate is rather low

(calculated TOF for butanol: 23.3 h^{-1}), and, as mentioned by the authors, complex **52** is oxygen sensitive, "resulting in decomposition and thus lower conversions".

Therefore, in order to improve the attractiveness of the the acceptorless dehydrogenative transformation of primary alcohols to corresponding acid salts, further development aiming at improvement of the catalytic activity and catalyst robustness is highly desirable.

1.6 Selective deuteration of alcohols

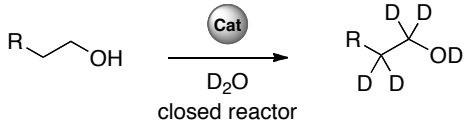

Scheme 1.28 *Selective deuteration of alcohols.*

Selective deuteration of alcohols can be used for the synthesis of deuterated pharmaceuticals and other biologically active compounds[86]. The deuterated alcohols find applications in biochemical enzymatic rate studies and in new materials R&D[86].

However, even recently, the desired labelled alcohols are still being produced from reaction of esters or aldehydes with alkali metal deuteride salts[87]. On the other hand, the original source of deuterium, deuterium oxide, remains inexpensive. Up to now, only a little attention has been paid to direct selective deuteration of alcohols. In 2003, Yamada *et al* disclosed a cobalt catalyst that could reduce aldehydes with $NaBD_4$, leading to enantioselective deuteration[88]. Baratta reported an homogeneous catalytic system using osmium or ruthenium pincer complexes that works efficiently in the presence of deuterated isopropyl alcohol as solvent[89]. In 2011, Jia used a catalytic system composed of [(*p*-cymene)$RuCl_2$], ethanolamine and KOH for deuteration of alcohol at the β position of the substrate[90].

In 2013, Milstein developed a simple catalytic system for the selective deuteration of alcohols, using inexpensive deuterium oxide as deuterium source[91]. The author reported a highly efficient system for selective deuteration of α and β positions of primary and secondary alcohols using catalysts **52** and **53**. Both catalysts

were tested under different sets of conditions using 1-hexanol as the model substrate (Table 1.12).

Table 1.12 *Selective deuteration of 1-hexanol*[‡][91].

entry	cata. (mol %)	base (mol)	deuteration yield (%) α; β
1	**53** (1.0)	/	0; 0
2	**53** (10.0)	/	80; 0
3	**52** (0.2)	NaOH (110)	94; 20
4	**52** (0.2)	NaOH (10)	78; 0
5	**52** (0.2)	NaOH (300)	94; 14
6	/	NaOH (110)	0; 0
7	**52** (0.2)	NaOH (20)	92; 10
8[†]	**52** (0.1)	NaOH (20)	90; 10

[‡] *n* (1-hexanol): 0.5 mmol; *V* (D_2O): 0.4 mL; 120 °C; 24 h under argon; closed system.

[†] under air.

Without catalyst, no deuteration products were observed (Table 1.12, entry 6). Catalyst **53** allowed to obtain 80 % of α-deuterated 1-hexanol under base-free conditions providing that a rather large catalyst loading was used (Table 1.12, entry 1 vs. 2). With catalyst **52** at lower loading, *i.e.* 0.2 mol %, and NaOH in substoechiometric amount, *i.e.* 20 mol %, the best compromise between productivity and selectivity was found, with yields of 92 % and 10 % for the α and β positions respectively (Table 1.12, entry 7). According to the authors, the presence of deuterium in the β position is not deleterious for most application.

For catalyst **52**, Milstein proposed that under basic conditions, a monohydride PNN-Ru complex **53** could be formed by release of HCl from **52** (Scheme 1.29). Addition of D_2O on complex **53** led to complex **A**, which released OHD and results in complex **B**. After further isomerizations, complex **C** and **D** were generated. Repeating the sequence of **53** to **D**, complex **D** transformed into complex **E** (Scheme 1.29).

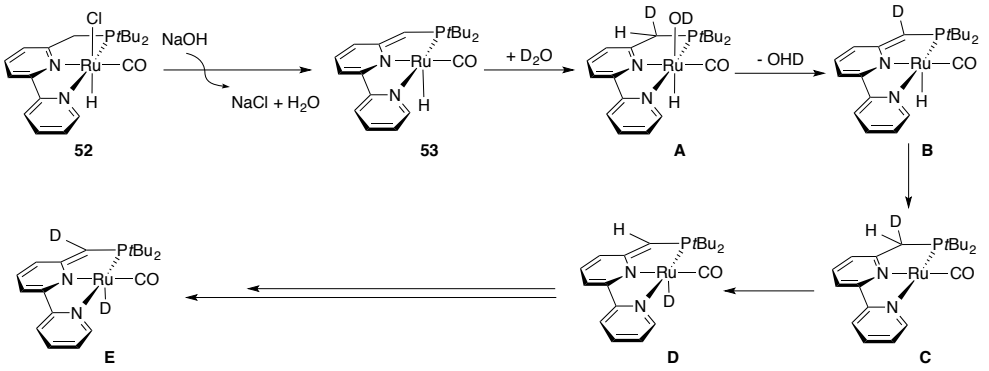

Scheme 1.29 *Formation of complex **E** from catalyst **52**.*

The authors further proposed the catalytic cycle represented on Scheme 1.30. The key step is the coordinated aldehyde formation and its addition to D_2 (complex **G** to **J**). The formation of CD_2 from CHD at α position proceed via identical mechanism but starting with an already partially α-deuterated alcohol.

Since it involves the temporary transformation of the alcohol to a carbonyl species (complex **E** to **H**), the selective deuteration of alcohols could also be viewed as a reaction based on dehydrogenative activation.

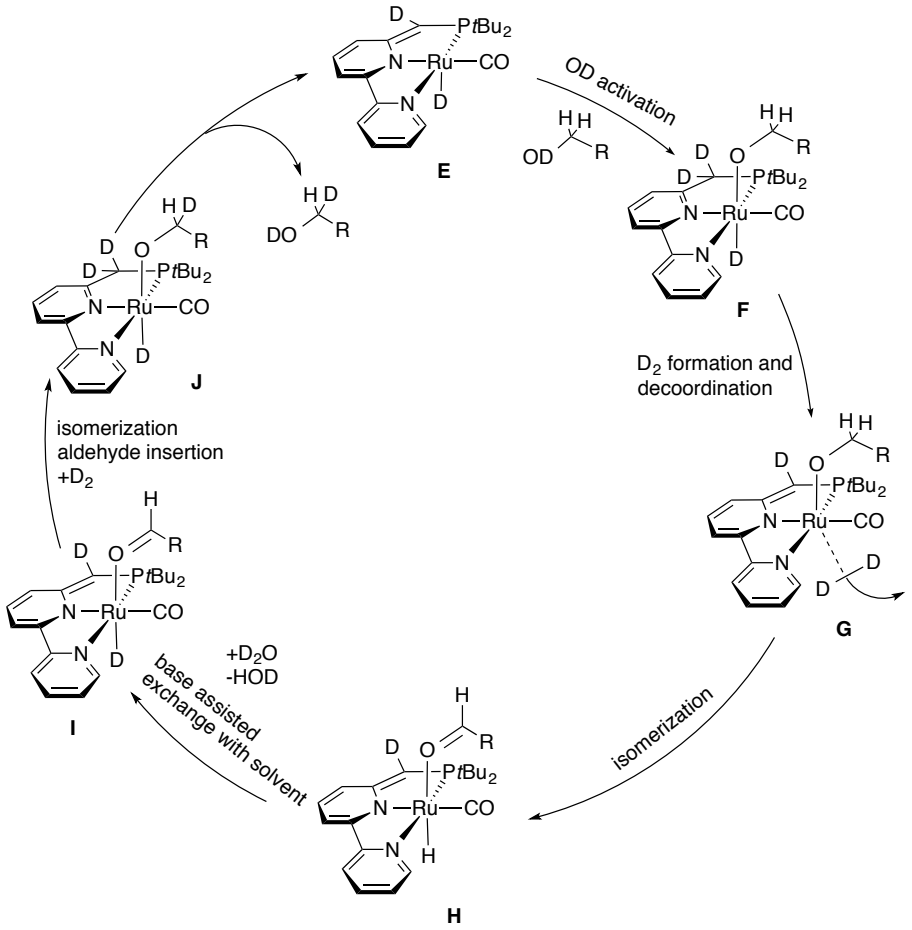

Scheme 1.30 *Proposed catalytic cycle for selective deuteration of alcohols with complexes **52** and **53**.*

1.7 Objective of the present thesis

In summary, catalytic transformations of alcohols by dehydrogenative activation are highly desirable routes to produce esters, acids, *etc*. The sole byproduct, molecular hydrogen is valuable in itself.

Catalysts for efficient ethanol dehydrogenation to ethyl acetate have been reported in the literature simultaneously to the work disclosed in the present thesis. However, all reported catalysts require addition of a base.

Catalytic transformation of alcohols to corresponding carboxylic acid salts and hydrogen has been reported, but the described catalyst is oxygen sensitive and has a rather low catalytic activity.

Hence, the objective of the present thesis is to develop highly active catalysts for alcohol dehydrogenation to produce esters under neat and neutral conditions, targeting ethanol as the most challenging substrate. In parallel we aim at developing oxygen stable and highly active catalysts for transformation of alcohols to corresponding carboxylic acid salts and hydrogen. As another reaction based on dehydrogenative activation, selective deuteration catalysed with highly efficient catalysts, is also set as a target reaction.

Ruthenium pincer complexes having non-innocent ligand have shown their potential in catalytic transformations of alcohols by dehydrogenative activation.

Herein in the present thesis, a series of PNP ruthenium pincer complexes are therefore investigated for alcohols dehydrogenation to produce esters, transformation of alcohols to corresponding carboxylic acid salts and hydrogen and selective deuteration of alcohols. Several reaction parameters were comprehensively analysed and structure-activity relationship have been investigated.

1.8 Outline of the present thesis

The present thesis is constituted of 5 chapters. In the first introduction chapter, the background of the present work is introduced. Based on the analysis of reported work, the unsolved challenges are pointed out.

The second chapter describes the experimental methods and procedures as well as the calculations used.

In Chapter 3, we report on the acceptorless dehydrogenative coupling of primary alcohols. For this transformation, two types of catalysts (*in situ* and isolated) are tested. The influence of reaction time, temperature and catalyst loading are investigated; different primary alcohols are used as substrates, in most cases, 1-butanol is employed as a model substrate. Finally ethanol dehydrogenation is investigated under neat and neutral conditions.

Chapter 4 is devoted to the acceptorless dehydrogenation of alcohols to corresponding acid salts. Two types of catalysts (*in situ* and isolated) are tested for this transformation. The influence of reaction time and catalyst loading are investigated; catalysts stability under air and catalyst recycling are also studied. In addition, the use of the developed catalysts for the selective deuteration of alcohol is reported.

In the final chapter, a general discussion based on all the reported results is made and perspectives for the present work are given.

1.9 References

[1] REN21, *Renewables 2013 Global Status Report*, http://www.ren21.net/REN21Activities/GlobalStatusReport.aspx.

[2] P. Y. Dapsens, C. Mondelli, J. Pérez-Ramírez, *ACS Catal.* **2012**, *2*, 1487-1499.

[3] *Biomass Energy Centre*, http://www.biomassenergycentre.org.uk.

[4] *Archaeological Wood, Vol. 225*, American Chemical Society, **1989**.

[5] D. M. Teegarden, *Polymer Chemistry: Introduction to an Indispensable Science*, NSTA Press, National Science Teachers Association, **2004**.

[6] M. Pauly, K. Keegstra, *Plant J.* **2008**, *54*, 559-568.

[7] J. I. Qazi, N. Chaudhary, S. S. Mirza, in *Biofuel Production-Recent Developments and Prospects*, **2011**, pp. 247-292.

[8] J. Shokri, K. Adibkia, in *Cellulose - Medical, Pharmaceutical and Electronic Applications*, **2013**, pp. 47-66.

[9] F. D. Marques-Marinho, C. D. Vianna-Soares, in *Cellulose - Medical, Pharmaceutical and Electronic Applications*, **2013**, pp. 141-162.

[10] A. Baptista, I. Ferreira, J. Borges, in *Cellulose - Medical, Pharmaceutical and Electronic Applications*, **2013**, pp. 1-18.

[11] S. Wang, Y. Yu, in *Cellulose - Medical, Pharmaceutical and Electronic Applications*, **2013**, pp. 195-214.

[12] D. S. Hon, *Cellulose* **1994**, *1*, 1-25.

[13] J. M. Moran-Mirabal, in *Cellulose - Fundamental Aspects*, **2013**, pp. 1-44.

[14] E. M. Rubin, *Nature* **2008**, *454*, 841-845.

[15] T. Werpy, G. Petersen, in *Top Value Added Chemicals from Biomass: Volume I -- Results of Screening for Potential Candidates from Sugars and Synthesis Gas*, National Renewable Energy Lab., Golden, CO (US), **2004**.

[16] J. E. Holladay, J. F. White, J. J. Bozell, D. Johnson, in *Top Value-Added Chemicals from Biomass - Volume II—Results of Screening for Potential Candidates from Biorefinery Lignin*, Pacific Northwest National Laboratory (PNNL), Richland, WA (US), **2007**.

[17] J. J. Bozell, G. R. Petersen, *Green Chem.* **2010**, *12*, 539-554.

[18] A. Stark, *Energy Environ. Sci.* **2011**, *4*, 19-32.

[19] M. Ni, D. Y. C. Leung, M. K. H. Leung, K. Sumathy, *Fuel Process. Technol.* **2006**, *87*, 461-472.

[20] K. Nakashima, K. Yamaguchi, N. Taniguchi, S. Arai, R. Yamada, S. Katahira, N. Ishida, H. Takahashi, C. Ogino, A. Kondo, *Green Chem.* **2011**, *13*, 2948-2953.

[21] G. Jurgens, S. Survase, O. Berezina, E. Sklavounos, J. Linnekoski, A. Kurkijärvi, M. Väkevä, A. van Heiningen, T. Granström, *Biotechnol. Lett* **2012**, *34*, 1415-1434.

[22] K. p. Michael, N. Steffi, D. r. Peter, in *Biofuel Production-Recent Developments and Prospects*, **2011**, pp. 451-486.

[23] S. B. Bankar, S. A. Survase, H. Ojamo, T. Granstrom, *RSC Adv.* **2013**, *3*, 24734-24757.

[24] G. Reuss, W. Disteldorf, A. O. Gamer, A. Hilt, in *Ullmann's Encyclopedia of Industrial Chemistry*, Wiley-VCH Verlag GmbH & Co. KGaA, **2000**.

[25] C. Parmeggiani, F. Cardona, *Green Chem.* **2012**, *14*, 547-564.

[26] K. Yamaguchi, K. Mori, T. Mizugaki, K. Ebitani, K. Kaneda, *J. Am. Chem. Soc.* **2000**, *122*, 7144-7145.

[27] M. S. Sigman, D. R. Jensen, *Acc. Chem. Res.* **2006**, *39*, 221-229.

[28] C. Gunanathan, D. Milstein, *Science* **2013**, *341*.

[29] C. Gunanathan, D. Milstein, *Acc. Chem. Res.* **2011**, *44*, 588-602.

[30] M. H. S. A. Hamid, P. A. Slatford, J. M. J. Williams, *Adv. Synth. Catal.* **2007**, *349*, 1555-1575.

[31] D. Morton, D. J. Cole-Hamilton, *J. Chem. Soc., Chem. Commun.* **1987**, 248-249.

[32] D. Morton, D. J. Cole-Hamilton, I. D. Utuk, M. Paneque-Sosa, M. Lopez-Poveda, *J. Chem. Soc., Dalton Trans.* **1989**, 489-495.

[33] D. Morton, D. J. Cole-Hamilton, *J. Chem. Soc., Chem. Commun.* **1988**, 1154-1156.

[34] L.-C. Yang, T. Ishida, T. Yamakawa, S. Shinoda, *J. Mol. Catal. A: Chem.* **1996**, *108*, 87-93.

[35] Y. Takano, M. Á. Herranz, N. Martín, S. G. Radhakrishnan, D. M. Guldi, T. Tsuchiya, S. Nagase, T. Akasaka, *J. Am. Chem. Soc.* **2010**, *132*, 8048-8055.

[36] A. J. Johansson, E. Zuidema, C. Bolm, *Chem. Eur. J.* **2010**, *16*, 13487-13499.

[37] N. Sieffert, R. Réocreux, P. Lorusso, D. J. Cole-Hamilton, M. Bühl, *Chem. Eur. J.* **2014**, *20*, 4141-4155.

[38] T. Matsubara, Y. Saito, *J. Mol. Catal.* **1994**, *92*, 1-8.

[39] G. R. A. Adair, J. M. J. Williams, *Tetrahedron Lett.* **2005**, *46*, 8233-8235.

[40] H. Junge, M. Beller, *Tetrahedron Lett.* **2005**, *46*, 1031-1034.

[41] H. Junge, B. Loges, M. Beller, *Chem. Commun.* **2007**, 522-524.

[42] A. Dobson, S. D. Robinson, *Inorg. Chem.* **1977**, *16*, 137-142.

[43] A. Dobscn, S. D. Robinson, *J. Organomet. Chem.* **1975**, *87*, C52-C53.

[44] C. W. Jung, P. E. Garrou, *Organometallics* **1982**, *1*, 658-666.

[45] G. B. W. L. Ligthart, R. H. Meijer, M. P. J. Donners, J. Meuldijk, J. A. J. M. Vekemans, L. A. Hulshof, *Tetrahedron Lett.* **2003**, *44*, 1507-1509.

[46] J. van Buijtenen, J. Meuldijk, J. A. J. M. Vekemans, L. A. Hulshof, H. Kooijman, A. L. Spek, *Organometallics* **2006**, *25*, 873-881.

[47] Y. Shvo, D. Czarkie, Y. Rahamim, D. F. Chodosh, *J. Am. Chem. Soc.* **1986**, *108*, 7400-7402.

[48] B. L. Conley, M. K. Pennington-Boggio, E. Boz, T. J. Williams, *Chem. Rev.* **2010**, *110*, 2294-2312.

[49] Y. Blum, Y. Shvo, *J. Organomet. Chem.* **1985**, *282*, C7-C10.

[50] J. H. Choi, N. Kim, Y. J. Shin, J. H. Park, J. Park, *Tetrahedron Lett.* **2004**, *45*, 4607-4610.

[51] K.-i. Fujita, N. Tanino, R. Yamaguchi, *Org. Lett.* **2006**, *9*, 109-111.

[52] K.-i. Fujita, T. Yoshida, Y. Imori, R. Yamaguchi, *Org. Lett.* **2011**, *13*, 2278-2281.

[53] R. Kawahara, K.-i. Fujita, R. Yamaguchi, *J. Am. Chem. Soc.* **2012**, *134*, 3643-3646.

[54] R. Kawahara, K.-i. Fujita, R. Yamaguchi, *Angew. Chem. Int. Ed.* **2012**, *51*, 12790-12794.

[55] G. Zeng, S. Sakaki, K.-i. Fujita, H. Sano, R. Yamaguchi, *ACS Catal.* **2014**, *4*, 1010-1020.

[56] S. Musa, I. Shaposhnikov, S. Cohen, D. Gelman, *Angew. Chem. Int. Ed.* **2011**, *50*, 3533-3537.

[57] K. Oded, S. Musa, D. Gelman, J. Blum, *Catal. Commun.* **2012**, *20*, 68-70.

[58] D. Milstein, *Top. Catal.* **2010**, *53*, 915-923.

[59] C. Gunanathan, D. Milstein, in *Bifunctional Molecular Catalysis, Vol. 37* (Eds.: T. Ikariya, M. Shibasaki), Springer Berlin Heidelberg, **2011**, pp. 55-84.

[60] J. Zhang, M. Gandelman, L. J. W. Shimon, H. Rozenberg, D. Milstein, *Organometallics* **2004**, *23*, 4026-4033.

[61] M. Nielsen, A. Kammer, D. Cozzula, H. Junge, S. Gladiali, M. Beller, *Angew. Chem. Int. Ed.* **2011**, *50*, 9593-9597.

[62] Y. Blum, D. Reshef, Y. Shvo, *Tetrahedron Lett.* **1981**, *22*, 1541-1544.

[63] Y. Blum, Y. Shvo, *J. Organomet. Chem.* **1984**, *263*, 93-107.

[64] S. Murahashi, T. Naota, K. Ito, Y. Maeda, H. Taki, *J. Org. Chem.* **1987**, *52*, 4319-4327.

[65] J. Zhang, G. Leitus, Y. Ben-David, D. Milstein, *J. Am. Chem. Soc.* **2005**, *127*, 10840-10841.

[66] J. Zhang, M. Gandelman, L. J. W. Shimon, D. Milstein, *Dalton. Trans.* **2007**, 107-113.

[67] C. Gunanathan, L. J. W. Shimon, D. Milstein, *J. Am. Chem. Soc.* **2009**, *131*, 3146-3147.

[68] J. Zhang, E. Balaraman, G. Leitus, D. Milstein, *Organometallics* **2011**, *30*, 5716-5724.

[69] M. H. G. Prechtl, K. Wobser, N. Theyssen, Y. Ben-David, D. Milstein, W. Leitner, *Catal. Sci. Technol.* **2012**, *2*, 2039-2042.

[70] E. Fogler, M. A. Iron, J. Zhang, Y. Ben-David, Y. Diskin−Posner, G. Leitus, L. J. W. Shimon, D. Milstein, *Inorg. Chem.* **2013**, *52*, 11469-11479.

[71] R. Langer, I. Fuchs, M. Vogt, E. Balaraman, Y. Diskin-Posner, L. J. W. Shimon, Y. Ben-David, D. Milstein, *Chem. Eur. J.* **2013**, *19*, 3407-3414.

[72] M. Bertoli, A. Choualeb, A. J. Lough, B. Moore, D. Spasyuk, D. G. Gusev, *Organometallics* **2011**, *30*, 3479-3482.

[73] D. Spasyuk, D. G. Gusev, *Organometallics* **2012**, *31*, 5239-5242.

[74] D. Spasyuk, S. Smith, D. G. Gusev, *Angew. Chem. Int. Ed.* **2012**, *51*, 2772-2775.

[75] D. Spasyuk, S. Smith, D. G. Gusev, *Angew. Chem. Int. Ed.* **2013**, *52*, 2538-2542.

[76] M. Bertoli, A. Choualeb, D. G. Gusev, A. J. Lough, Q. Major, B. Moore, *Dalton. Trans.* **2011**, *40*, 8941-8949.

[77] X. Yang, *ACS Catal.* **2013**, *3*, 2684-2688.

[78] A. Friedrich, M. Drees, J. Schmedt auf der GuÃànne, S. Schneider, *J. Am. Chem. Soc.* **2009**, *131*, 17552-17553.

[79] M. Nielsen, H. Junge, A. Kammer, M. Beller, *Angew. Chem. Int. Ed.* **2012**, *51*, 5711-5713.

[80] R. A. Sheldon, *Chem. Soc. Rev.* **2012**, *41*, 1437-1451.

[81] G. Tojo, M. Fernandez, *Oxidation of Primary Alcohols to Carboxylic Acids: A Guide to Current Common Practice*, Springer, **2007**.

[82] T. Zweifel, J.-V. Naubron, H. Grützmacher, *Angew. Chem. Int. Ed.* **2009**, *48*, 559-563.

[83] S. Annen, T. Zweifel, F. Ricatto, H. Grützmacher, *ChemCatChem* **2010**, *2*, 1286-1295.

[84] M. Trincado, H. Grützmacher, F. Vizza, C. Bianchini, *Chem. Eur. J.* **2010**, *16*, 2751-2757.

[85] E. Balaraman, E. Khaskin, G. Leitus, D. Milstein, *Nat. Chem.* **2013**, *5*, 122-125.

[86] J. Atzrodt, V. Derdau, T. Fey, J. Zimmermann, *Angew. Chem. Int. Ed.* **2007**, *46*, 7744-7765.

[87] Q. Wang, X. Sheng, J. H. Horner, M. Newcomb, *J. Am. Chem. Soc.* **2009**, *131*, 10629-10636.

[88] D. Miyazaki, K. Nomura, H. Ichihara, Y. Ohtsuka, T. Ikeno, T. Yamada, *New J. Chem.* **2003**, *27*, 1164-1166.

[89] G. Bossi, E. Putignano, P. Rigo, W. Baratta, *Dalton. Trans.* **2011**, *40*, 8986-8995.

[90] S. K. S. Tse, P. Xue, C. W. S. Lau, H. H. Y. Sung, I. D. Williams, G. Jia, *Chem. Eur. J.* **2011**, *17*, 13918-13925.

[91] E. Khaskin, D. Milstein, *ACS Catal.* **2013**, 448-452.

Chapter 2 Experimental

2.1 General information

All experiments were carried out under argon atmosphere using a glovebox or a vacuum line using standard Schlenk techniques unless some special conditions were pointed out. All ruthenium complexes and tridentate ligands were stored under argon.

GC–FID/MS was carried out on Agilent 7890A (flame ionization detector and MS detector) instruments equipped with a Zebron ZB-Bioethanol column (30 m column length x 0.25 mm internal diameter x 1.00 μm film thickness) with helium as carrier gas.

All ^{1}H NMR or ^{31}P NMR spectra were recorded on a Bruker Avance 300 NMR spectrometer. ^{1}H NMR chemical shifts were reported in ppm (δ) downfield from tetramethylsilane, ^{31}P NMR chemical shifts were reported in ppm (δ) downfield from H_3PO_4 and referenced to an external 85 % solution of phosphoric acid in D_2O. Common abbreviations used in the NMR experiments were as follows: b, broad; s, singlet; d, doublet; t, triplet; q, quartet; sp, septet; m, multiplet; v, virtual.

2.2 Organic synthesis procedures

Gas: argon was purchased from Praxair (Argon 6.0).

Substrates and solvents: 1-butanol (Aldrich, 99.9 %), ethanol (Merck KGaA, 99.9 %), 1-pentanol (Aldrich, 99 %), 1-octanol (Aldrich, 99.9 %), 1-tetradecanol (Aldrich, 97 %), 2-methyl-1-butanol (Aldrich, 99.0 %), 2-ethyl-1-hexanol (Aldrich, 99.6 %), 2-propanol (Aldrich, 99.5 %), cyclohexanol (Fluka, 99.0 %), dimethylaminoethanol (Aldrich, 99.5 %), acetone (Verbièse, 99.5 %), dichloromethane (Verbièse, 99.8 %), ethyl acetate (Verbièse, 99.5 %), cyclohexane (Aldrich, 99.9 %). The substrates and solvents were dried by 20 wt. % 3Å molecular sieves, then degassed by argon flushing and stored under argon.

Deuterated chemicals: deuterium oxide (99.96 % D), chloroform-d (99.80 % D), were from Euriso-top and used without further purification. Dichloromethane-d_2 (Aldrich, 99.96 % D), tetrahydrofuran-d_8 (Euriso-top, 99.50 % D) and benzene-d_6 (Euriso-top, 99.50 % D) were degassed and stored in a glovebox.

Bases: sodium hydroxide (Aldrich, 98 %), sodium ethoxide (Fluka, 95 %) were used as recieved.

Ruthenium complexes: $[RuH(BH_4)(CO)((Ph_2PC_2H_4)_2NH)]$ (trade name: Ru-MACHO-BH, Strem chemicals, 98 %), $[RuHCl(CO)((Ph_2PC_2H_4)_2NH)]$ (trade name: Ru-MACHO, Strem chemicals, 98 %), carbonylhydrido[6-(di-*t*-butylphosphinomethylene)-2-(N,N-diethylaminomethyl)-1,6-dihydropyridine]ruthenium(II) (trade name: Milstein catalyst, Strem chemicals, 98 %), dichlorotriphenylphosphine[2-(diphenylphosphino)-N-(2-pyridinylmethyl)ethanamine] ruthenium(II) (Aldrich, 97 %), $[RuCl_2(PPh_3)((EtSC_2H_4)_2NH)]$ (Aldrich, 97 %), $[RuH_2(CO)(PPh_3)_3]$ (Strem chemicals, 99 %), $[RuH_2(PPh_3)_4]$ (Aldrich), $[RuCl_2(PPh_3)_4]$ (Aldrich), $[RuHCl(CO)(PPh_3)_3]$ (Aldrich), $[RuCl_2(p\text{-cymene})]_2$ (Strem chemicals, 98 %) were stored under argon and used as received.

Ligands: $(iPr_2PC_2H_4)_2NH$ (Strem chemicals, 97 %), $(Cy_2PC_2H_4)_2NH$ (Strem chemicals, 97 %), $(tBu_2PC_2H_4)_2NH$ (Aldrich, 10 wt. % in THF), $(Ph_2PC_2H_4)_2NH$ (Strem chemicals, 97 %) were stored under argon and used as received.

Reagents for syntheses: $NaBH_4$ (Fluka, 99 %), $NaHBEt_3$ (Aldrich, 1.0 M in toluene), PMe_3 (Aldrich, 1.0 M in THF) were used as received.

Other complexes were produced according to the following synthetic details:

(All the following complex synthesis were done by Dr. Guillaume Raffa)

2.2.1 $[RuHCl(CO)((R_2PC_2H_4)_2NH)]$ (R = *i*Pr, Cy, *t*Bu)

2.2.1.1 $[RuHCl(CO)((iPr_2PC_2H_4)_2NH)]$

Under argon, a suspension of [RuHCl(CO)(PPh_3)$_3$] (0.999 g, 1.04 mmol) and (iPr$_2$PC$_2$H$_4$)$_2$NH (0.357 g, 1.17 mmol) in diglyme (10 mL) was stirred magneticaly and heated at 165 °C for 1 h to give a clear yellow solution. The solution was left to cool down and let at room temperature for 18 h to give a precipitate. At 0 °C, pentane (10 mL) was added and the suspension was left standing for 1 h. The supernatant was carefully removed via a syringe, and the solid was washed with diethylether (3 x 5 mL) and finally dried under reduced pressure (1 x 10^{-3} mbar, RT) to give the product as a pale yellow powder (0.317 g, 64 % yield).

^{31}P NMR (^{1}H decoupled) (CD_2Cl_2, 121.5 MHz): δ. 74.7 ppm (^{1}H and ^{31}P NMR spectra in agreement with literature data, see: [1]).

2.2.1.2 [RuHCl(CO)(($Cy_2PC_2H_4)_2NH$)]

Under argon, a suspension of [RuHCl(CO)(PPh_3)$_3$] (1.000 g, 1.05 mmol) and ($Cy_2PC_2H_4)_2NH$ (0.498 g, 1.07 mmol) in diglyme (10 mL) was stirred magnetically and heated at 165 °C for 19 h. The suspension was left to cool down to room temperature and the supernatant was carefully removed via a syringe. The solid was washed with diethylether (3 x 5 mL) and finally dried under reduced pressure (1 x 10^{-3} mbar, RT) to give the product as a pale yellow powder (0.518 g, 78 % yield).

^{31}P NMR (^{1}H decoupled) (CD_2Cl_2, 121,5 MHz): δ. 65.6 ppm (^{1}H and ^{31}P NMR spectra in agreement with literature data, see:[2]).

2.2.1.3 [RuHCl(CO)((tBu$_2$PC$_2$H$_4$)$_2$NH)]

Under argon, a suspension of [RuHCl(CO)(PPh_3)$_3$] (200 mg, 0.210 mmol) and (tBu$_2$PC$_2$H$_4$)$_2$NH (10 wt % in THF; 0.230 mmol) was concentrated under reduced pressure giving a brownish powder. Then, diglyme (2 mL) was added and the suspension was stirred magnetically and heated at 165 ^{o}C for 1 h giving a yellow solution. The solution was left to cool down to room temperature to give a white precipitate. The supernatant was carefully removed via a syringe, and the solid was washed three times with diethylether (3 x 5 mL) and finally dried under reduced

pressure (1 x 10^{-3} mbar, RT) to give the product as a white powder (106.5 mg, yield: 96 %).

^{1}H NMR ($CDCl_3$, 400 MHz): δ (ppm). -16.02 (t; *J* = 19.7; 1H; Ru*H*; 18 % minor isomer); -21.9 (t; *J* = 18.6 Hz; 1H; Ru*H*; 82 % major isomer)

^{1}H NMR (^{31}P decoupled) ($CDCl_3$, 400 MHz): δ (ppm). 6.34 (*broad* s; 1H; N*H*); 3.43-3.40 (m; 2H; C*H*N); 2.39 (ddd; *J* = 24.0; 12.8 and 5.5 Hz; 2H; C*H*N); 2.26 (td; *J* = 12.8 and 5.5 Hz; 2H; C*H*P); 2.16 (dd; *J* = 12.8 and 4.0; 2H; C*H*P); 1.38 (s; 18H; *t*Bu); 1.31 (s; 18H; *t*Bu).

^{31}P NMR (^{1}H decoupled) ($CDCl_3$, 162 MHz): δ (ppm). 88.15 (s; 84 %; major isomer) and 87.0 (s; 16 %; minor isomer).

2.2.2 [RuH(BH_4)(CO)(($R_2PC_2H_4)_2$NH)] (R = *i*Pr, Cy)

2.2.2.1 [RuH(BH_4)(CO)(($iPr_2PC_2H_4)_2$NH)]

Under argon, a solution of $NaBH_4$ (5 mg, 0.24 mmol) in ethanol (2 mL) was added to a suspension of [RuHCl(CO)(($iPr_2PC_2H_4)_2$NH)] (50 mg, 0.08 mmol) in toluene (8 mL). The suspension was stirred magneticaly and heated at 65 °C for 2.5 h to give an opalescent solution. The solvents were removed under vacuum (1 x 10^{-3} mbar, RT) and the white residue was extracted with dichloromethane (3 x 5 mL). The combined organic phase was concentrated under reduced pressure (1 x 10^{-3} mbar, RT) to give the product as a white powder (30 mg, yield 62 %).

^{1}H NMR (CD_2Cl_2, 300 MHz): δ. 3.90 (large; 1H; N*H*); 3.30 - 3.12 (m; 2H); 2.56 - 2.44 (m; 2H); 2.30 - 2.21 (m; 2H); 1.94 - 1.82 (m; 2H); 1.38 (dd; J_{HP} = 16,2 Hz; J_{HH} = 7,5 Hz; 6H); 1.28 - 1.14 (m; 18H); -1.92 - -2.69 (large; 4H; Ru*H*B*H*$_3$); -13.53 (t, J_{HP} = 17,7 Hz; 1H; Ru*H*).

^{31}P NMR (^{1}H decoupled) (CD_2Cl_2, 121.5 MHz): δ. 77.7 ppm.

2.2.2.2 [RuH(BH_4)(CO)(($Cy_2PC_2H_4)_2$NH)]

Under argon, a solution of $NaBH_4$ (48 mg, 1.37 mmol) in ethanol (12 mL) was added to a suspension of [RuHCl(CO)(($Cy_2PC_2H_4)_2NH$)] (200 mg, 0.43 mmol) in toluene (16 mL). The suspension was stirred magneticaly and heated at 65 °C for 4 h to give an opalescent solution. The solvents were removed under vacuum (1 x 10^{-3} mbar, RT) and the white residue was extracted with dichloromethane (3 x 5 mL). The combined organic phase was concentrated under reduced pressure (1 x 10^{-3} mbar, RT) to give the product as a white powder (171 mg, yield 88 %).

^{1}H NMR (CD_2Cl_2, 300 MHz): δ. 3.85 (large; 1H; N*H*); 3.27 - 3.09 (m; 2H); 2.27 - 2.10 (m; 8H); 1.96 - 1.68 (m; 20H); 1.61 - 1.20 (m; 22H); -2.19 - -2.50 (large; 4H; Ru*H*B*H*$_3$); -13.60 (t, J_{HP} = 17.9 Hz; 1H; Ru*H*).

^{31}P NMR (^{1}H decoupled) (CD_2Cl_2, 121.5 MHz): δ. 68.9 ppm.

2.2.3 [$RuH_2(CO)((R_2PC_2H_4)_2NH)$] (R = *i*Pr, Ph)

2.2.3.1 [$RuH_2(CO)((iPr_2PC_2H_4)_2NH)$]

Under argon, a commercial solution of $NaHBEt_3$ (1 M in toluene; 0.45 mL, 0.45 mmol) was added to a suspension of [RuHCl(CO)(($iPr_2PC_2H_4)_2NH$)] (221 mg, 0.468 mmol) in tetrahydrofuran (8 mL). The system was stirred magnetically at room temperature for 18 h to give an opalescent yellow solution. The solution was concentrated under reduced pressure (1 x 10^{-3} mbar, RT) to yield a yellow solid. The solid was dissolved in toluene (8 mL) and the obtained suspension was filtered over a sintered glass filter. The filtrate was concentrated under reduced pressure (1 x 10^{-3} mbar, RT) to give the product as a yellow powder (181 mg, yield: 89 %).

^{1}H NMR (C_6D_6, 300 MHz): δ. 2.20 - 2.04 (m; 3H); 1.92 - 1.83 (m; 4H); 1.66 - 1.54 (m; 2H); 1.36 - 1.27 (m; 24H); 1.01 - 0.91 (m; 2H); -6.18 - -6.46 (m; 2H; Ru*H*$_2$).

^{31}P NMR (^{1}H decoupled) (C_6D_6, 121.5 MHz): δ. 91.1 ppm (^{1}H and ^{31}P NMR spectra in agreement with literature data, see:[1]).

2.2.3.2 [$RuH_2(CO)((Ph_2PC_2H_4)_2NH)$]

Under argon, a suspension of [RuHCl(CO)($(Ph_2PC_2H_4)_2NH$)] (244 mg, 0.402 mmol) in dry THF (32 mL) was treated by a commercially available solution of $NaHBEt_3$ (1 M in toluene; 0.42 mL, 0.42 mmol). The mixture was magnetically stirred for 18 h at RT giving an opalescent yellow solution. The solution was filtered over a sintered glass filter and the salt washed with THF. The solution was concentrated under reduced pressure to few mL and layered with pentane giving at room temperature a white powder (106 mg, yield: 46 %).

The ^{1}H NMR (C_6D_6, 300 MHz) spectrum exhibits a complex signal at –5.97 ppm consisting of two triplet of doublet (J = 20.0 and 5.0 Hz) coherent with a *trans*-dihydride complex. Unfortunately this signal evolves slowly to a triplet (J = 20.0 Hz). Actually the accurate structure of this complex is not fully known and sill under investigation. The ^{31}P NMR (^{1}H decoupled) (C_6D_6, 121.5 MHz) spectrum exibits a broad signal at 65.5 ppm.

2.2.4 [RuH(CO)($R_2PC_2H_4)_2N$]] (R = *t*Bu)

Under argon, a solution of [RuHCl(CO)((tBu$_2PC_2H_4)_2NH$)] (98 mg, 0.185 mmol) in dry toluene (2 mL) was treated by a commercial solution of $NaHBEt_3$ (1 M in toluene; 0.21 mL, 0.21 mmol). The mixture was stirred magnetically at RT for 18 h to give an opalescent orange–yellow solution. The solution was filtred over a sintered glass filter and the salt was washed with a few mL of toluene. The filtrate was concentrated under reduced pressure until 1– 2 ml and layered with pentane to give at RT a yellow powder (71 mg, yield: 78 %).

^{1}H NMR (C_6D_6, 400 MHz): δ (ppm). -20.87 (t; J = 16.4 Hz; Ru*H*)

^{1}H NMR (^{31}P decoupled) (C_6D_6, 400 MHz): δ. 3.49 (dd; J = 12.0 and 8.0 Hz; 2H; CHN); 3.18 – 3.10 (m; 2H; CHN); 1.92 (ddd; J = 14.2, 5.6 and 1.2 Hz; 2H; CHP); 1.82 (ddd; J = 14.2; 10.0 and 8.0 Hz; 2H; CHP); 1.28 (s; 18H; *t*Bu); 1.24 (s; 18H; *t*Bu).

^{31}P NMR (^{1}H decoupled) (C_6D_6, 162 MHz): δ (ppm). 110.0 (s)

2.2.5 $[RuCl_2((i\text{Pr}_2PC_2H_4)_2NH)]_2$

Prepared according to[3] as follows:

Under argon, $(i\text{Pr}_2PC_2H_4)_2NH$ (499 mg; 1.63 mmol) was added to a suspension of $[RuCl_2(p\text{-cymene})]_2$ (500 mg; 0.81mmol) in tetrahydrofuran (20 mL). The red-orange solution was stirred magnetically and heated at 70°C for 24 h during which a yellow powder slowly precipitates. The solvent was reduced to a few mL under reduced pressure (1 x 10^{-3} mbar, RT). The system was cooled down to 0 °C and pentane (30 mL) was added to give a yellow precipitate. The solid was separated by filtration, washed with pentane (3 x 10 mL) and dried under reduced pressure (1 x 10^{-3} mbar, RT) (494 mg, yield: 64 %).

^{1}H NMR (CD_2Cl_2, 300 MHz): δ = 6.22 (s, 1H, N*H*), 3.17 - 2.99 (m, 2H, NCH_2), 2.88 - 2.71 (m, 2H, PC*H*$(CH_3)_2$), 2.65 - 2.44 (m, 2H, NCH_2), 2.15 - 2.01 (m, 2H, CH_2P), 2.01 - 1.91 (m, 2H, PC*H*$(CH_3)_2$), 1.51 - 1.41 (m, 6H, CH_3), 1.41 - 1.36 (m, 6H, CH_3), 1.36 - 1.28 (m, 6H, CH_3), 1.24 - 1.16 (m, 6H, CH_3).

^{31}P NMR (^{1}H decoupled) (CD_2Cl_2, 121.5 MHz): δ. 72.5 ppm (s). (^{1}H and ^{31}P NMR spectra in agreement with literature data, see: [3])

2.2.6 $[RuCl_2(PMe_3)(i\text{Pr}_2PC_2H_4)_2NH]$

Prepared according to[3] as follows:

Under argon, a commercial solution of PMe_3 in tetrahydrofuran (1M, 503 µL, 0.503 mmol) was added via syringe to a suspension of $[RuCl_2((i\text{Pr}_2PC_2H_4)_2NH)]_2$ (0.200 g, 0.209 mmol) in tetrahydrofuran. After all solid was dissolved (15 - 20 min), the solution was evaporated to dryness under reduced pressure (1 x 10^{-3} mbar, RT) to give the product as light orange powder. (159 mg, yield: 74 %).

^{1}H NMR (THF-d_8, 300 MHz): δ = 3.50 (1H, N*H*), 2.95 (m, 2H, PC*H*(CH_3)$_3$), 2.80 (m, 2H, CH_2P), 2.8 - 2.7 (m, 2H, NCH_2), 2.42 (m, 2H, NCH_2), 1.88 (m, 2H, CH_2P), 1.59 (d, J_{HP} = 8.32 Hz, 9H, P(CH_3)$_3$), 1.40 (m, 2H, CH_2P), 1.28 (m, 6H, CH_3), 1.28 - 1.15 (m, 18H, CH_3).

^{31}P NMR (^{1}H decoupled) (THF-d_8, 121.5 MHz): δ. 38.77 (d, J_{PP} = 30.1 Hz, 2P, *Pi*Pr$_2$), 6.00 (t, J_{PP} = 30.1 Hz, 1P, *P*Me$_3$). (^{1}H and ^{31}P NMR spectra in agreement with literature data, see: [3])

2.3 Catalytic testing procedures

2.3.1 Typical procedure for acceptorless dehydrogenative coupling of alcohols

In a glovebox, the required amount of catalyst (typically 15.4 mg, 0.0262 mmol) was weighed in a Schlenk tube containing a stir bar. The required amount of alcohol (typically 10 mL, 109 mmol) was added via a syringe under an argon atmosphere. The Schlenk tube was then equipped with a reflux condenser topped with an argon bubbler. The system was heated by an oil bath and stirred magnetically. Liquid samples (typically 1 mL) were periodically taken to monitor the reaction progress over time. Liquid samples were weighed, mixed with a known amount of internal standard (cyclohexane) and diluted with dichloromethane. Samples were then analyzed by GC-FID/MS for determination of conversion, yield, turnover number, turnover frequency and mass balance (see 2.5.1.3 and 2.5.1.4). Alternatively, liquid samples were diluted with $CDCl_3$ and analyzed by ^{1}H NMR for determination of yield, turnover number and turnover frequency (see 2.5.1.5).

2.3.2 Typical procedure for acceptorless dehydrogenation of alcohols to corresponding acid salts

2.3.2.1 Standard procedure for catalytic performance measurement

In a glovebox, the required amount of sodium hydroxide (typically 2.19 g, 54.8 mmol) and catalyst (typically 33.2 mg, 0.0546 mmol) were weighed in a Schlenk tube containing a stir bar. Under argon, the required amount of 1-butanol (typically 5 mL,

54.6 mmol) and water (typically 2 mL, 111 mmol) were added via syringes. The Schlenk tube was equipped with a reflux condenser topped with an argon bubbler. The system was heated by an oil bath and stirred magnetically.

After the desired reaction time, water was added (15 mL) the mixture was acidified using hydrochloric acid (typically 7.0 g, 34 wt. % solution, 65 mmol HCl) and extracted with ethyl acetate (5 x 20 mL). To the combined organic phase, a known amount of internal standard (cyclohexane) was added. The samples were analyzed by GC-FID/MS for determination of conversion, yield, turnover number, turnover frequency and mass balance (see 2.5.2).

2.3.2.2 Test of catalyst recyclability

In a glovebox, the required amount of sodium hydroxide (typically 2.19 g, 54.8 mmol) and catalyst (typically 33.2 mg, 0.0546 mmol) were weighed in a Schlenk tube containing a stir bar in a glovebox. The required amount of 1-butanol (typically 5 mL, 54.6 mmol), water (typically 2 mL, 111 mmol) and toluene (typically 5 mL) were added via syringes under argon. The Schlenk tube was equipped with a reflux condenser topped with an argon bubbler. The system was heated by an oil bath and stirred magnetically.

After the desired reaction time, water (15 mL) was added to the crude reaction mixture, the system was stirred magnetically for few minutes until all solid products became soluble. After settling, the aqueous phase was separated and the organic phase was further washed with water (15 mL), the water phase was separated and combined with the previous one.

To the catalyst containing organic phase, fresh substrate (1-butanol, typically 5 mL, 54.6 mmol) and fresh base solution (typically 2.19 g sodium hydroxide in 2 mL water) were added. The system was heated via oil bath and stirred magnetically to start another catalytic test. The procedure was repeated several times to evalutate the catalyst recyclability.

For analysis, the combined aqueous phases (30 mL) used for product extraction at the end of each run, were acidified with hydrochloric acid (typically 7.0 g 34 wt. % solution, 65 mmol HCl) and extracted with ethyl acetate (5 x 30 mL). To the combined organic phase, a known amount of internal standard (cyclohexane) was added and the samples were analyzed by GC-FID/MS for determination of yield and conversion.

2.3.3 Typical procedure for selective deuteration of alcohols

In a glovebox, the required amount of base (typically 12 mg, 0.3 mmol) and catalyst (typically 3.64 mg, 0.006 mmol) were weighed in a glass tube (volume of the tube: 7.3 mL) containing a stir bar. Under air, the required amount of alcohol (typically 222 mg, 3 mmol) and deuterium oxide (typically 2.4 mL, 133 mmol) were added. The tube was then closed, heated by an oil bath and stirred magnetically. After desired reaction time, liquid samples were analyzed by ^{1}H NMR for determination of yields (see 2.5.3). When required, known amount of internal standard (1,4-dioxane) was added to the reaction crude before analysis by ^{1}H NMR.

2.4 Analytical methods

2.4.1 Analysis by GC-FID/MS

For GC-FID/MS analysis, the following oven temperature program was used:

50 ^{o}C, 4 min;

then 5 ^{o}C min^{-1} to 105 ^{o}C;

then 10 ^{o}C min^{-1} to 200 ^{o}C, and keep at 200 ^{o}C for 3.5 min.

The total duration for this temperature program is 28 minutes.

Helium was used as a carrier gas. The temperatures set for inlet and FID detector were 250 ^{o}C and 300 ^{o}C respectively. The inject volume was 0.1 mL with a split ratio of 40: 1. The total gas flow was 41.574 mL min^{-1} with a split flow of 37.633 mL min^{-1} and a septum purge flow of 3 mL min^{-1}.

For both alcohols acceptorless dehydrogenative coupling reactions (using 1-butanol and ethanol as substrate) and the acceptorless dehydrogenation of 1-butanol to butyric acid salt reaction, GC-FID/MS was used for product identification and quantification using the abovedescribed analysis conditions. The chromatograms obtained from the FID signal were used for quantification of the different products. MS was only used for product identification.

Typical FID chromatograms obtained for the acceptorless dehydrogenative coupling of 1-butanol, for the acceptorless dehydrogenative coupling of ethanol and for the acceptorless dehydrogenation of 1-butanol to butyric acid salt are shown in Fig. 2.1, Fig. 2.2 and Fig. 2.3, respectively.

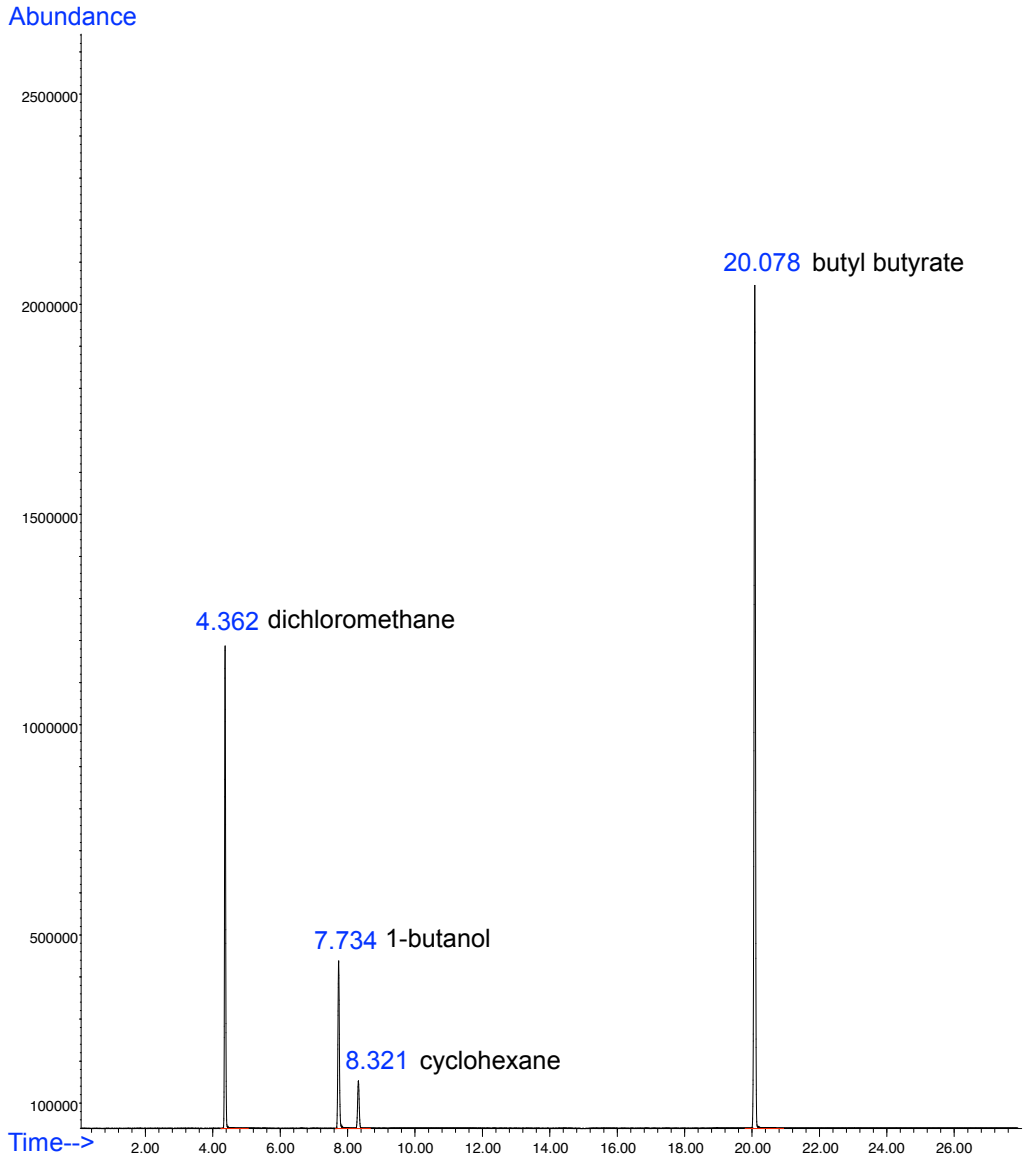

Fig. 2.1 *A typical FID chromatogram obtained for the acceptorless dehydrogenative coupling of 1-butanol.*

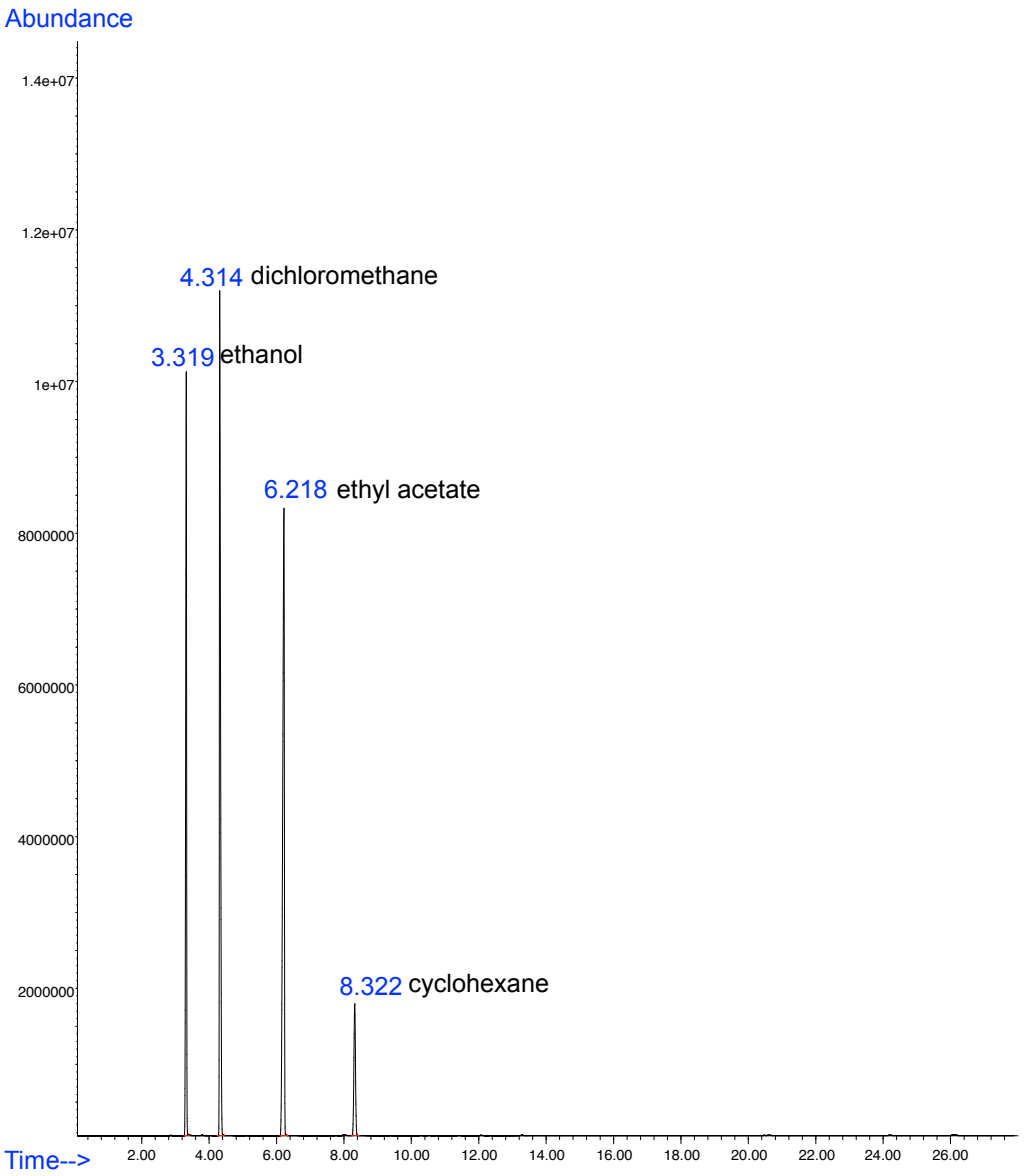

Fig. 2.2 *A typical FID chromatogram obtained for the acceptorless dehydrogenative coupling of ethanol.*

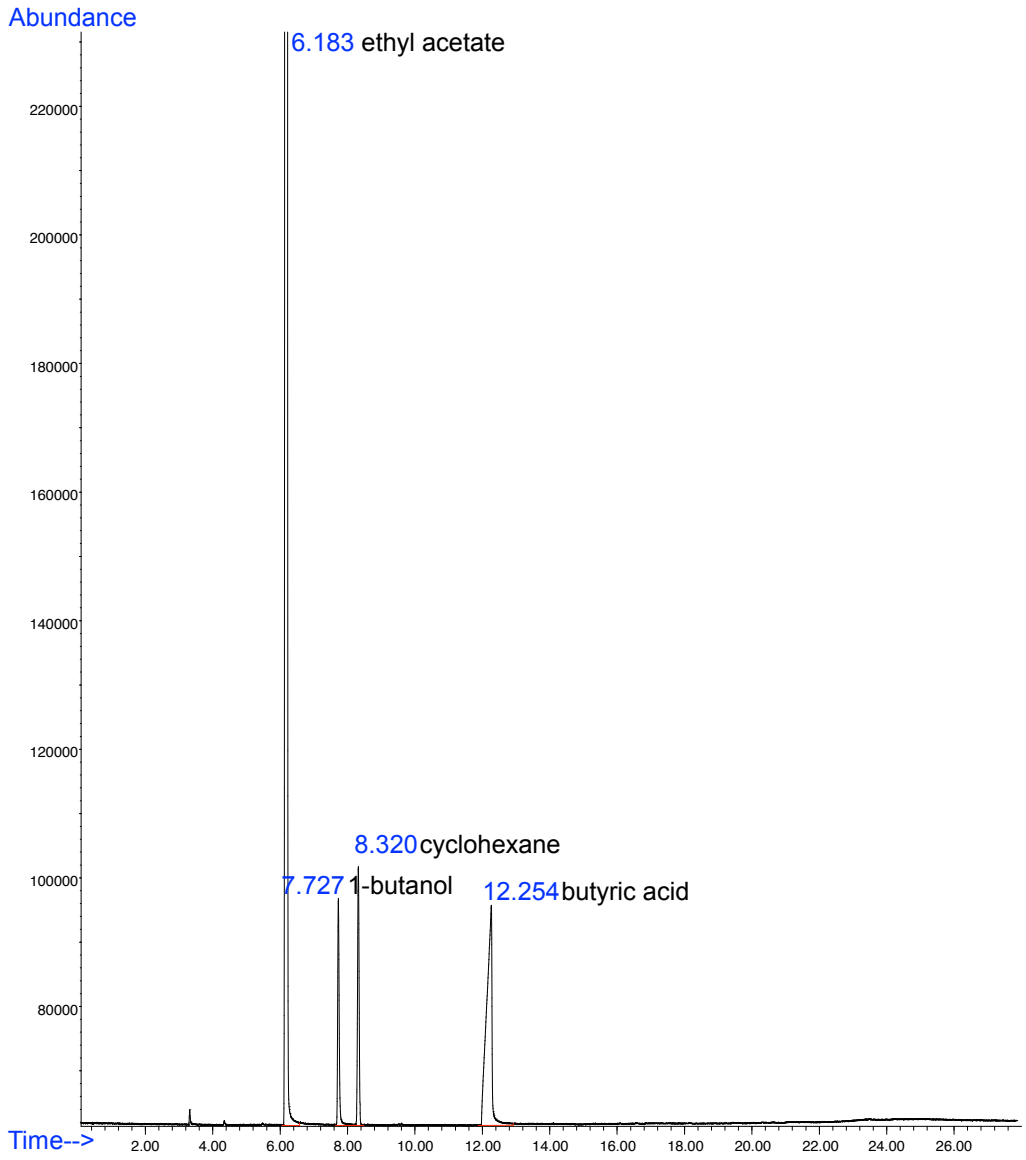

Fig. 2.3 *A typical FID chromatogram obtained for the acceptorless dehydrogenation of 1-butanol to butyric acid salt.*

2.4.2 Analysis by NMR

Acceptorless dehydrogenative coupling reactions using different substrates than ethanol and 1-butanol were analyzed by ^{1}H NMR. From the ^{1}H NMR spectra, the signal typical for the alcohol, a triplet at 3.6 ppm, and the signal typical for the ester, triplet at 4.0 were integrated.

Typical ^{1}H NMR spectra for 1-octanol, octyl octanoate and a crude reaction sample collected during the acceptorless dehydrogenative coupling of octanol are shown in Fig. 2.4 (a, b, c respectively).

The progress of alcohol deuteration reactions were followed by ^{1}H NMR.

Typical ^{1}H NMR spectra for 1-butanol before and after selective deuteration are shown in Fig. 2.5 (a, b respectively).

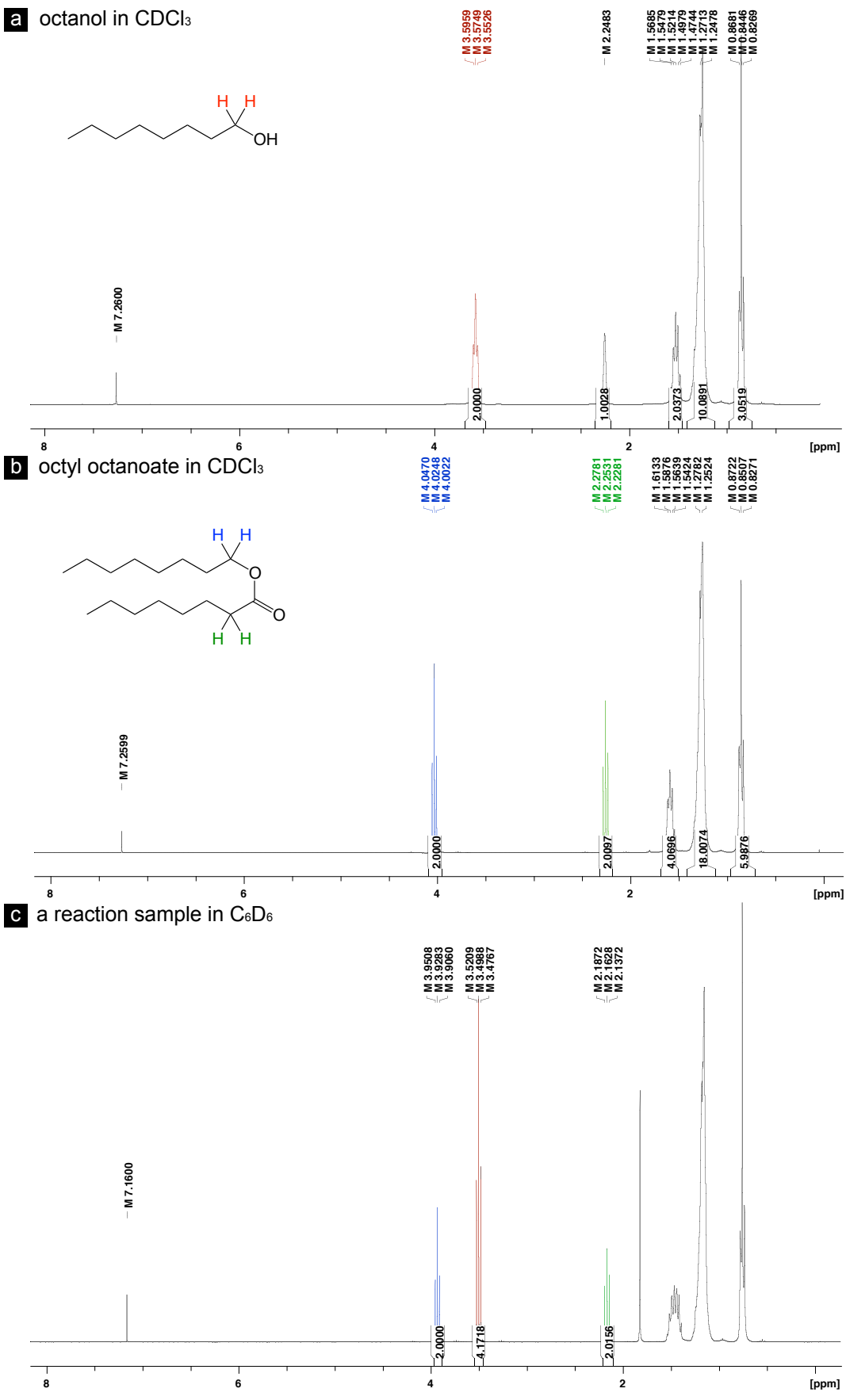

Fig. 2.4 *Typical ^{1}H NMR spectra for dehydrogenative coupling of octanol.*

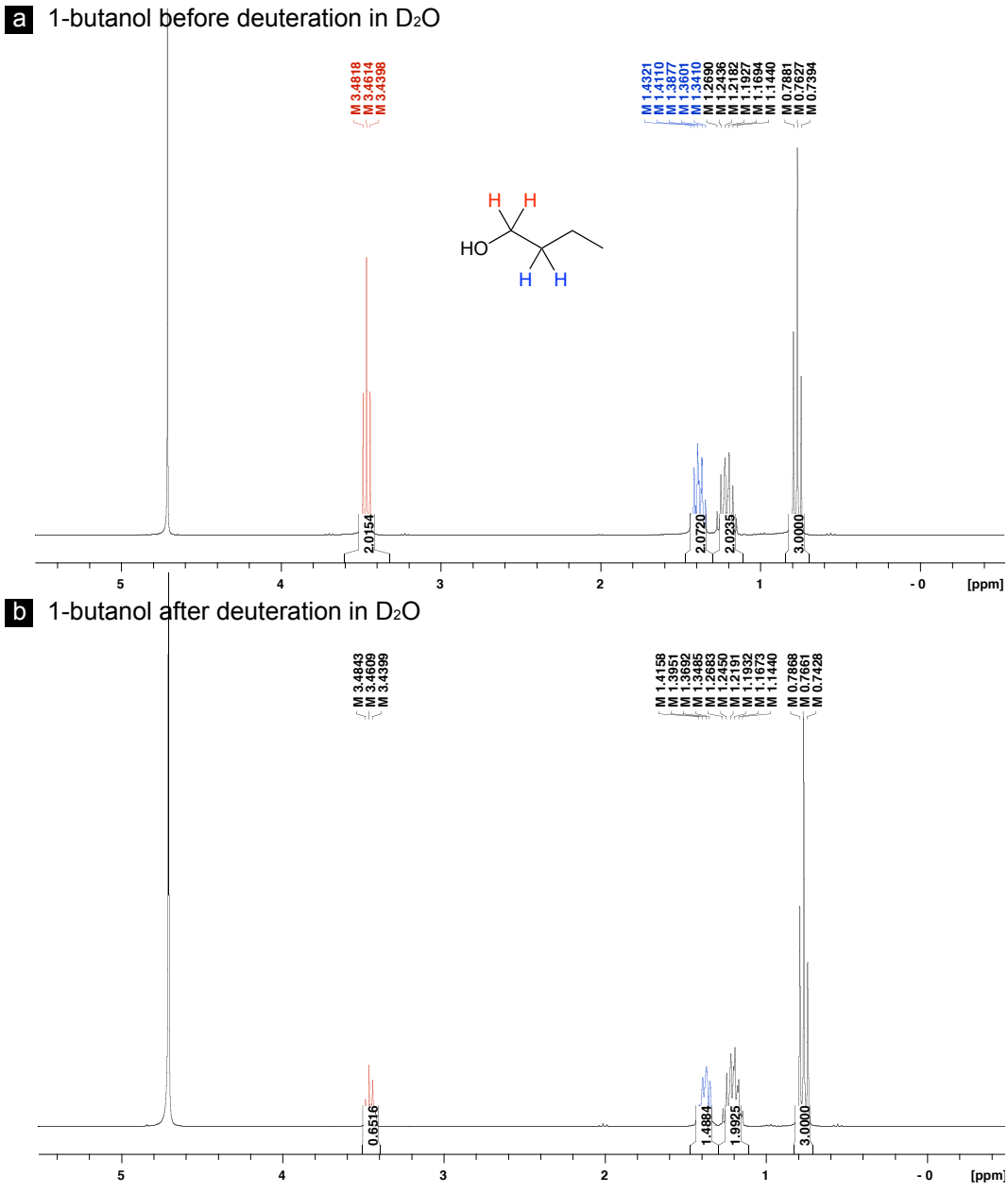

Fig. 2.5 *Typical ^{1}H NMR spectra for selective deuteration of 1-butanol.*

2.5 Calculations

2.5.1 Acceptorless dehydrogenative coupling of alcohols

For 1-butanol and ethanol, GC-FID/MS was used for analysis (Fig. 2.1 and Fig. 2.2 shows typical FID spectra). Identification of the different products was made by comparison with authentic samples and/or the fragmentation arising from the MS spectra. For quantification, the FID chromatograms were integrated and calculation were made according to the following calibrations.

2.5.1.1 GC calibrations for 1-butanol and butyl butyrate

For calibration, samples containing known amount of 1-butanol, butyl butyrate and cyclohexane (internal standard) were analyzed by GC-FID and the chromatograms were integrated in order to obtain the response factor *(f)* of substrate and product against the internal standard cyclohexane.

Amount of substance (*n*) for 1-butanol, butyl butyrate and cyclohexane was calculated, respectively.

$$n_x = m_x / M_x \qquad \textbf{Eq. 2.1}$$

(M_x = molecular weight of compound *x*)

The response factor for each compound against the internal standard, f_x (*x* = *BuOH* or *BB, BuOH* = 1-butanol, *BB* = butyl butyrate) was given by the slope of the linear regressions from the plot of n_x/n_{std} (*std* = cyclohexane) as a function of PA_x/PA_{std} (*PA* = FID peak area, Fig. 2.6).

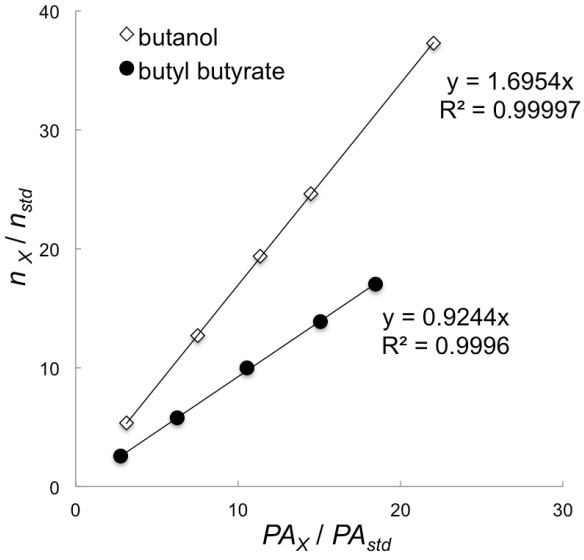

Fig. 2.6 *Linear regressions of n_x/n_{std} as a function of PA_x/PA_{std} (x = butanol or butyl butyrate).*

2.5.1.2 GC calibrations for ethanol and ethyl acetate

For ethanol calibration, samples with known amount of ethanol, ethyl acetate and cyclohexane (= internal standard) were analyzed by GC-FID and the chromatograms

were integrated in order to obtain the response factor *(f)* of substrate and product against the internal standard.

Amount of substance (*n*) for ethanol, ethyl acetate and cyclohexane was then calculated, respectively (see Eq. 2.1).

The response factor for each compound against the internal standard f_x ($x = EtOH$ or EA, $EtOH$ = ethanol, EA = ethyl acetate) was given by the slope of the linear regressions from the plot of n_x/n_{std} (std = cyclohexane) as a function of PA_x/PA_{std} (PA = FID peak area, Fig. 2.7).

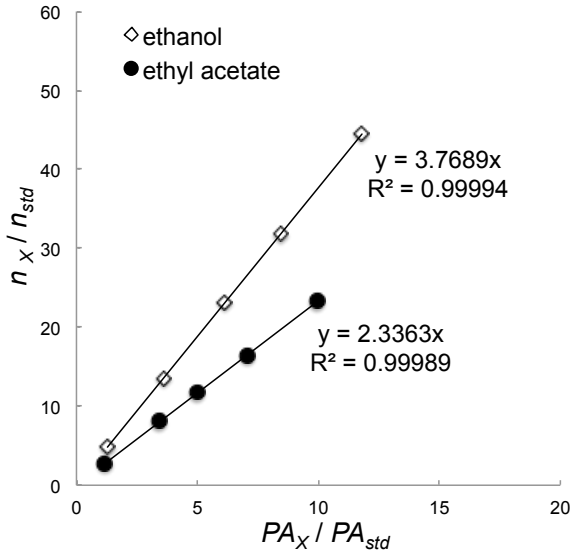

Fig. 2.7 *Linear regressions of n_x/n_{std} as a function of PA_x/PA_{std} (x = ethanol or ethyl acetate).*

2.5.1.3 Calculations for testing using 1-butanol

The amount of 1-butanol and butyl butyrate in the samples collected at desired reaction time *t* (n^t_{BuOH}, n^t_{BB}) were calculated as follows:

$$n^t_{BuOH} = n^t_{std} \cdot f_{BuOH} \cdot \frac{PA^t_{BuOH}}{PA^t_{std}} \qquad \textbf{Eq. 2.2}$$

$$n^t_{BB} = n^t_{std} \cdot f_{BB} \cdot \frac{PA^t_{BB}}{PA^t_{std}} \qquad \textbf{Eq. 2.3}$$

Conversion (C^t), the yield to butyl butyrate (Y^t_{BB}), the turnover number (TON^t), the turnover frequency (TOF^t) and the mass balance (MB^t) for a reaction at time t were calculated as follows:

$$C^t = \left[1 - \frac{n^t_{BuOH}}{(m^t + 2n^t_{BB}M_{H_2}) / M_{BuOH}}\right] \cdot 100\% \qquad \textbf{Eq. 2.4}$$

$$Y^t_{BB} = \frac{2n^t_{BB}}{(m^t + 2n^t_{BB}M_{H_2}) / M_{BuOH}} \cdot 100\% \qquad \textbf{Eq. 2.5}$$

$$TON^t = \frac{Y^t_{BB}}{[Ru]} = \frac{2n^t_{BB}}{(m^t + 2n^t_{BB}M_{H_2}) / M_{BuOH} \cdot [Ru]} \qquad \textbf{Eq. 2.6}$$

$$TOF^t = \frac{TON^t}{t} = \frac{2n^t_{BB}}{(m^t + 2n^t_{BB}M_{H_2}) / M_{BuOH} \cdot [Ru] \cdot t} \qquad \textbf{Eq. 2.7}$$

$$MB^t(\%) = \frac{n^t_{BuOH} + 2n^t_{BB}}{(m^t + 2n^t_{BB}M_{H_2}) / M_{BuOH}} \cdot 100\% \qquad \textbf{Eq. 2.8}$$

(m^t = mass of the sample collected for analysis at the reaction time t; the term $2n^t_{BB}M_{H2}$ corresponds to the mass loss of the sample during reaction time *0* to t due to hydrogen evolution, due to the reaction stoechiometry, 2 mol of H_2 were lost for each mol of butyl butyrate produced; [Ru] = catalyst concentration = n_{Ru}/n^0_{BuOH})

2.5.1.4 Calculations for tests using ethanol

The amount of ethanol and ethyl acetate in the samples collected at desired reaction time t (n^t_{EtOH}, n^t_{EA}) were calculated as follows:

$$n^t_{EtOH} = n^t_{std} \cdot f_{EtOH} \cdot \frac{PA^t_{EtOH}}{PA^t_{std}} \qquad \textbf{Eq. 2.9}$$

$$n^t_{EA} = n^t_{std} \cdot f_{EA} \cdot \frac{PA^t_{EA}}{PA^t_{std}} \qquad \textbf{Eq. 2.10}$$

The conversion (C^t), the yield to ethyl acetate (Y^t_{EA}), the turnover number (TON^t), the turnover frequency (TOF^t) and the mass balance (MB^t) for a reaction at time t were calculated as follows:

$$C^t = \left[1 - \frac{n^t_{EtOH}}{(m^t + 2n^t_{EA}M_{H_2}) / M_{EtOH}}\right] \cdot 100\% \qquad \textbf{Eq. 2.11}$$

$$Y^t_{BB} = \frac{2n^t_{EA}}{(m^t + 2n^t_{EA}M_{H_2}) / M_{EtOH}} \cdot 100\% \qquad \textbf{Eq. 2.12}$$

$$TON^t = \frac{Y^t_{EA}}{[Ru]} = \frac{2n^t_{EA}}{(m^t + 2n^t_{EA}M_{H_2}) / M_{EtOH} \cdot [Ru]} \qquad \textbf{Eq. 2.13}$$

$$TOF^t = \frac{TON^t}{t} = \frac{2n^t_{EA}}{(m^t + 2n^t_{EA}M_{H_2}) / M_{EtOH} \cdot [Ru] \cdot t} \qquad \textbf{Eq. 2.14}$$

$$MB^t(\%) = \frac{n^t_{EtOH} + 2n^t_{EA}}{(m^t + 2n^t_{EA}M_{H_2}) / M_{EtOH}} \cdot 100\% \qquad \textbf{Eq. 2.15}$$

(m^t = mass of the sample collected for analysis at the reaction time t; the term $2n^t_{EA}M_{H2}$ corresponds to the mass loss of the sample during reaction time *0* to t due to hydrogen evolution, due to the reaction stoechiometry, 2 mol of H_2 were lost for each mol of ethyl acetate produced; [*Ru*] = catalyst concentration = n_{Ru}/n^0_{EtOH})

2.5.1.5 Calculations for tests using other alcohols

For alcohols other than 1-butanol and ethanol, ^{1}H NMR spectroscopy was used for analysis (a typical ^{1}H NMR spectrum for acceptorless dehydrogenative coupling of 1-octanol is shown in Fig. 2.4).

From the ^{1}H NMR spectra, the signal typical for the alcohol, a triplet at 3.6 ppm, and the signal typical for the ester, triplet at 4.0 were integrated. The peak area of these two peaks ($PA_{3.6}$, $PA_{4.0}$) were used to represent the amount of the alcohol and correponding ester.

The yield to ester (Y^t_E), the turnover number (TON^t) and the turnover frequency (TOF^t) for a the sample collected at reaction time t were calculated as follows:

$$Y^t_E = \frac{2PA_{4.0}}{2PA_{4.0} + PA_{3.6}} \cdot 100\% \qquad \textbf{Eq. 2.16}$$

$$TON^t = \frac{Y_E^t}{[Ru]} \qquad \textbf{Eq. 2.17}$$

$$TOF^t = \frac{TON^t}{t} \qquad \textbf{Eq. 2.18}$$

([Ru] = catalyst concentration = $n_{Ru}/n^0_{subsrate}$)

2.5.1.6 Calculations of the initial turnover frequency TOF_0

For all acceptorless dehydrogenative coupling reactions, the initial turnover frequency, TOF_0, was determined from the plot of the turnover number as a function of time (Fig. 2.8 shows a typical example). The TOF_0 was obtained from the slope of linear regression calculated on the initial linear part of the plot (typically the first 1 h of reaction).

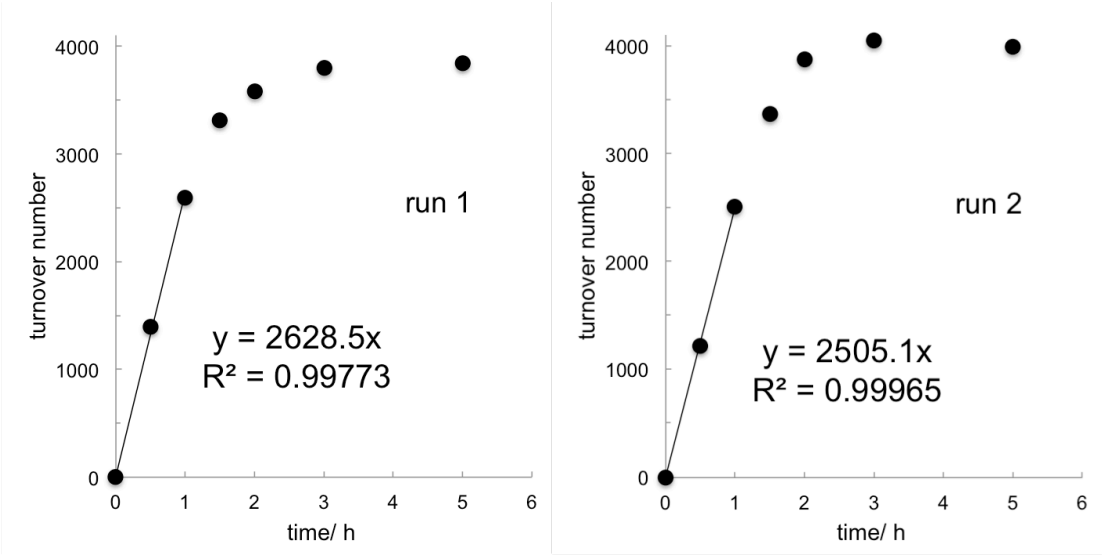

Fig. 2.8 *Calculation of initial TOF_0.*

In some cases, under the same reaction conditions with the same catalyst, the catalytic tests were duplicated to ensure reproducibility (see Fig. 2.8). Thus, the initial TOF_0 was calculated from the average level of run 1 and run 2, and an error margin was given (for instance in Fig. 2.8, average TOF_0 = (2629 + 2505) / 2 = 2567 h^{-1}, the error margin = (2629 - 2505) / 2 = 62 h^{-1}, simply the initial TOF_0 was expressed as TOF_0 = 2567 ± 62 h^{-1}).

2.5.2 Acceptorless dehydrogenation of alcohols to corresponding acid salts

For this reaction, GC-FID/MS was used for analysis (a typical FID chromatogram is shown in Fig. 2.3). Identification of the different products was made by comparison with authentic samples and/or the fragmentation arising from the MS spectra. For quantification, the FID chromatogram were integrated and calculation were made according to the following calibrations.

2.5.2.1 GC calibrations for butanol and butyric acid

For calibration, samples with known amount of 1-butanol, butyric acid and cyclohexane were analyzed by GC and the FID chromatograms were integrated in order to obtain the response factor (*f*) of substrate and product against the internal standard.

Amount of substance (*n*) for 1-butanol, butyric acid and cyclohexane was then calculated, respectively (see Eq. 2.1).

The response factor for each compound against the internal standard, f_x (x = *BuOH* or *BA*, was given by the slope of the linear regressions from the plot of n_x/n_{std} as a function of PA_x/PA_{std} (Fig. 2.9).

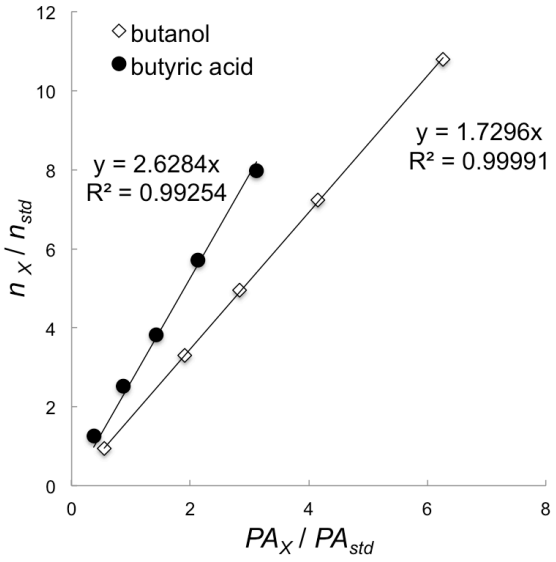

Fig. 2.9 *Linear regressions of n_x/n_{std} as a function of PA_x/PA_{std} (x = butanol or butyric*

acid).

2.5.2.2 Calculations

The amount of 1-butanol and butyric acid in the reaction crude after the desired reaction time *t* (n^t_{BuOH}, n^t_{BA}) were calculated as follows:

$$n^t_{BuOH} = n^t_{std} \cdot f_{BuOH} \cdot \frac{PA^t_{BuOH}}{PA^t_{std}} \quad \textbf{Eq. 2.19}$$

$$n^t_{BA} = n^t_{std} \cdot f_{BA} \cdot \frac{PA^t_{BA}}{PA^t_{std}} \quad \textbf{Eq. 2.20}$$

The conversion (C^t), the yield to butyric acid (Y^t_{BA}), the turnover number (TON^t) and the turnover frequency (TOF^t) for the reaction at reaction time *t* were calculated as follows:

$$C^t = \left(1 - \frac{n^t_{BuOH}}{n^0_{BuOH}}\right) \cdot 100\% \quad \textbf{Eq. 2.21}$$

$$Y^t_{BA} = \frac{n^t_{BA}}{n^0_{BuOH}} \cdot 100\% \quad \textbf{Eq. 2.22}$$

$$TON^t = \frac{Y^t_{BA}}{[Ru]} \quad \textbf{Eq. 2.23}$$

$$TOF^t = \frac{TON^t}{t} \quad \textbf{Eq. 2.24}$$

(n^0_{BuOH} = amount for 1-butanol used at the beginning of the reaction, [*Ru*] = catalyst concentration = n_{Ru}/n^0_{BuOH})

2.5.3 Selective deuteration of alcohols

Similar analysis method can be found in[4].

2.5.3.1 Calculations for testing using 1-butanol

For the deuteration reactions, ^{1}H NMR spectroscopy was used for quantitative analysis (typical ^{1}H NMR spectrum for selective deuteration of of 1-butanol is shown

in Fig. 2.5). As it can be seen from the comparison of ^{1}H NMR spectra for 1-butanol before and after reaction, upon deuteration the peak areas for the signals corresponding to the proton on the α and β positions (3.5 ppm and 1.5 ppm, respectively) decrease compared to the signals of the γ CH_2 and terminal CH_3 groups (1.2 ppm and 0.8 ppm, respectively), unchanged by the reaction.

Therefore, the deuteration yield for the α position and the β position (Y^t_α, Y^t_β) at reaction time *t* were calculated as follows:

$$Y^t_\alpha = \frac{2/3 - PA^t_{3.5}/PA^t_{0.8}}{2/3} \cdot 100\% \qquad \textbf{Eq. 2.25}$$

$$Y^t_\beta = \frac{2/3 - PA^t_{1.4}/PA^t_{0.8}}{2/3} \cdot 100\% \qquad \textbf{Eq. 2.26}$$

2.5.3.2 Calculations for tests using ethanol

For ethanol, since all protons were affected by the deuteration reaction, known amount 1,4-dioxane was used as an internal standard for analysis. The 1,4-dioxane shows a sole singlet at 3.6 ppm on ^{1}H NMR spectrum, which was separated from typical ethanol signals at 3.5 ppm and 1.0 ppm. Therefore, the deuteration yield for the α position and the β position (Y^t_α, Y^t_β) at reaction time *t* were calculated as follows:

$$Y^t_\alpha = \frac{2n^0_{EtOH} - 8n_{DX} \cdot PA^t_{3.5}/PA^t_{3.6}}{2n^0_{EtOH}} \cdot 100\% \qquad \textbf{Eq. 2.27}$$

$$Y^t_\beta = \frac{3n^0_{EtOH} - 8n_{DX} \cdot PA^t_{1.0}/PA^t_{3.6}}{3n^0_{EtOH}} \cdot 100\% \qquad \textbf{Eq. 2.28}$$

(n^0_{EtOH} = amount of ethanol used at the beginning of the reaction, n_{DX} = amount of 1,4-dioxane added after the reaction)

2.6 References

[1] M. Bertoli, A. Choualeb, A. J. Lough, B. Moore, D. Spasyuk, D. G. Gusev, *Organometallics* **2011**, *30*, 3479-3482.

[2] M. Nielsen, E. Alberico, W. Baumann, H.-J. Drexler, H. Junge, S. Gladiali, M. Beller, *Nature*

2013, *495*, 85-89.

[3] M. Käß, A. Friedrich, M. Drees, S. Schneider, *Angew. Chem. Int. Ed.* **2009**, *48*, 905-907.

[4] E. Khaskin, D. Milstein, *ACS Catal.* **2013**, 448-452.

Chapter 3 Acceptorless dehydrogenative coupling of primary alcohols

Acceptorless dehydrogenative coupling of primary alcohols is an environmentally friendly and atom-efficient route to produce symmetrical esters (Scheme 3.1). In this transformation, the only co-product is hydrogen, which is valuable in itself as a clean energy source and a clean reduction agent. Compared with the traditional esterification reaction using an acid and an alcohol, the evolved hydrogen can shift the reaction equilibrium to completion and thus overcome thermodynamic limitations.

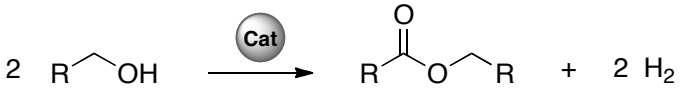

Scheme 3.1 *Acceptorless dehydrogenative coupling of primary alcohols.*

In recent years, several complexes of ruthenium and osmium coordinated by non-innocent pincer ligands have been developed as catalysts for this reaction[1-7]. Several papers on this reaction have appeared simultaneously to the work described in the present thesis[8-14].

As discussed in Chapter 1, dehydrogenation of primary alcohols, especially ethanol, under neat and neutral conditions still remains a challenging transformation.

In order to gain an insight on this reaction, 1-butanol was used as a model substrate. The reaction was further extended to other primary alcohols including ethanol.

Both *in situ* formed and isolated ruthenium complexes were studied as catalysts for the dehydrogenative coupling of primary alcohols.

The *in situ* formed catalysts consist of an equimolar mixture of a PNP ligand and a ruthenium precursor, which are believed to transform into a ruthenium PNP pincer complex under reaction conditions. In this chapter, section 3.1 presents our studies on

in situ formed catalysts and section 3.2 presents our studies on isolated catalysts for the dehydrogenative coupling of primary alcohols.

3.1 *In situ* formed catalysts

In 2011, Beller and co-workers reported that the complex $[RuH_2(CO)(PPh_3)_3]$ **1a** with one equivalent of the PNP ligand $(iPr_2PC_2H_4)_2NH$ **2a** was active for the dehydrogenation of iso-propanol and ethanol[7]. This represented at the time the highest reaction rate with TOF_0 of 1483 h^{-1} after 2 h using 3.1 ppm of catalyst for the dehydrogenation of ethanol under mild conditions (neat, base-free, at ethanol reflux temperature, *i.e.* 78 °C). However, conversion were not reported and products were just described as "formation of acetaldehyde and ethyl acetate, both in substantial amounts". Calculation indicates that, under their reaction conditions, ethanol conversion after 2 h of reaction is only 0.9 %.

Based on this report, we investigated the use of *in situ* formed catalysts for the acceptorless dehydrogenative coupling of primary alcohols.

3.1.1 Complex formation

In order to investigate the *in situ* catalyst formation, a solution of $[RuH_2(CO)(PPh_3)_3]$ **1a** and 1 equivalent of PNP ligand $(Cy_2PC_2H_4)_2NH$ **2b** in 1-butanol was refluxed under argon for 30 minutes ([Ru] = 240 ppm). The obtained yellow solution was then analysed by $^{31}P\{^1H\}$ NMR spectroscopy (Fig. 3.1.iii). From the NMR spectra, it appears that none of the signals corresponding to the free PNP ligand **2b (**Fig. 3.1.ii**)** nor to the starting $[RuH_2(CO)(PPh_3)_3]$ **1a (**Fig. 3.1.i**)** complex remained. Two new distinct signals appeared: one singlet at 64.0 ppm and one singlet at -5.5 ppm with a peak area ratio of 2 to 3 respectively. The signal at -5.5 ppm corresponds to free PPh_3 expelled from the starting $[RuH_2(CO)(PPh_3)_3]$ **1a** complex, which is confirmed by comparison with $^{31}P\{^1H\}$ NMR of free PPh_3 in C_6D_6 (Fig. 3.2). The singlet at 64.0 ppm is in agreement with the PNP ligand being coordinated to the ruthenium with both phosphorus atoms being equivalent.

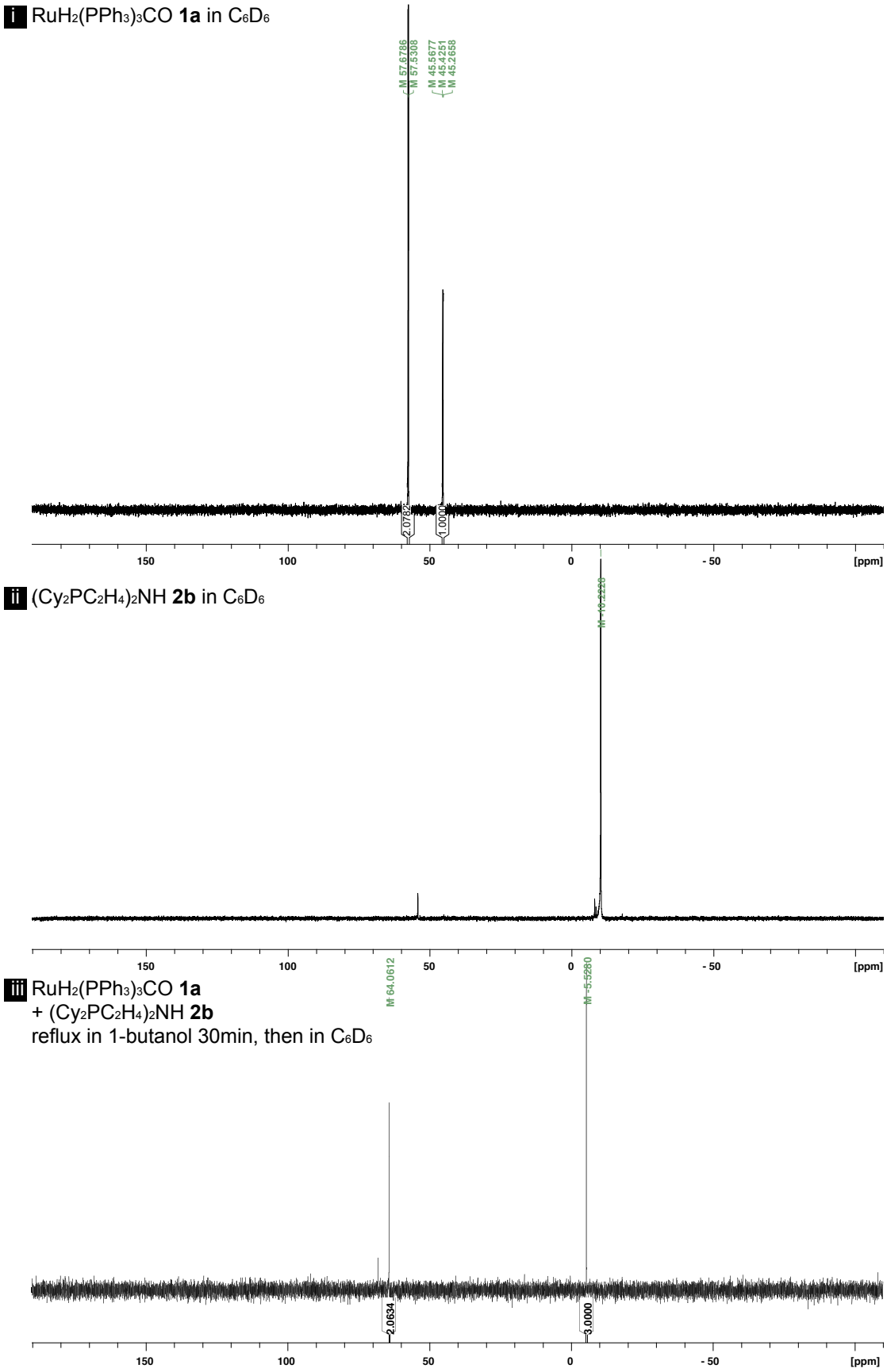

Fig. 3.1 *$^{31}P\{^{1}H\}$ NMR of an in situ formed catalyst.*

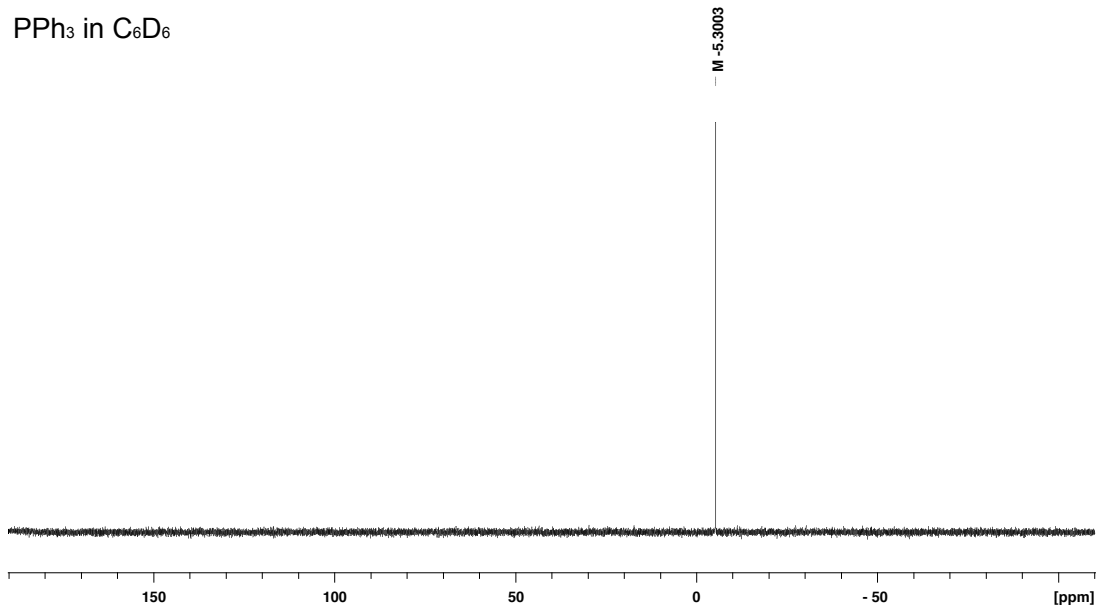

Fig. 3.2 *$^{31}P\{^{1}H\}$ NMR of free PPh_3.*

Based on these facts, one can reasonably suppose that upon refluxing in 1-butanol, the complex $[RuH_2((CO)PPh_3)_3]$ **1a** is being transformed into a ruthenium PNP pincer complex by substitution of the PPh_3 by the PNP ligand that coordinates the ruthenium center (Scheme 3.2).

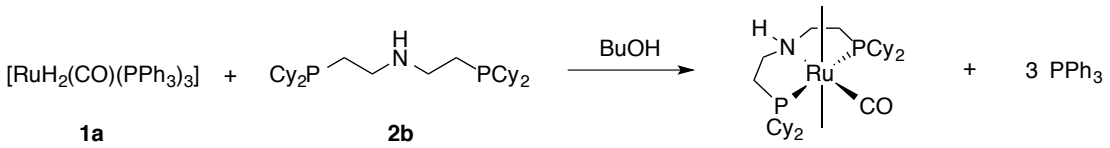

Scheme 3.2 *Proposed in situ catalyst formation.*

3.1.2 Screening of *in situ* formed catalysts

As shown previously, PNP ligands are able to substitute monodentate phosphine from ruthenium complexes in butanol under reflux. We therefore investigated the use of *in situ* formed catalysts for the dehydrogenative coupling of 1-butanol using ruthenium dihydride complexes bearing at least three labile phosphines as ruthenium source together with PNP ligands. In order to test whether PNP ligands are required to ensure catalytic activity, the complexes $[RuH_2(CO)(PPh_3)_3]$ **1a** and $[RuH_2(PPh_3)_4]$ **1b** were refluxed in butanol (b.p.= 118 °C) without additional ligand. Under these conditions no reaction was observed (Table 3.1 entries 1 and 5 and Fig. 3.4). When

using one equivalent of a PNP ligand having either iso-propyl, or cyclohexyl substituents at the phosphorus atom, **2a** or **2b**, together with complexes $[RuH_2(CO)(PPh_3)_3]$ **1a** or $[RuH_2(PPh_3)_4]$ **1b**, butyl butyrate was obtained with yields higher than 80 % after 3 h of reactions (Fig. 3.4). At any reaction time, the selectivity was found to be higher than 99 %, the reaction mixture being free of any side products, only containing unreacted 1-butanol and the desired ester (Moreover, all carbon balances were found to be in the range of 100 ± 5 %). *In situ* catalysts using complex **1b** as ruthenium source were found to be slightly more active than with **1a**. Initial turnover frequencies, TOF_0, ranging from 2358 h^{-1} to 2565 h^{-1} were obtained with ruthenium precursor **1b** while **1a** gave TOF_0 ranging from 1891 h^{-1} to 2078 h^{-1} with ligands **2a** and **2b** (Table 3.1, entries 2, 3, 6 and 7). Changing from iso-propyl to cyclohexyl substituents at the phosphorus atom of the PNP ligand did not seem to affect significantly the activity of the obtained catalyst (Table 3.1, entry 2 vs. 3 and entry 6 vs. 7). However, when more bulky PNP ligand **2c,** having tertio-butyl substituents at the phosphorus atom, was used with complexes **1a** and **1b** less than 5 % of the ester product was obtained and TOF_0 lower than 100 h^{-1} were observed (Table 3.1 entries 4 and 8 and Fig. 3.4). This dramatic fall in activity could be due to the bulkiness of ligand **2c** that impedes the formation of the Ru-PNP complex or forms a Ru-PNP complex that is too crowded to interact with the substrate.

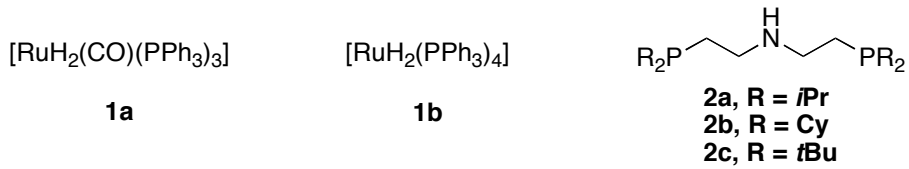

Fig. 3.3 *Precursors to in situ formed catalysts.*

Table 3.1 *Dehydrogenative coupling of 1-butanol using in situ formed catalysts*[‡].

entry	Ru	PNP	Ru / butanol	TOF_0 (h^{-1})	max. TON	max. yield (%)
1	**1a**	/	220 ppm	0	0	0
2		**2a**	218 ppm	2078	3970 (7 h)	95.1 (7 h)
3		**2b**	242 ppm	1950 ± 76	4100 (3 h)	99.2 (3 h)
4		**2c**	237 ppm	43	260 (32 h)	5.9 (32 h)
5	**1b**	/	242 ppm	0	0	0
6		**2a**	236 ppm	2358	4160 (4 h)	98.1 (4 h)
7		**2b**	238 ppm	2565	3500 (4 h)	83.1 (4 h)
8		**2c**	242 ppm	25	120 (5 h)	2.9 (5 h)

[‡]reaction conditions: Ru / ligand: 1; *V* (1-butanol): 10 mL; applied temperature: 130 °C; under argon.

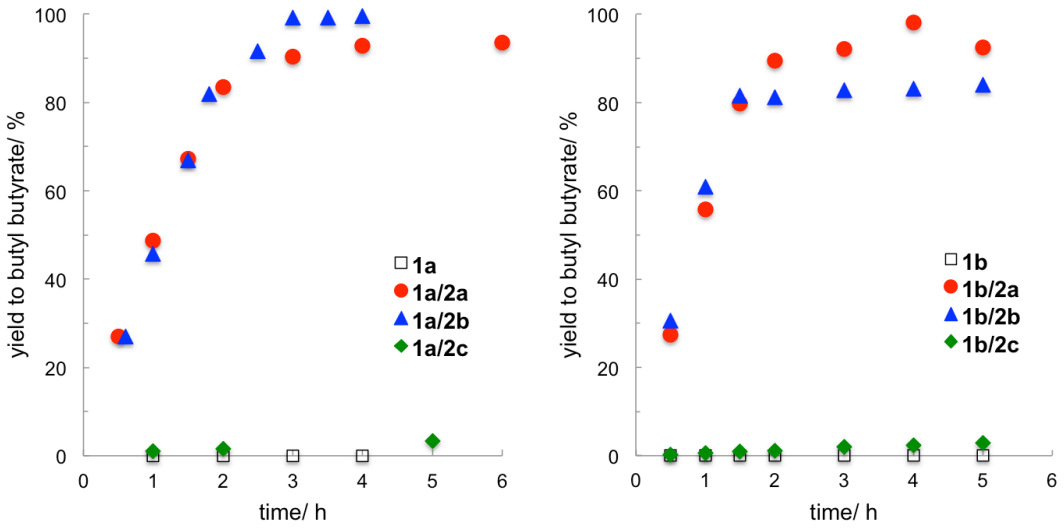

Fig. 3.4 *Evolution of the ester yield as a function of time during the dehydrogenative coupling of 1-butanol catalysed by in situ catalysts with ruthenium precursor **1a** (left) and **1b** (right).*

3.1.3 Influence of the reaction conditions

3.1.3.1 Catalyst concentration

Acceptorless dehydrogenative coupling of 1-butanol was carried out in the presence of different loadings of equimolar mixtures of ruthenium precursor $[RuH_2(CO)(PPh_3)_3]$ **1a** and PNP pincer ligand $(Cy_2PC_2H_4)_2NH$ **2b** (240, 100, 60 and 20 ppm).

For each catalyst concentration, the catalytic tests were duplicated to ensure reproducibility and accurate measurement of the reaction rate expressed as the initial turnover frequency, TOF_0. The reproducibility was found to be excellent with relative

error lower than 4 % on the TOF_0 measurement for catalysts loading higher than 20 ppm (see Fig. 3.5 for an example of reaction duplication and Table 3.2 for TOF_0 with error margin).

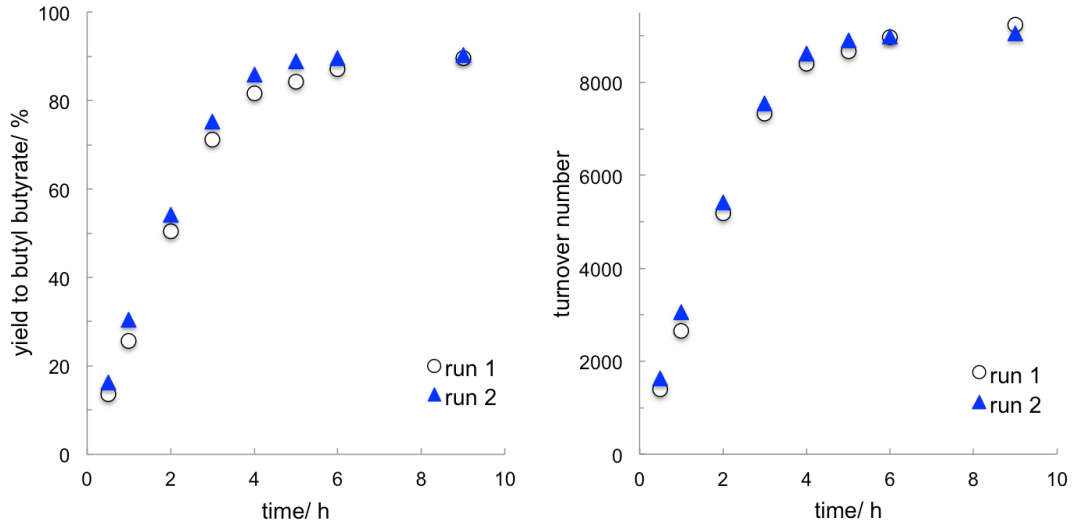

Fig. 3.5 *Evolution of the ester yield (left) and TON (right) as a function of time during the dehydrogenative coupling of 1-butanol catalysed by* ***1a/2b****, 100 ppm.*

At all the investigated loadings, the catalytic system formed by equimolar mixture of **1a** and **2b** was found to be very active. Decrease of the catalyst concentration leads, as expected, to a decrease of the general productivity. With a loading of 240 ppm, a yield of 99 % of ester was obtained after 3 h, while with a loading of 100 ppm, an ester yield of *ca.* 72 % was obtained after the same reaction time. With lower catalysts loadings of 59 ppm and 20 ppm, ester yields of 53 % and 24 % were obtained after the same reaction time (3 h), respectively. Evolution of the yield as a function of time at the different catalyst loading shows that the net ester production rate decrease with the catalyst loading indicating that reaction rate is dependent on the catalyst concentration (Fig. 3.6, left). One can also note that at catalyst loadings lower than 100 ppm, the ester production rate decreased before reaching high conversion indicating that catalyst deactivates after prolonged reaction time. This becomes more pronounced at very low loading, as observed with a 20 ppm catalyst loading, were a plateau is reached after 8 h of reaction. Nevertheless, turnover

number as high as 26900 could be obtained with a 20 ppm catalyst loading, evidencing the robustness of the catalytic system.

Surprisingly, when expressing the TON as a function of time for the different catalyst loading, one can observe that the lowest catalyst loading lead to the more active catalytic systems with higher TOF_0 (Fig. 3.6, right, Table 3.2). This suggests that the overall reaction kinetic is not first order relative to the catalyst concentration since this would lead to TOF_0 independant of the catalyst concentration. This could arise from "reservoir" effects with catalyst dimerisation and dissociation. However, one should bear in mind that since these results report on *in situ* catalysts, active catalysts may form as the reaction proceed and clear conclusions regarding kinetics cannot be drawn.

Table 3.2 *Influence of catalyst concentration on dehydrogenative coupling of 1-butanol catalysed by* ***1a/2b***[‡].

entry	[Ru] (ppm)	TOF_0 (h^{-1})	max. TON	max. yield (%)
1	242	1950 ± 76	4100 (3 h)	99.2 (3 h)
2	100	2708 ± 94	9050 (9 h)	90.3 (9 h)
3	59	3055 ± 4	14600 (9 h)	86.5 (9 h)
4	20	3802 ± 514	26900 (9 h)	52.6 (9 h)

[‡]standard conditions: catalyst: **1a/2b**; Ru / ligand: 1; applied temperature: 130 °C; under argon.

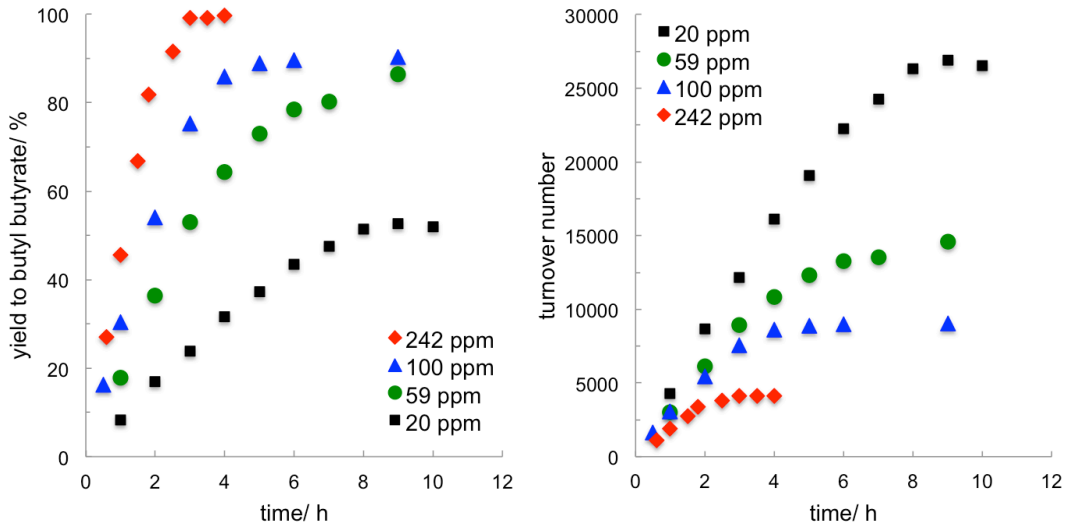

Fig. 3.6 *Evolution of the ester yield (left) and TON (right) as a function of time during the dehydrogenative coupling of 1-butanol catalysed by* ***1a/2b*** *at different loading.*

3.1.3.2 Reaction temperature

Acceptorless dehydrogenative coupling of 1-butanol in the presence of equimolar mixtures of $[RuH_2(CO)(PPh_3)_3]$ **1a** and PNP pincer ligand $(Cy_2PC_2H_4)_2NH$ **2b** (**1a** = **2b** = 240 ppm) was investigated at different reaction temperatures: 90, 110 and 130 °C (Table 3.3 and Fig. 3.7).

Table 3.3 *Influence of reaction temperature on dehydrogenative coupling of 1-butanol catalysed by* ***1a/2b***[‡].

entry	Ru / butanol	temp. (°C)	TOF_0 (h^{-1})	max. TON	max. yield (%)
1	242 ppm	130	1950 ± 76	4100 (3 h)	99.2 (3 h)
2	243 ppm	110	500	3800 (8 h)	90.5 (8 h)
3	240 ppm	90	100	1980 (20 h)	47.5 (20 h)

[‡]standard conditions: catalyst: **1a/2b**; Ru / ligand: 1; *V* (1-butanol): 10 mL; under argon; temperature refers to the applied temperature.

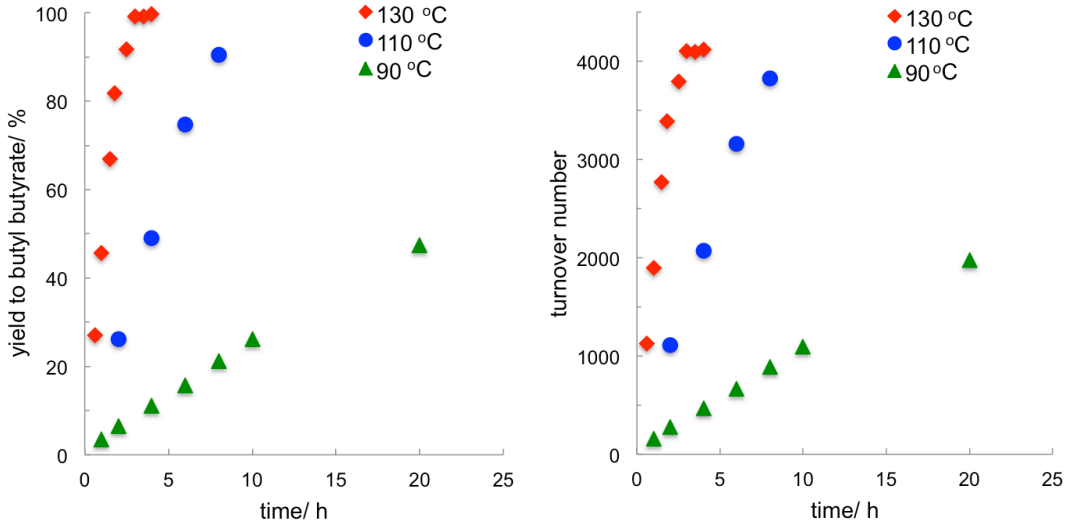

Fig. 3.7 *Evolution of the ester yield (left) and TON (right) as a function of time during the dehydrogenative coupling of 1-butanol catalysed by* ***1a/2b*** *at different temperatures.*

The catalytic system formed by **1a**/**2b** was found to be active at a temperature as low as 90 °C. As expected, lower reaction temperature leads to lower TOF_0.

From the TOF_0 obtained at different temperatures, the activation energy of acceptorless dehydrogenative coupling of 1-butanol using *in situ* formed catalyst **1a/2b** was calculated using Arrhenius equation (Eq. 3.1).

$$\ln TOF_0 = \frac{-E_a}{R}\frac{1}{T} + \ln A \qquad \textbf{Eq. 3.1}$$

(*T*, reaction temperature in kelvin; A, prefactor; R, ideal gas constant; E_a, activation energy)

In our case, ln TOF_0, 1/T is calculated as in Table 3.4.

Table 3.4 *Calculation of activation energy.*

entry	T (K)	TOF_0	ln TOF_0	1/T	E_a (kJ mol^{-1})
1	363.15	103.4	4.64	2.75E-03	
2	383.15	501.3	6.21	2.61E-03	89.4
3	403.15	1950	7.58	2.48E-03	

The slope of the linear regressions from the plot of ln TOF_0 as a function of 1/T is then given in Fig. 3.8. From the slope, the activation energy was calculated and was found to be equal to 89.4 kJ mol^{-1}.

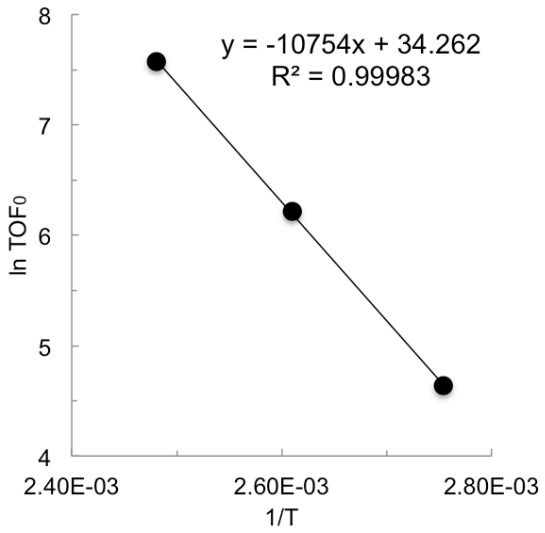

Fig. 3.8 *Linear regressions ln TOF_0 as a function of 1/T.*

Following the investigation on the influence of catalyst concentration and reaction temperature (3.1.3.1 and 3.1.3.2), we chose the following conditions as "benchmark" conditions: Ru/1-butanol : 240 ppm; applied temperature : 130 ^oC. These conditions allows obtaining simultaneously active catalysts ($TOF_0 \approx 2000\ h^{-1}$) and productive catalysts (yield > 90 %).

3.1.4 Other substrates

In addition to 1-butanol, 1-pentanol and 2-methyl-1-butanol were used as substrates. In the presence of equimolar mixtures of **1a** and **2b,** these substrates are readily converted into the corresponding esters (see Table 3.5 and Fig. 3.9).

Table 3.5 *Dehydrogenative coupling of different primary alcohols using catalyst* ***1a/2b***[‡].

entry	substrate	Ru / alcohol	TOF_0 (h^{-1})	max. TON	max. yield (%)
1	1-butanol	242 ppm	1950 ± 76	4100 (3 h)	99.2 (3 h)
2	1-pentanol	240 ppm	1660	3750 (5 h)	90.0 (5 h)
3	2-methylbutanol	232 ppm	1340	3650 (6 h)	84.4 (6 h)

[‡]standard conditions: catalyst: **1a/2b**; Ru / ligand: 1; *V* (alcohol): 10 mL; applied temperature: 130 °C; under argon.

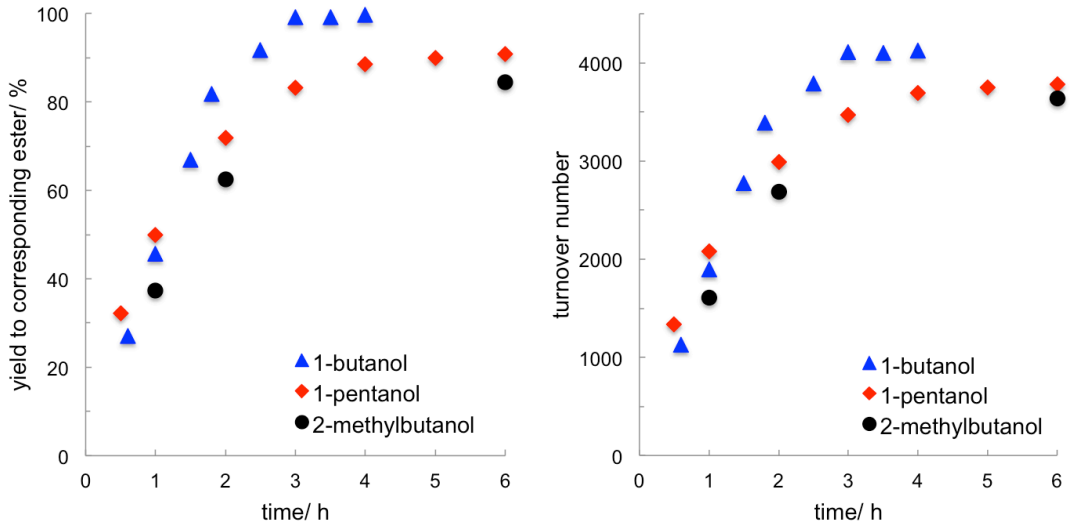

Fig. 3.9 *Evolution of the ester yield (left) and TON (right) as a function of time during the dehydrogenative coupling of different alcohols catalysed by* ***1a/2b.***

For all the three investigated alcohols, the catalytic system generated by equimolar mixture of **1a** and **2b** was found to be very active with initial turnover frequencies higher than 1300 h^{-1}. For 1-pentanol the activity was found to be slightly lower than for butanol with TOF_0 of 1660 h^{-1} and 1950 h^{-1}, respectively. For 2-methylbutanol the TOF_0 further drops to 1340 h^{-1}which is likely due to the superior steric hindrance of this branched alcohol. Nevertheless, a yield of 84.4 % can still be reached with this bulky alcohol after 6 h of reaction.

3.2 Isolated catalysts

Following our investigation on the use of *in situ* formed catalysts, we turned our attention to isolated and well-defined ruthenium PNP complexes for the acceptorless dehydrogenative coupling of primary alcohols.

3.2.1 Screening of isolated catalysts

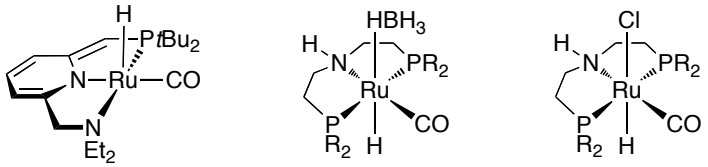

3 **4a, R = Ph** **4b, R = *i*Pr** **5a, R = Ph** **5b, R = *i*Pr** **5c, R = Cy**

Fig. 3.10 *Structures of isolated catalysts.*

As a starting point, we investigated the use of Milstein's dearomatized PNN catalyst **3** for the base-free acceptorless dehydrogenative coupling of 1-butanol (Fig. 3.10, entry 1 in Table 3.6 and Fig. 3.11). This catalyst was found to be an order of magnitude less active than our previousely developed *in situ* formed catalysts. Butyl butyrate yields of 19 % were obtained after 5 h of reaction using Milstein's catalyst **3** while almost quantitative yields were obtained after 3 h using catalyst **1a/2b** under identical conditions.

We then tested a series of isolated aliphatic Ru/PNP complexes (see structures in Fig. 3.10). Regarding their structure, the investigated complexes differ from the nature of the substituents at the phosphorus atoms, phenyl, iso-propyl or cyclohexyl, and the nature of the ligand *trans* to the hydride, chloride or borohydride.

Under base-free conditions, complexes bearing a borohydride ligand **4a** and **4b** proved to be very active for the dehydrogenative coupling of 1-butanol with TOF_0 ranging from 2500 h^{-1} to 2770 h^{-1} and quantitative yields were obtained after 3 h of reaction (Table 3.6 entries 2 and 3, Fig. 3.11). Moreover, at any reaction time, the

selectivity was found to be higher than 99 %, the reaction mixture being free of any side products, only containing unreacted 1-butanol and the desired ester.

Complexes having a chloride ligand **5a-5c** were found to be completely inactive in the absence of a base (Table 3.6, entries 4 to 6 and Fig. 3.11). Upon addition of sodium ethoxide (1.3 mol % relative to 1-butanol), these complexes led to catalytic systems displaying similar activity to borohydride complexes, **4a-b** (Table 3.6, entries 7 to 9 and Fig. 3.12). However, sodium ethoxide induced the formation of heavier alcohols via Guerbet reaction, and also led to the formation of a small amount of ethanol. These alcohols are detected in the reaction media as mixed esters with butanol accounting for ~2 % of the products, hence decreasing the reaction selectivity.

Table 3.6 *Dehydrogenative coupling of 1-butanol with isolated catalysts*[‡].

entry	cata. (Ru / butanol)	TOF_0 (h^{-1})	max. TON	max. yield (%)
1	**3** (241 ppm)	60	3550 (23 h)	85.4 (23 h)
2	**4a** (244 ppm)	2567 ± 62	3800 (3 h)	92.7 (3 h)
3	**4b** (262 ppm)	2770	3710 (3 h)	97.3 (3 h)
4	**5a** (218 ppm)	0	0	0
5	**5b** (236 ppm)	0	0	0
6	**5c** (249 ppm)	0	0	0
7[†]	**5a** (225 ppm)	2590	3770 (3 h)	84.9 (3 h)
8[†]	**5b** (233 ppm)	2470	3770 (3 h)	87.9 (3 h)
9[†]	**5c** (243 ppm)	2480	3930 (6 h)	95.6 (6 h)

[‡]standard conditions: *V* (1-butanol): 10 mL; applied temperature: 130 °C; under argon.

[†]in presence of 1.3 mol % NaOEt.

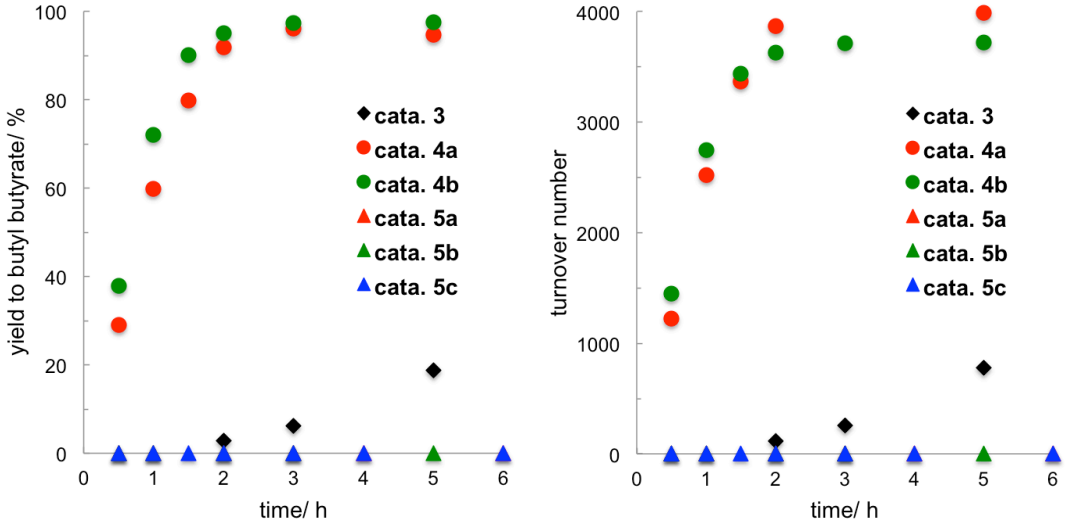

Fig. 3.11 *Evolution of the ester yield (left) and TON (right) as a function of time during the dehydrogenative coupling of 1-butanol catalysed by isolated catalysts* ***4a-b*** *and* ***5a-c*** *under base-free conditions.*

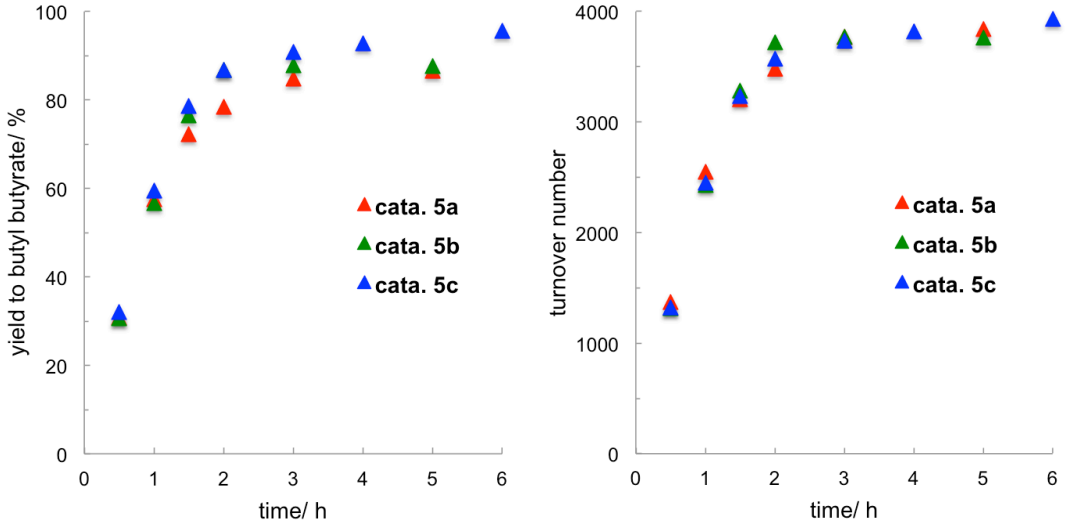

Fig. 3.12 *Evolution of the ester yield (left) and TON (right) as a function of time during the dehydrogenative coupling of 1-butanol catalysed by isolated catalysts* ***5a-c*** *with 1.3 mol % NaOEt.*

Presumably, complexes bearing borohydride ligand are transformed under reaction conditions into the putative active unsaturated monohydride amido ruthenium complex **A** by loss of borane and hydrogen. On the other hand, chloride complexes are stable under reaction conditions and a base is required to remove HCl to form the monohydride amido ruthenium complex **A** (Scheme 3.3).

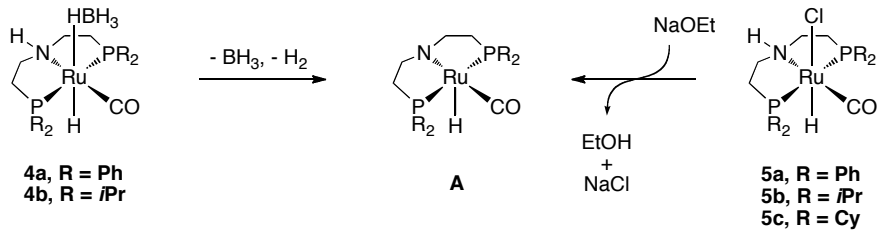

Scheme 3.3 *Formation of unsaturated monohydride amido ruthenium complex **A** from complexes **4a-b** and **5a-c**.*

No significant differences in activity were observed with variation of the substituents at the phosphorus atoms. For borohydride complexes, more electron donating *iso*-propyl phosphine led to only slightly more active catalyst than with less basic phenylphosphine (complex **4a** vs. **4b**; Table 3.6 entry 2 vs. 3). For hydridochloro ruthenium complexes **5a-c**, almost no differences in activity were observed indicating the very little influence of the phosphorus substituents on the catalyst activity (Table 3.6, entries 7 to 9).

3.2.2 Influence of catalyst concentration

Having established that aliphatic PNP pincer ruthenium complexes bearing HBH_3 ligand are very active catalysts under base-free conditions for the acceptorless dehydrogenative coupling of 1-butanol, we investigated the influence of the catalyst concentration on the reaction. Therefore, acceptorless dehydrogenative coupling of 1-butanol was carried out with four different loadings of complex **4a**: 500, 240, 100 and 20 ppm (Table 3.7 and Fig. 3.14). For each catalyst concentration, the catalytic tests were duplicated to ensure reproducibility and accurate measurment of the reaction rate expressed as the initial turnover frequency, TOF_0. The reproducibility was found to be excellent with relative error lower than 3 % on the TOF_0 measurement for catalysts loading higher than 20 ppm (see Fig. 3.13 for an example of reaction duplication and Table 3.7 for TOF_0 with error margin).

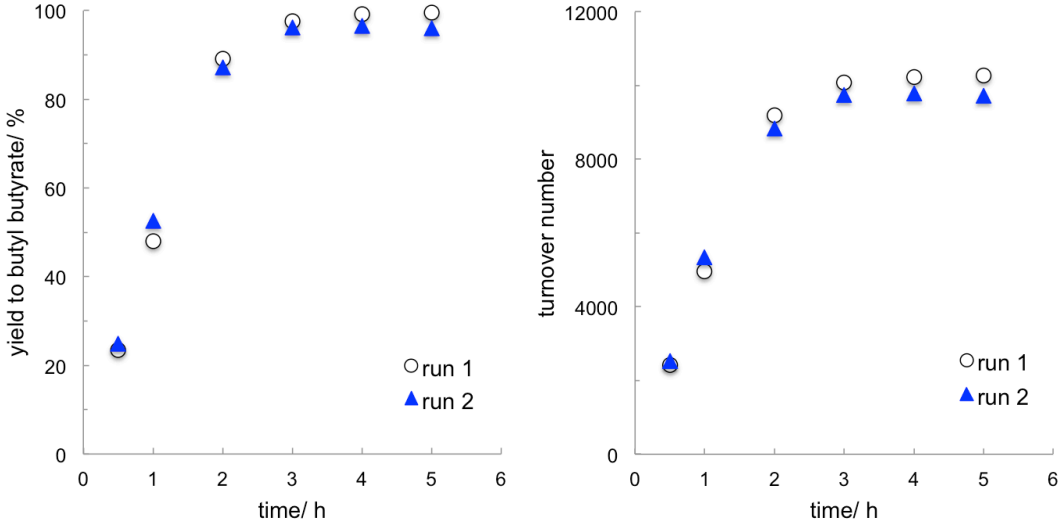

Fig. 3.13 *Evolution of the ester yield (left) and TON (right) as a function of time during the dehydrogenative coupling of 1-butanol catalysed by* ***4a****, 100 ppm.*

Very similar behaviour regarding the influence of catalyst concentration is observed with the *in situ* formed catalyst described above and isolated catalyst **4a** (see 3.1.3.1). Firstly, catalyst **4a** was found to be very active at all the investigated loadings. Secondly, the ester productivity was found, as expected, to decrease with decreasing the catalyst loading. With a loading of 500 ppm, a yield of 100 % of ester is obtained after 2 h, while with a loading of 240 ppm an ester yield of *ca.* 90 % is obtained after the same reaction time. With lower catalysts loadings of 100 ppm and 20 ppm, ester yields of 88 % and 70 % are obtained after 2 h and 9 h of reaction, respectively. The evolution of the yield as a function of time at the different catalyst loading shows that the net ester production rate decrease with the catalyst loading indicating that the reaction rate is dependant on the catalyst concentration (Fig. 3.14, left). One can also note that at very low catalyst loading, *i.e.* 20 ppm, the ester production rate decreases before reaching high conversion indicating that catalyst deactivates after prolonged reaction time. Nevertheless, turnover number as high as 35000 could be obtained at a 20 ppm catalyst loading, evidencing the robustness of the catalytic system.

Finally, when expressing the TON as a function of time for the different catalyst loading, one can again observe that the lower catalyst loading led to the more active catalytic systems with higher TOF_0 (Fig. 3.14, right and Table 3.7). As for *in situ* formed catalysts, this suggests that the overall reaction kinetic is not first order relative to the catalyst concentration since this would lead to TOF_0 independant of the catalyst concentration. This could arise from "reservoir" effects, were lower catalyst loading favours the dissociation of catalyst aggregates (dimers, etc) toward single active complexes. No evidences of such "dormant" catalytic species were found. Another possible explanation of this effect is that the reaction rate is limited by the hydrogen diffusion out of the liquid phase at higher catalyst loading while at very low catalyst loading the reaction rate is governed by chemical kinetics.

Table 3.7 *Influence of catalyst concentration on dehydrogenative coupling of 1-butanol catalysed by* ***4a***[‡].

entry	cata. conc. (ppm)	TOF_0 (h^{-1})	max. TON	max. yield (%)
1	507	2172 ± 41	1972 (2 h)	100 (2 h)
2	244	2567 ± 62	3800 (3 h)	92.7 (3 h)
3	99	4652 ± 28	9750 (3 h)	96.2 (3 h)
4	20	8171 ± 1098	35000 (8 h)	69.0 (8 h)

[‡]standard conditions: catalyst: **4a**; applied temperature: 130 °C; under argon.

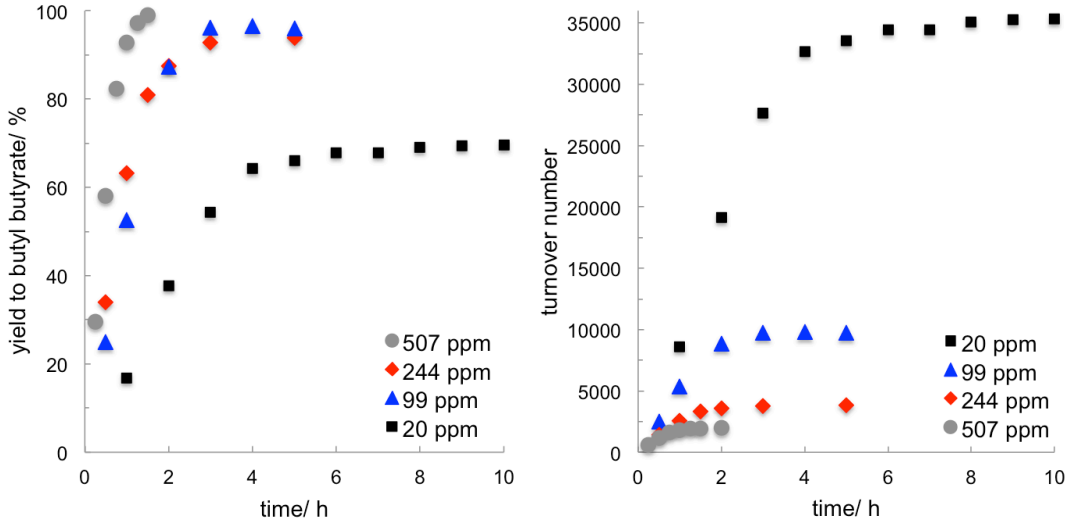

Fig. 3.14 *Evolution of the ester yield (left) and TON (right) as a function of time during the dehydrogenative coupling of 1-butanol catalysed by* ***4a*** *at different loading.*

3.2.3 Stability to water and air

Aliphatic PNP pincer ruthenium complexes bearing HBH_3 ligand are very active, selective and robust catalysts for the base-free acceptorless dehydrogenative coupling of primary alcohols. However, in order to be used for industrial production of esters, one important feature is their activity and stability in the presence of water and oxygen, which would avoid special handling care and intensive substrate purification. Therefore, we tested the activity of complex **4a** using 1-butanol without prior drying nor degassing hence containing dissolved oxygen and *ca.* 1000 ppm of water (determined by Karl-Fischer titration). Moreover, the reaction was conducted under air, without a protective argon atmosphere. Under these conditions, the catalyst displayed the same activity as when thoroughly degassed and dried 1-butanol (water content of *ca.* 8 ppm, determined by Karl-Fischer titration) was used as substrate and the reaction carried out under argon atmosphere (Table 3.8, entries 1 and 2; Fig. 3.15). In another test, catalyst **4a** was left standing in air for 6 days and was then tested for the acceptorless dehydrogenative coupling of non-purified 1-butanol. Under these conditions, catalysts **4a** displayed almost identical activity as when carefully stored and handled and using degassed and dried 1-butanol. Only a slight decrease of the TOF_0 and the maximum yield obtained could be observed (Table 3.8, entries 1 and 3; Fig. 3.15) .

These results illustrate the robustness of catalyst **4a** and indicate that it does not required intensive substrate purification nor special handling. This relative stability together with the high activity and selectivity make it a promising catalyst for industrial application.

Table 3.8 *Stability of catalyst **4a** to water and air in the dehydrogenative coupling of 1-butanol.*

entry	Ru / butanol	TOF_0 (h^{-1})	max. TON	max. yield (%)
1[‡]	244 ppm	2567 ± 62	3800 (3 h)	92.7 (3 h)
2[†]	252 ppm	2670	3670 (3 h)	92.5 (3 h)
3[§]	253 ppm	2130	3630 (3 h)	91.7 (3 h)

[‡]standard conditions: catalyst: **4a**; *V* (1-butanol): 10 mL; applied temperature: 130 °C; under argon.

[†]non-purified nor degassed 1-butanol (~1000 ppm water) was used, reaction performed under air.

[§]catalyst **4a** was aged in air for 6 days, non-purified nor degassed 1-butanol (~1000 ppm water) was used, reaction performed under air.

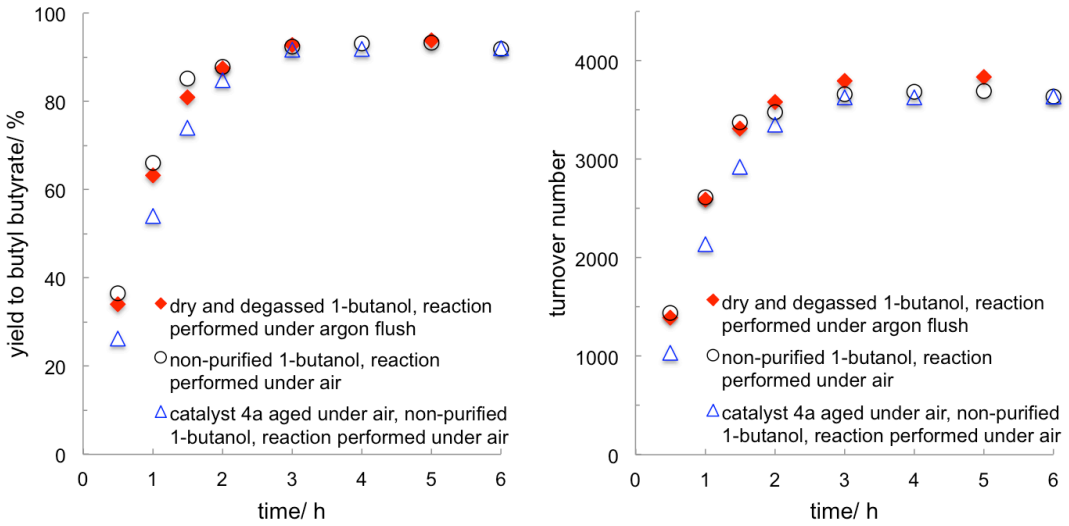

Fig. 3.15 *Evolution of the ester yield (left) and TON (right) as a function of time during the dehydrogenative coupling of 1-butanol catalysed by **4a** under different reaction conditions.*

3.2.4 Other substrates

In addition to 1-butanol, other alcohols such as 1-pentanol, 1-octanol 1-tetradecanol, 2-methyl-1-butanol and 2-ethyl-1-hexanol were also used as substrates for the acceptorless dehydrogenative coupling reaction in the presence of complex **4a** (Table 3.9 and Fig. 3.16). All these substrates were efficiently and selectively transformed into the corresponding symetrical esters in the presence of **4a**.

Compared with 1-butanol, heavier linear alcohols such as 1-pentanol, 1-octanol and 1-tetradecanol were transformed at slightly higher rate (entries 2-4 in Table 3.9). This may reflect a difference in reaction temperature since the applied temperature, 130 °C , is lower than the boiling point of these alcohols while butanol refluxes at

118 °C. Hence reaction temperature would be 130 °C for alcohols > C_5 and lower for butanol, *ca.* 118 °C. For branched primary alcohols such as 2-methyl-1-butanol and 2-ethyl-1-hexanol, the reaction rate, as expressed by the initial TOF_0 was found to be much lower than for 1-butanol, ranging from 1280 h^{-1} to 1640 h^{-1} for branched alcohol and 2567 h^{-1} for 1-butanol (Table 3.9, entries 1, 5 and 6). This may be due to the increased steric hindrance in the vicinity of the reacting alcohol function for the branched alcohols compared with the linear primary alcohols.

Table 3.9 *Dehydrogenative coupling of various primary alcohols catalysed by* ***4a***[‡].

entry	substrate	Ru / alcohol	TOF_0 (h^{-1})	max. TON	max. yield (%)
1	1-butanol	244 ppm	2567 ± 62	3800 (3 h)	92.7 (3 h)
2	1-pentanol	243 ppm	2380	3800 (3 h)	92.7 (3 h)
3	1-octanol	240 ppm	3230	3840 (4 h)	92.1 (4 h)
4	1-tetradecanol	225 ppm	3070	4200 (4 h)	94.2 (4 h)
5	2-methyl-1-butanol	238 ppm	1280	3600 (6 h)	85.8 (6 h)
6	2-ethyl-1-hexanol	234 ppm	1640	3860 (5 h)	90.5 (5 h)

[‡]standard conditions: catalyst: **4a**; *V* (alcohol): 10 mL; applied temperature: 130 °C; under argon.

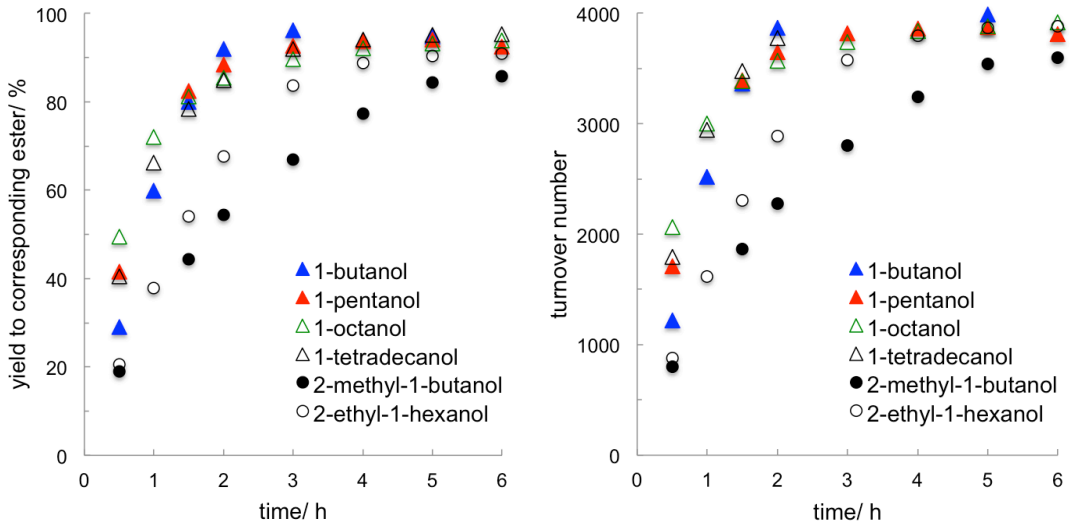

Fig. 3.16 *Evolution of the ester yield (left) and TON (right) as a function of time during the dehydrogenative coupling of various primary alcohols catalysed by* ***4a****.*

3.2.5 Production of butyraldehyde

For all the previousely described acceptorless dehydrogenative coupling reactions, ester is observed as the sole organic product. In some cases, traces of the intermediate aldehyde are detected but account for less than 1 % of the reaction mixture. Since all the reactions were performed under neat conditions, the intermediate aldehyde is instantly trapped by an alcohol molecule to give an hemiacetal that is quickly dehydrogenated to give the ester.

In order to produce aldehydes instead of esters, the formation of the intermediate hemiacetal needs to be impeded, which can be done by dilution of the reaction medium. Moreover, to avoid the reverse reaction, hydrogenation of the aldehyde, the ruthenium dihydride needs to be trapped using a sacrificial hydrogen acceptor.

Therefore, the dehydrogenation of 1-butanol using **4a** was carried in the presence of different amount of acetone acting as both a hydrogen acceptor and a diluent (Table 3.10 and Fig. 3.17).

Interestingly, when 5 mL acetone is added, butyl butyrate is observed as the final major product (entry 1 in Table 3.10 and Fig. 3.17, left). However, at the beginning of the reaction butylraldehyde is the major product with a yield of 18.8 % while the yield of buryl butyrate is 13.0 % after 15 minutes of reaction. As the reaction proceeds, the amount of butyraldehyde decreases while the yield to butyl butyrate increases overtime. This indicates that even with addition of 5 mL acetone, butyaldehyde can still react with 1-butanol to give the hemiacetal that is dehydrogenated to butyl butyrate. However, compared with neat conditions, the final amount of butyraldehyde is larger in presence of 5 mL acetone indicating that hemiacetal formation is slowed down to some extend.

When a larger amount of acetone is used, *i.e.* 90 mL, butyraldehyde is obtained as the major final product (Table 3.10 and Fig. 3.17, right). At the beginning of the reaction, butyraldehyde is obtained as the sole product. A small amount of ester builds

up only at the end of the reaction after 66 % of the alcohol was converted to the aldehyde. Interestingly, for both reaction conditions, 5 or 90 mL acetone, the total yield at different reaction time are similar indicating the catalyst activities seems unchanged by addition of a large amount of acetone.

The similar catalyst activity and opposite products distribution illustrate that addition of large excess of acetone successfully inhibit reactions between produced buryaldehyde and 1-butanol. At the end of the reaction, the yield to aldehyde reaches 70.0 % while the yield to ester is kept as low as 5.1 %.

In addition to the possibility of switching reaction product distribution, these results strongly support aldehyde as being an intermediate for esters formation from alcohols.

Table 3.10 *Production of butyraldehyde by 1-butanol dehydrogenation using catalyst* ***4a***[‡].

entry	Ru / butanol	reaction time (h)	yield to butyraldehyde (%)	yield to butyl butyrate (%)	TON
1[†]	0.958 %	0.25	18.8	13.0	33
		0.5	12.7	30.3	45
		1	10.4	49.9	63
		2	7.0	58.6	68
		3	6.2	70.9	80
2[§]	1.06 %	0.5	48.7	0.0	46
		1	66.4	0.0	62
		2	72.5	2.9	71
		3	70.4	3.8	70
		4	68.7	4.3	69
		5	70.0	5.1	71

[‡]standard conditions: catalyst: **4a**; *V* (1-butanol): 0.1 mL; applied temperature: 60 °C; under argon.

[†]5 mL acetone is used.

[§]90 mL acetone is used.

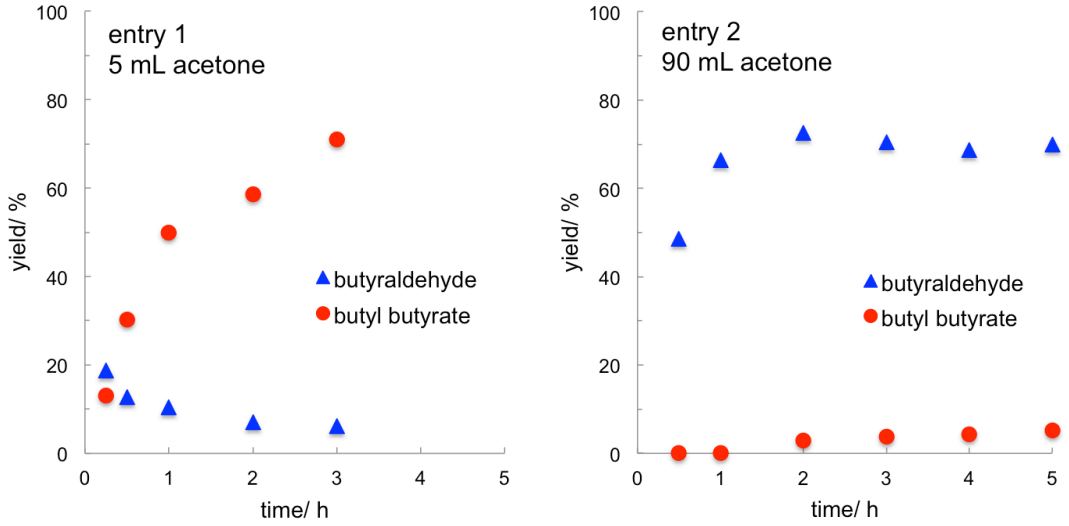

Fig. 3.17 *Evolution of the ester and aldehyde yield as a function of time during the transformation of 1-butanol catalysed by* ***4a*** *in the presence of added acetone, 5 mL (left) and 90 mL (right).*

3.2.6 Acceptorless dehydrogenative coupling of ethanol

Having estabilised the use of aliphatic PNP pincer ruthenium complexes with borohydrides ligands as efficient catalyst for the base-free acceptorless dehydrogenative coupling of primary alcohol such as 1-butanol and heavier ones, we investigated the transformation of ethanol. Due to its lower boiling point and its ease of decarbonylation, ethanol represents the most challenging substrate among all primary alcohols and its dehydrogenation under neat and neutral conditions remains an unsolved challenge (see chapter 1, 1.4.5).

The acceptorless dehydrogenative coupling of ethanol was carried out using the isolated catalyst **4a** under neat and neutral conditions (Table 3.11 and Fig. 3.18). To our delight, using a catalyst loading of 500 ppm, a yield higher than 90 % was obtained after 24 h of reaction, ethyl acetate being the sole reaction product. Moreover, the catalyst displayed a good activity under these mild conditions with a TOF_0 of 175 ± 2 h^{-1} and show no sign of deactivation with a steady increase of the TON with time (Fig. 3.18, right).These good results were confirmed by duplication of the experiment.

It is noteworthy that, to the best of our knowledge, this is the first example for such high yield to ethyl acetate for the acceptorless dehydrogenative coupling of ethanol under neat and neutral conditions.

Table 3.11 *Acceptorless dehydrogenation coupling of ethanol*[‡].

entry	Ru / ethanol	TOF_0 (h^{-1})	max. yield to ethyl acetate (%)	max. TON
run 1	527 ppm	175 ± 2	96.4 (24 h)	1830 (24 h)
run 2	505 ppm		90.3 (24 h)	1790 (24 h)

[‡]standard conditions: catalyst: **4a**; *V* (ethanol): 10 mL, applied temperature: 90 °C; under argon.

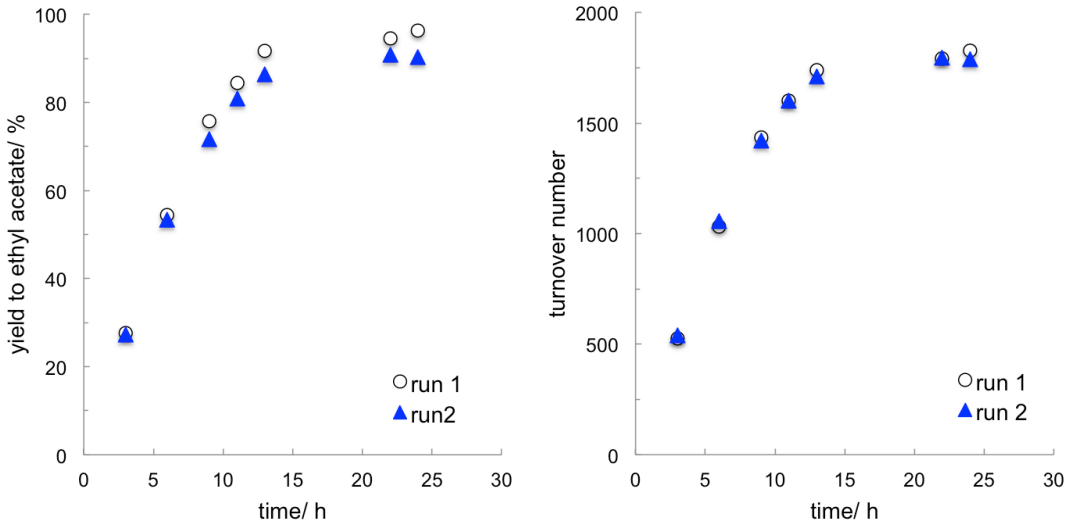

Fig. 3.18 *Evolution of the ester yield (left) and TON (right) as a function of time during the dehydrogenative coupling of ethanol catalysed by* ***4a***.

3.3 Conclusion

Two types of ruthenium-based catalysts, *in situ* formed and isolated catalysts, were studied for the acceptorless dehydrogenative coupling of primary alcohols. Using 1-butanol as model substrate, the catalyst structure was systematically varied and optimized. For both *in situ* formed and isolated catalysts, both the reaction conditions such as catalyst loading and reaction temperature were studied and optimized for the acceptorless dehydrogenative coupling reaction under neat and neutral conditions. Acceptorless dehydrogenative couplings of other primary alcohols (such as 1-pentanol and 2-methyl-1-butanol) were also tested. Moreover, isolated catalyst stability to water and air was studied. Reaction conditions were modified, by addition of a large excess of an "hydrogen accepting solvent", namely acetone, to

switch the selectiviy toward aldehyde production. Dehydrogenation of ethanol with high yield was finally performed under neat and neutral conditions.

Studies on *in situ* formed catalysts showed that the presence of a PNP ligand is crucial to ensure the conversion of 1-butanol to butyl butyrate. By using dihydride phosphinoruthenium complexes such as $[RuH_2(CO)(PPh_3)_3]$ **1a** or $[RuH_2(PPh_3)_4]$ **1b** without a non-innocent PNP ligand, no 1-butanol conversion was observed under the investigated reaction conditions. Addition of one equivalent of an aliphatic PNP ligand having alkyl substituents at the phosphorus led to the *in situ* formation of very active catalysts for the acceptorless dehydrogenative coupling of 1-butanol under base-free conditions. The catalyst loading could be decreased down to 20 ppm allowing to reach TON up to 26000. Influence of the catalyst concentration upon the reaction is unclear, improvement of the TOF_0 with decrease of the catalyst concentration suggests that the order relative to the catalyst concentration is lower than 1. This may arise from catalyst aggregate dissociation, *ie.* reservoir effect. Study of the reaction at different temperatures indicated that *in situ* formed catalysts are still active at 90°C. From an Arrhenius plot, an apparent activation of 89.4 kJ mol^{-1} was found.

For isolated catalysts, two families of complexes differing from the nature of the ligand *trans* to the hydride were investigated. Complexes bearing a chloride ligand were found to be inactive in absence of base while complexes bearing a borohydride are very active catalysts for the base-free dehydrogenative coupling of 1-butanol. The presence of a base is an essential factor for the activation of complexes bearing a chloride while complexes bearing a borohydride can self activate without any other additives. The use of sodium ethoxide induced base catalysed side reactions that resulted in the decrease of reaction selectivity. Activity of the isolated catalysts system was found to be unaffected by the nature of the substituent at the phosphorus atoms on the PNP ligand (phenyl, iso-propyl or cyclohexyl).

As observed for *in situ* formed catalysts, catalyst concentration strongly affects the reaction kinetics. An increase of the TOF_0 with decrease of the catalyst concentration was also observed. This may arise from a reservoir effect or alternatively from limitation of the reaction rate by hydrogen diffusion at high catalyst loadings.

Besides 1-butanol, both *in situ* formed and isolated catalysts are very active for the dehydrogenative coupling of other primary alcohols. For *in situ* formed catalyst, 1-pentanol and 2-methyl-1-butanol were tested; for isolated catalyst, 1-pentanol, 1-octanol, 1-tetradecanol, 2-methylbutanol and 2-ethylhexanol were investigated. Compared with 1-butanol, higher linear alcohols such as 1-pentanol, 1-octanol and 1-tetradecanol are transformed at similar rate, while branched primary alcohols such as 2-methylbutanol and 2-ethylhexanol are transformed at lower rate presumably due to increased steric hinderance.

The stability of the isolated catalyst was evidenced for catalyst **4a**. It was found to be stable to some extent to air and water, remaining active with non dried nor degassed substrate. Moreover the reaction could be carried out under air and the catalyst remained active even after exposure to air and moisture for 6 days.

Using a large amount of acetone as a "hydrogen accepting solvent", the product distribution could be dramatically switched from pure butyl butyrate to mainly butyraldehyde. This could be explained by inhibition of the reaction between the aldehyde and the alcohol by dilution and consumption of the ruthenium dihydride by the hydrogen acceptor. These results strongly evidence aldehyde as an intermediate for esters formation from alcohols. Moreover, aldehydes production can therefore be conducted on isolated catalyst **4a**.

Finally, catalyst **4a** was shown as the first efficient catalyst for ethanol dehydrogenation to ethyl acetate under neat and neutral conditions.

3.4 References

[1] J. Zhang, G. Leitus, Y. Ben-David, D. Milstein, *J. Am. Chem. Soc.* **2005**, *127*, 10840-10841.

[2] J. Zhang, M. Gandelman, L. J. W. Shimon, D. Milstein, *Dalton. Trans.* **2007**, 107-113.

[3] C. Gunanathan, L. J. W. Shimon, D. Milstein, *J. Am. Chem. Soc.* **2009**, *131*, 3146-3147.

[4] J. Zhang, E. Balaraman, G. Leitus, D. Milstein, *Organometallics* **2011**, *30*, 5716-5724.

[5] M. Bertoli, A. Choualeb, D. G. Gusev, A. J. Lough, Q. Major, B. Moore, *Dalton. Trans.* **2011**, *40*, 8941-8949.

[6] M. Bertoli, A. Choualeb, A. J. Lough, B. Moore, D. Spasyuk, D. G. Gusev, *Organometallics* **2011**, *30*, 3479-3482.

[7] M. Nielsen, A. Kammer, D. Cozzula, H. Junge, S. Gladiali, M. Beller, *Angew. Chem. Int. Ed.* **2011**, *50*, 9593-9597.

[8] M. Nielsen, H. Junge, A. Kammer, M. Beller, *Angew. Chem. Int. Ed.* **2012**, *51*, 5711-5713.

[9] M. H. G. Prechtl, K. Wobser, N. Theyssen, Y. Ben-David, D. Milstein, W. Leitner, *Catal. Sci. Technol.* **2012**, *2*, 2039-2042.

[10] E. Fogler, M. A. Iron, J. Zhang, Y. Ben-David, Y. Diskin−Posner, G. Leitus, L. J. W. Shimon, D. Milstein, *Inorg. Chem.* **2013**, *52*, 11469-11479.

[11] R. Langer, I. Fuchs, M. Vogt, E. Balaraman, Y. Diskin-Posner, L. J. W. Shimon, Y. Ben-David, D. Milstein, *Chem. Eur. J.* **2013**, *19*, 3407-3414.

[12] D. Spasyuk, D. G. Gusev, *Organometallics* **2012**, *31*, 5239-5242.

[13] D. Spasyuk, S. Smith, D. G. Gusev, *Angew. Chem. Int. Ed.* **2012**, *51*, 2772-2775.

[14] D. Spasyuk, S. Smith, D. G. Gusev, *Angew. Chem. Int. Ed.* **2013**, *52*, 2538-2542.

Chapter 4 Acceptorless dehydrogenation of alcohols to corresponding acid salts

Acceptorless dehydrogenation of alcohols to corresponding acid salts is an attractive novel catalytic transformation developed in 2013[1] (Scheme 4.1, see chapter 1, 1.5). Compared with the traditional method for alcohol oxidation, no toxic solvent or strong oxidant is used. Instead, water acts, under basic conditions, as oxygen atom source and hydrogen gas is produced as the only co-product.

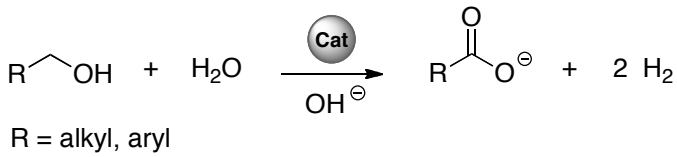

Scheme 4.1 *Acceptorless dehydrogenation of alcohols to corresponding acid salts.*

For this transformation, Milstein *et al* reported the use of an aromatic PNN pincer ruthenium complex (Scheme 4.2). For this system, the authors proposed that reaction network follows a dehydrogenative coupling sequence. The alcohol is dehydrogenated to give an aldehyde that reacts with water to give a hydrate that is finally dehydrogenated to give the carboxylic acid product, which is deprotonated in the basic reaction medium (Scheme 4.2).

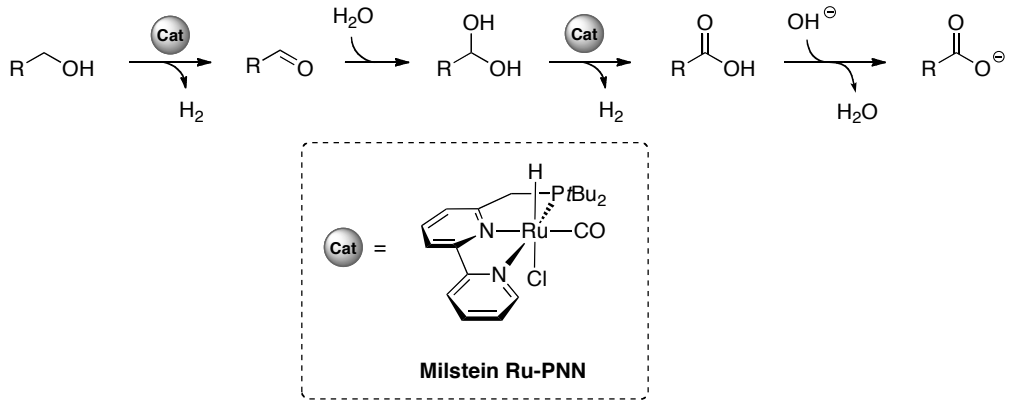

Scheme 4.2 *Reaction network for the acceptorless dehydrogenation of alcohols to corresponding acid salts.*

While high yield can be obtained with Milstein's PNN complex, namely 84 % yield to butyl butyrate after 18 h using 0.2 mol % of catalyst, the reaction rate is rather low (calculated TOF for butanol: 23.3 h^{-1})[1]. Moreover, the authors pointed out that the catalyst is oxygen sensitive ("resulting in decomposition and thus lower conversions"), limiting its practical use.

In this chapter, the use of two types of catalysts, *in situ* formed and isolated, are investigated for the dehydrogenation of alcohol to carboxylate salts. The *in situ* formed catalysts consist of a ruthenium precursor with an equimolar amount of a PNP ligand, which, as shown in Chapter 3, are transformed into a ruthenium PNP pincer complex under reaction conditions. The isolated catalysts refer to well-defined ruthenim PNP pincer complexes.

In addition, both types of catalysts, *in situ* formed and isolated, were also used for the selective deuteration of alcohols.

4.1 Screening of catalysts

4.1.1 *In situ* formed catalysts

As shown in section 3.1.1, PNP ligands are able to substitute monodentate phosphines from ruthenium complexes in 1-butanol under reflux. These *in situ* formed catalysts were used for the acceptorless dehydrogenative coupling of 1-butanol (see section 3.1.2). Herein, we further used these *in situ* formed catalysts for the acceptorless dehydrogenation of 1-butanol to butyric acid salt as a model reaction. Five ruthenium precursors and four PNP ligands were used to generate a large set of *in situ* formed catalysts (see structures in Fig. 4.1).

Ruthenium precursors

$[RuHX(CO)(PPh_3)_3]$	$[RuHX(PPh_3)_4]$	$[RuCl_2(p\text{-cymene})]_2$
1a; X = H **1b**; X = Cl	**2a**; X = H **2b**; X = Cl	**3**

PNP ligands

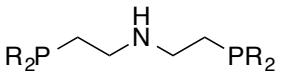

4a; R = Ph
4b; R = *i*Pr
4c: R = Cy
4d: R = *t*Bu

Fig. 4.1 *Structures of ruthenium precursors and PNP ligands used for the in situ formed catalysts.*

The reactions were carried out using an equimolar mixture of the ruthenium precursor with the PNP ligand at a catalyst loading of 1000 ppm. Water (2 mL) and base (1 equivalent to butanol) were added and the system refluxed for 3 h.

Table 4.1 *Dehydrogenation of 1-butanol to butyric acid salts catalysed by in situ formed catalysts*[‡].

entry	Ru	ligand	Ru / butanol	yield to butyric acid (%)	TOF_{3h} (h^{-1})
1	/	/	/	0	0
2	**1a**	/	1005 ppm	0	0
3	**1b**	/	966 ppm	0	0
4	**2a**	/	977 ppm	0	0
5	**2b**	/	971 ppm	0	0
6	**3**	/	1007 ppm	0	0
7	**1a**	**4a**	1025 ppm	69.6	226
8		**4b**	1003 ppm	81.6	271
9		**4c**	1019 ppm	80.1	262
10		**4d**	999 ppm	10.6	35
11	**1b**	**4b**	1003 ppm	80.7	268
12		**4c**	989 ppm	75.6	255
13	**2a**	**4b**	970 ppm	75.2	258
14		**4c**	976 ppm	55.9	191
15	**2b**	**4b**	997 ppm	65.9	220
16		**4c**	973 ppm	54.7	188
17	**3**	**4b**	953 ppm	64.1	224
18		**4c**	995 ppm	58.3	195

[‡]reaction conditions: *V* (1-butanol): 5 mL; *V* (water): 2 mL; *m* (NaOH): 2.19 g; 3 h; reflux under argon. For *in situ* formed catalysts, sodium hydroxide and water were added 2 minutes after the heating of Ru precursor and equimolar ligand in 1-butanol at applied temperature 130 °C.

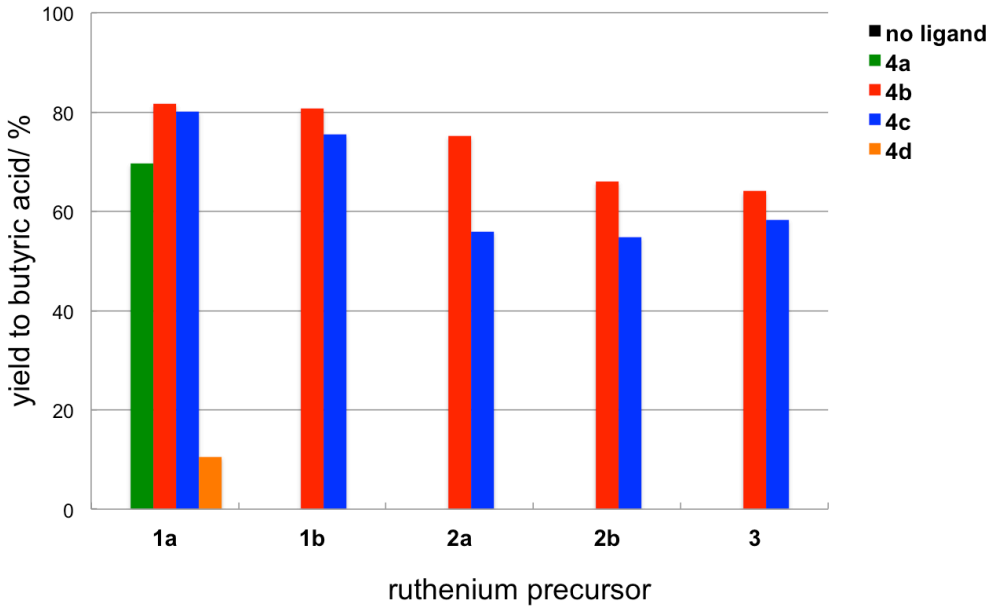

Fig. 4.2 *Dehydrogenation of 1-butanol to butyric acid salts catalysed by in situ formed catalysts.*

Without addition of catalyst, no conversion of 1-butanol was observed under the reaction conditions (Table 4.1, entry 1). Also, when the ruthenium precursors **1a-b**, **2a-b** or **3** were used without additional PNP ligand, no conversion of 1-butanol was observed under the reaction conditions (Table 4.1, entries 2-6). When any of the ruthenium precursors **1a-b**, **2a-b** or **3** were used with any of the PNP ligands **4a-d**, 1-butanol was converted to butyrate salt with yields ranging from 10 to 80 % (Table 4.1, entries 7-18; Fig. 4.2). Moreover, the selectivity for each catalyst was found to be higher than 99 %, the reaction mixture being free of any side products, only containing unreacted 1-butanol and the desired butyric acid (Moreover, all carbon balances were found to be in the range of 100 ± 7 %, for analysis, the produced sodium butyrate was treated with HCl and thus presented as free acid, see details in 2.3.2, chapter 2).

This suggests that PNP ligands are crucial to ensure reactivity. Moreover, as observed for dehydrogenative coupling, one can imagine that under reaction conditions, the PNP ligand is bound to the ruthenium by replacing phosphine or cymene ligands from the precursors to form active ruthenium PNP pincer complexes.

When comparing the use of different ligands with ruthenium precursor **1a**, one can observe that the nature of the substituents at the phosphorus atoms has an impact on the reactivity of the resulting catalyst. Yields higher than 80 % can be obtained with electron donating PNP ligand **4b** and **4c** having *iso*-propyl and cyclohexyl substituents respectively (Table 4.1, entries 8 and 9 and Fig. 4.2). A lower yield of 70 % was obtained with the PNP ligand **4a** having electron withdrawing phenyl substituent (Table 4.1, entry 7 and Fig. 4.2). Use of the bulky PNP ligand **4d** resulted in an impressive drop in catalyst activity, *i.e.* 10 % yield, presumably due to the increased steric hinderance of the ligand (Table 4.1, entry 10 and Fig. 4.2). Use of ligand **4b** and **4c** together with other precursors **1b**, **2a-b** and **3** resulted in active catalysts allowing obtaining butyric acid salt with yields ranging from 55 to 75 % (Table 4.1, entries 11-18 and Fig. 4.2). Moreover, with all ruthenium presursors, ligand **4b** gave more active catalysts compare to ligand **4c** presumably due to reduced steric hindrance of the *iso*-propyl group (Table 4.1, entry 8 vs. 9, 11 vs. 12, 13 vs.14, 15 vs. 16 and 17 vs.18; and Fig. 4.2).

With PNP ligands **4b** and **4c**, all ruthenium precursors led to active catalysts. However, differences in activity are observed depending on the precursor structure. Carbonyl ruthenium complexes $[RuH_2(CO)(PPh_3)_3]$ **1a** and $[RuHCl(CO)(PPh_3)_3]$ **1b** gave the more active catalysts (Table 4.1, entries 8, 9, 11 and 12; Fig. 4.2). Substitution of one of the hydride by a chloride did not have a significant impact on the catalyst activity with yields between 75 and 80 % obtained with dihydride and hydridochloride ruthenium complexes **1a** and **1b** (entries 8 vs.11 and 9 vs.12; Fig. 4.2). Substitution of the carbonyl in **1a-b** by a triphenylphosphine as in precursors $[RuH_2(PPh_3)_4]$ **2a** and $[RuHCl(PPh_3)_4]$ **2b** led to less active catalysts giving butyric acid salt yields ranging from 55 to 75 % (Table 4.1, entries 13-16; Fig. 4.2). For these precursors, substitution of an hydride by a chloride led to a decrease in catalyst activity only with PNP ligand **4b** (Table 4.1, entries 13 vs.15 and 14 vs.16; Fig. 4.2). The ruthenium dimer **3** gave catalysts with similar activities to ruthenium complex

[$RuHCl(PPh_3)_4$] **2b** (Table 4.1, entries 17 and 18; Fig. 4.2)**.** This suggests that *p*-cymene ligand can readily be replaced by the PNP ligands under reaction conditions and that the presence of an hydride on the ruthenium precursor is not required to ensure formation of an active catalyst.

4.1.2 Isolated catalysts

Following our investigation on *in situ* formed catalysts, we then studied the use of well-defined and isolated ruthenium PNP complexes for acceptorless dehydrogenation alcohols to carboxylic acid salt.

A small library of related carbonyl ruthenium PNP pincer complexes **5a-c**, **6a-b**, **7b** as well as trimethylphosphinoruthenium dichloride PNP pincer complex **8b** and Schneider's ruthenium PNP pincer dimer **9b** were used for the dehydrogenation of 1-butanol to butyric acid salt as model reaction (Fig. 4.3). The reactions were carried out using the ruthenium pincer PNP complexes at a catalyst loading of 1000 ppm. Water (2 mL) and base (1 equivalent to butanol) were added and the system refluxed for 3 h at applied temperature, 130 °C.

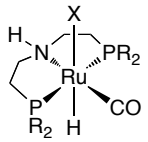

X =	Cl	HBH_3	H
R = Ph	**5a**	**6a**	
R = *i*Pr	**5b**	**6b**	**7b**
R = Cy	**5c**		

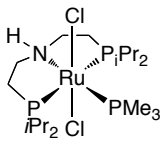

8b

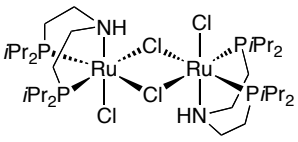

9b

Fig. 4.3 *Structures of the ruthenium PNP complexes.*

Table 4.2 *Dehydrogenation of 1-butanol to butyric acid salt catalysed by isolated ruthenium-PNP complexes*[‡].

entry	cata. (Ru / butanol)	yield to butyric acid (%)	TOF_{3h} (h^{-1})
1	**5a** (950 ppm)	81.6	286
2	**5b** (1011 ppm)	78.1	258
3	**5c** (1022 ppm)	82.0	267
4	**6a** (1006 ppm)	86.1	285
5	**6b** (1008 ppm)	77.7	257
6	**7b** (991 ppm)	74.8	251
7	**8b** (1001 ppm)	41.7	139
8	**9b** (980 ppm)	76.7	261

[‡]reaction conditions: *V* (1-butanol): 5 mL; *V* (water): 2 mL; *m* (NaOH): 2.19 g; 3 h; reflux under argon.

All the tested complexes were found to be active for the dehydrogenation of butanol to butyric acid salt with selectivities higher than 99 % (Table 4.2). With the exception of the trimethylphosphino ruthenium dichloride PNP pincer complex **8b**, all complexes allowed obtaining yields surerior to 75 %. This seems to indicate that substitition of the carbonyl by less π-accepting trimethylphosphine is detrimental to the complex activity. For all other complexes, no major difference in activity could be observed. Complexes with PNP ligands having electron withdrawing phenyl substituents at the phosphorus atom were found to be slightly more active (Table 4.2, entries 1 and 4). For complexes with a PNP ligand having iso-propyl substituents at the phosphorus, **5b**, **6b**, **7b** and **9b**, almost identical activities were found regardless of the nature of the other ligands (Table 4.2, entries 2, 5, 6 and 8). This suggests that under reaction conditions, all the complexes are transformed into the same active catalyst.

When compared with Milstein's aromatic ruthenium PNN catalyst, the tested aliphatic PNP ruthenium complexes were found to be much more active[1]. Milstein *et al* reported a yield of 84 % to butyric acid after 18 h with a catalyst loading of 2000 ppm which corresponds to a TOF of 23.3 h^{-1}. With the aliphatic PNP ruthenium complexes, yields between 75 and 86 % were obtained using half catalyst loading, *i.e.* 1000 ppm, and much shorter reaction time, 3 h. If compared on a TOF basis, these

catalysts are 10 times more active with TOF ranging from 250 h^{-1} to 280 h^{-1} against 23.3 h^{-1} for aromatic ruthenium PNN complex.

4.2 Optimization of the reaction conditions

Having developed active catalysts, we investigated the influences of water amount, catalyst concentration and reaction time for the dehydrogenation of 1-butanol to butyric acid salt using catalyst **5a**.

4.2.1 Influence of water

Dehydrogenation of 1-butanol to butyric acid salt using complex **5a** was carried in the presence of various amounts of added water (Table 4.3).

Table 4.3 *Dehydrogenation of 1-butanol to butyric acid salt catalysed by **5a** in the presence of various amount of water*[‡].

entry	amount of water (mL)	Ru / butanol	yield to butyric acid (%)	TOF_{3h} (h^{-1})
1	0.5	1014 ppm	69.9	230
2	1	1007 ppm	64.2	213
3	2	950 ppm	81.6	286
4	3	990 ppm	56.9	192
5	4	982 ppm	49.0	166

[‡]reaction conditions: catalyst: **5a**; *V* (1-butanol): 5 mL; *m* (NaOH): 2.19 g; 3 h; reflux under argon.

The performance of the reaction was found to be influenced by the amount of water present in the system.The product yield increased with the water amount up to a point where further addition of water resulted in a decrease of the product yield. Under our conditions, 2 mL of water was found to be the optimum. Reasons for this behaviour are unclear.

4.2.2 Influence of catalyst concentration

Dehydrogenation of 1-butanol to butyric acid salt using complex **5a** was carried with different catalyst loadings: 950, 484, 235, 93 and 20 ppm (Table 4.4).

Table 4.4 *Dehydrogenation of 1-butanol to butyric acid salt with different loadings of* ***5a***[‡].

entry	catalyst concentration (ppm)	yield to butyric acid (%)	TOF_{3h} (h^{-1})
1	950	81.6	286
2	484	65.4	451
3	235	52.3	741
4	93	24.3	875
5	21	8.1	1281

[‡]reaction conditions: catalyst: **5a**; *V* (1-butanol): 5 mL; *V* (water): 2 mL; *m* (NaOH): 2.19 g; 3 h; reflux under argon.

Complex **5a** was active at all the investigated loadings. As expected, the obtained product yield at fixed time, 3 h, increased with the catalyst loading. This indicates that reaction rate is dependant on the catalyst concentration. When considering the variation of the TOF at 3 h with the catalyst loading, one can observe an increase of the TOF with decreased catalyst loading. TOF as high as 1281 h^{-1} is obtained with a catalyst loading of 20 ppm while with 950 ppm catalyst, the TOF is reduced 4.4 times falling to 286 h^{-1} (Table 4.4 entries 1 and 5). This suggests that the overall reaction kinetic is not first order relative to the catalyst concentration since this would lead to TOF_0 independant of the catalyst concentration. As pointed out for dehydrogenative coupling reactions, this could arise from "reservoir" effects, where lower catalyst concentration may favour the dissociation of catalyst aggregates (dimers, etc) toward single active complexes. No evidences of such "dormant" catalytic species were found. Another possible explanation of this effect is that the reaction rate is limited by the hydrogen diffusion out of the liquid phase at higher catalyst loading while at very low catalyst loading the reaction rate is governed by chemical kinetics.

When crossing results from the study on the influence of water amount and catalyst concentration, it appeared that using a catalyst loading of 950 ppm together with 2 mL water provided the optimum reaction conditions allowing to obtain butyric acid yield of 81.6 % (Fig. 4.4).

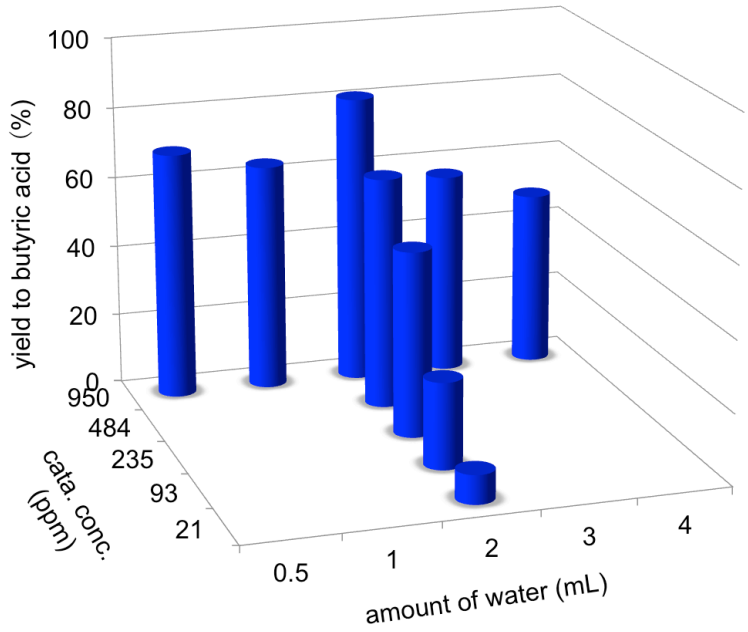

Fig. 4.4 *Influences of catalyst concentration and water amount on the dehydrogenation of 1-butanol to butyric acid salt catalysed by* ***5a*** .

4.2.3 Evolution of yield as a function of time

Direct monitoring of the reaction by gas chromatography or NMR is complicated because of the basic aqueous media used to perform the transformation. Therefore, in order to obtain the profile of yield and TON as a function of time, several dehydrogenation reactions of 1-butanol to butyric acid salt catalysed by **5a** were performed using different reaction times (Table 4.5, Fig. 4.5).

Table 4.5 *Dehydrogenation of 1-butanol to butyric acid salt catalysed by* ***5a*** *at different reaction times*[‡].

entry	Ru / butanol	time (h)	yield to butyric acid (%)	TON	TOF (h^{-1})
1	1012 ppm	1	52.2	516	516 (1 h)
2	1011 ppm	2	68.4	676	338 (2 h)
3	950 ppm	3	81.6	858	286 (3 h)
4	998 ppm	4	85.0	851	213 (4 h)
5	1021 ppm	5	82.0	803	161 (5 h)

[‡]reaction conditions: catalyst: **5a**; *V* (1-butanol): 5 mL; *V* (water): 2 mL; *m* (NaOH): 2.19 g; reflux under argon.

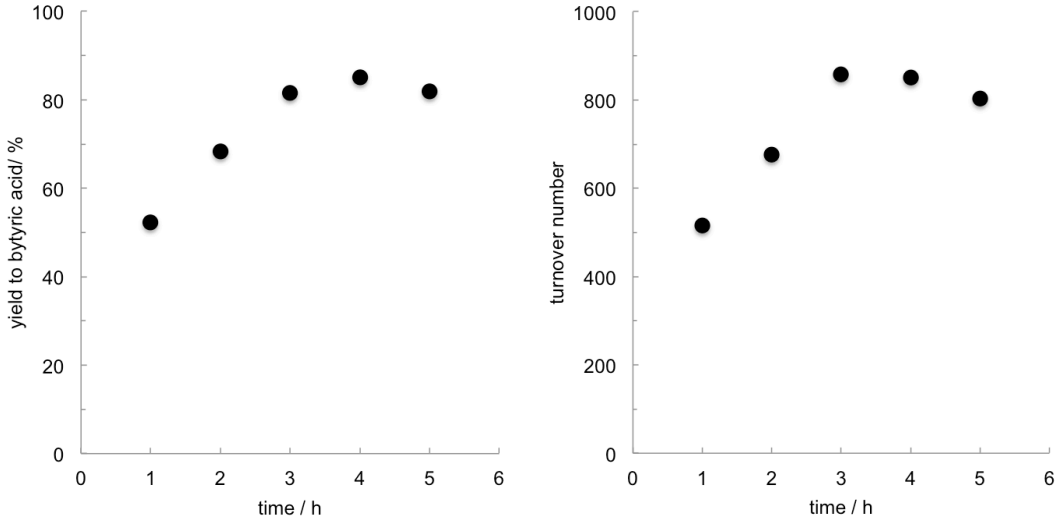

Fig. 4.5 *Evolution of the acid yield (left) and TON (right) as a function of time during the dehydrogenation of butanol to butyric acid catalysed by* ***5a****.*

Yields and TONs were found to increase with time up to 3 - 4 h of reaction were a plateau is reached around 85 % of product. The TOF steadily decreased during the reaction which maybe due to dilution of the reacting alcohol and base. Therefore, the catalyst activity is higher than previously observed as the initial TOF is most likely close to 500 h^{-1}, as measured at 1 h, than 280 h^{-1} measured at 3 h were the reaction had already slowed down.

4.3 Air stability

Aliphatic PNP pincer ruthenium complexes are very active and selective catalysts for acceptorless dehydrogenation of 1-butanol to butyric acid salt. However, from an industrial point of view, the catalyst stability in the presence of oxygen is also one important feature. Therefore, we tested the activity of complexes **5a** and **6a** using 1-butanol without prior degassing, hence containing dissolved oxygen. Moreover, the reaction was conducted under air, without a protective argon atmosphere. Under these conditions, the catalysts displayed very similar activity as when thoroughly degassed 1-butanol was used as substrate and the reaction carried out under argon atmosphere (Table 4.6, entries 1 vs. 2 and 4 vs. 5). In another test, catalyst **5a** was left standing in air for 6 days and was then tested for the acceptorless dehydrogenation of

non-purified 1-butanol. Under these conditions, catalysts **5a** displayed almost identical activity as when carefully stored and handeled and using degassed 1-butanol. (Table 4.6, entry 3).

These results illustrate the robustness of catalysts **5a** and **6a** and indicate that it does not required intensive substrate purification nor special handling. This relative stability together with the high activity and selectivity makes them promising catalysts for industrial application.

Table 4.6 *Air stability of catalysts **5a** and **6a**.*

entry	cata.	Ru / butanol	yield to butyric acid (%)	TOF_{3h} (h^{-1})
1[‡]	**5a**	950 ppm	81.6	286
2[†]		984 ppm	82.1	278
3[§]		993 ppm	81.7	274
4[‡]	**6a**	1006 ppm	86.1	285
5[†]		994 ppm	78.6	263

[‡]reaction conditions: *V* (1-butanol): 5 mL; *V* (water): 2 mL; *m* (NaOH): 2.19 g; reflux under argon.

[†]non-purified nor degassed 1-butanol was used, reaction performed under air.

[§]catalyst **5a** was aged in air for 6 days, non-purified nor degassed 1-butanol was used, reaction performed under air.

4.4 Catalyst recycling

For most homogeneous catalytic processes, catalyst recycling is complicated which limits their industrial application. For some cases however, using biphasic reaction systems, such a recycling can be carried out successfuly at the industrial scale. Aqueous-biphasic hydroformylation of propene being the best-known example.

For dehydrogenation of 1-butanol to butyric acid salt, it is worth noticing that the product is soluble in water, and on the other hand, the catalyst is soluble in organic solvent. This open up the opportunity of product separation making it possible to recycle the catalyst.

Therefore, the reaction was carried out with **5a** using toluene as "catalyst immobilising phase" and after the desired reaction time, water was used to extract the

product (Fig. 4.6). The organic catalyst-containing phase was recovered by phase separation and could be used for the transformation of added fresh substrate.

Fig. 4.6 *Separation of catalyst **5a** in toluene (top) and product in water (bottom).*

This strategy was used for recycling of catalyst **5a** in the dehydrogenation of 1-butanol to butyric acid salts. Recycling was carried for two different reaction times, 3 h and 6 h (Table 4.7 and Fig. 4.7).

Table 4.7 *Catalyst recycling for the dehydrogenation of 1-butanol to butyric acid salts using catalyst* ***5a***[‡].

entry	recycle No.	Ru / butanol	yield to butyric acid (%)	TOF_{3h} / TOF_{6h} (h^{-1})
	1	1006 ppm	59.5	197
	2	1014 ppm	52.7	173
i[†]	3	1014 ppm	65.4	215
	4	997 ppm	51.6	173
	5	994 ppm	56.5	189
	1	997 ppm	61.3	102
	2	1024 ppm	64.0	104
ii[§]	3	1023 ppm	72.8	119
	4	1000 ppm	72.7	121
	5	1005 ppm	75.0	124

[‡]reaction conditions: catalyst: **5a**; *V* (1-butanol): 5 mL; *V* (water): 2 mL; *V* (toluene): 5 mL; *m* (NaOH): 2.19 g.

[†]3 h reflux under argon.

[§]6 h reflux under argon.

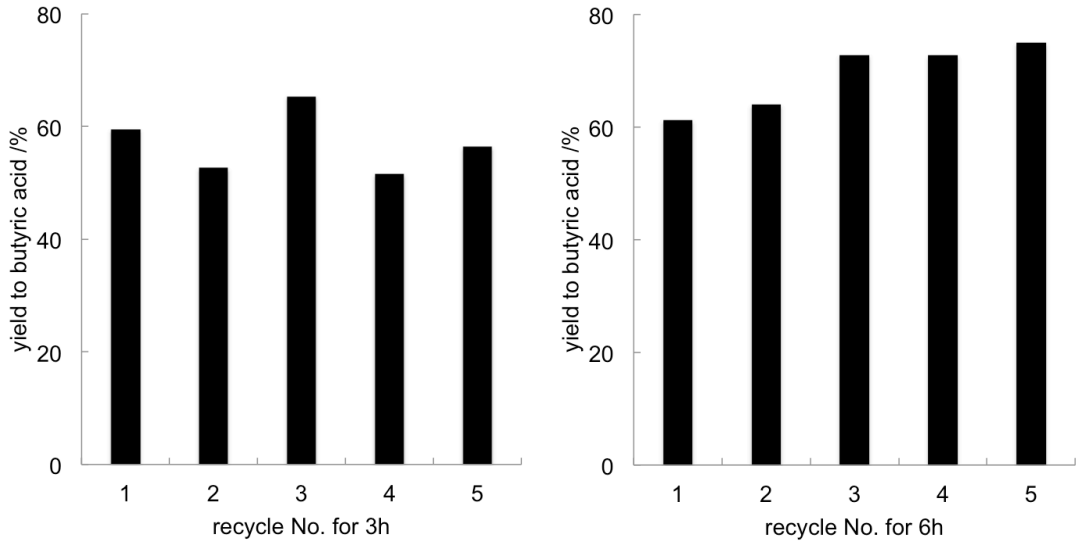

Fig. 4.7 *Catalyst recycling for the dehydrogenation of 1-butanol to butyric acid salts using catalyst* ***5a*** *(left: 3 h reaction; right: 6 h reaction).*

Using this biphasic strategy, the catalyst could be used for 5 consecutive runs. When recycling was performed after 3 h of reaction, the yields were found to vary randomly between 52 and 65 % (Table 4.7, entry i; Fig. 4.7, left). This may be due to the fact that unreacted 1-butanol partitions between the toluene phase containing the catalyst and the aqueous phase during product extraction. This partitionning will depend on the conversion obtained after reaction. Therefore, on the next run, the

amount of butanol is greater than the added fresh butanol. This will change the substrate to catalyst ratio, which affects the kinetics, and modify the observed yield. When each run was carried out for 6 h, the yield was found to increase from 62 to 75 % (Table 4.7, entry ii; Fig. 4.7, right). This observed increase also is likely to be due to the partitioning of 1-butanol at the end of the reaction. However, these results indicates that the catalyst can be recycled and used for 5 consecutive runs maintaining its activity.

To the best of our knowledge this is the first example of catalyst recycling for this transformation and more generaly for ruthenium PNP pincer complexes.

4.5 Dehydrogenation of butyl butyrate

Traditionally, esters are saponified under basic conditions to give the corresponding carboxylic acid salt and the alcohol in equimolar ratio (**Fig. 4.8**).

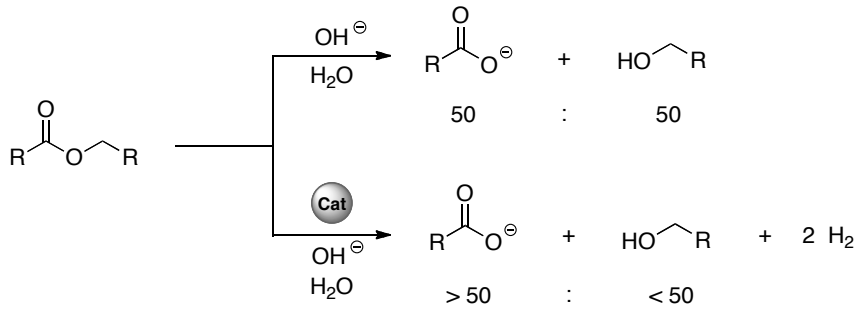

Fig. 4.8 *Uncatalysed (top) and catalysed (bottom) saponification of esters.*

We thought that by using a dehydrogenation catalyst, the produced alcohol could further reacts to give the carboxylic acid salt together with hydrogen and hence a yield to carboxylate higher than 50 % can be reached.

Therefore, butyl butyrate was tested at applied temperature, 130 °C under basic aqueous conditions for 3 h with 2000 ppm of catalyst **5a** (Table 4.8).

Table 4.8 *Dehydrogenation of butyl butyrate*[‡].

entry	yield to butyric acid (%)	TOF_{3h} (h^{-1})
1	73.3	125

[‡]reaction conditions: catalyst: **5a**; Ru / butyl butyrate: 1955 ppm; *V* (butyl butyrate): 4.5 mL; *V* (water): 2 mL; *m* (NaOH): 2.19 g; applied temperature 130 °C; 3 h under argon.

Using such conditions, 73 % yield to butyric acid salt was obtained. This shows that dehydrogenation of the butanol arising from saponification is taking place. Such methodology could be used to improve yields of saponification reactions.

4.6 Reaction pathway

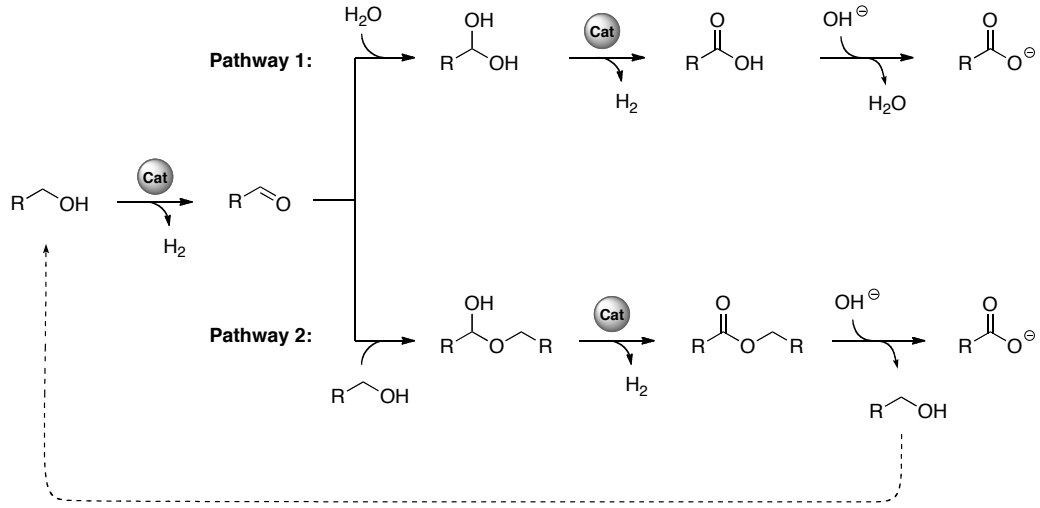

Scheme 4.3 *Two possible reaction pathways for acceptorless dehydrogenation of primary alcohols to corresponding acid salts.*

Dehydrogenation of primary alcohols to carboxylic acid salts can proceed via two distinct reaction pathways (Scheme 4.3). Alcohol can be dehydrogenated to an aldehyde that further reacts with water to give a hydrate that is dehydrogenated to give a carboxylic acid, which is then deprotonated in the basic reaction media. Alternatively, the reaction may proceed as the dehydrogenative coupling yielding an ester that is then hydrolysed under basic conditions. The alcohol resulting from the ester hydrolysis reacts again to form an ester that is subsequently hydrolysed. This sequence repeats itself until all alcohol is converted to the carboxylate salt. For this pathway, all the steps have been independently evidenced with the dehydrogenative coupling of alcohol to esters and the transformation of esters to carboxylic acid salts.

In order to get insight into the operative reaction pathway for the dehydrogenation of primary alcohols to carboxylic acid salts, the two following experiments were carried out (Scheme 4.4 and Table 4.9). Firstly butanol was reacted using 1 mol % catalyst **6a** under identical reaction conditions used for synthesis of carboxylic acid salts but without base. This resulted in the formation of an equimolar mixture of ester and carboxylic acid. Under these conditions the catalyst only made one turnover. Secondly, pure butyl butyrate was reacted under identical conditions. This resulted in the hydrolysis of only 0.06 % of the ester to the carboxylic acid. Since the yield of this hydrolysis is about 10 times lower than the one observed for the first reaction, it means that the produced butyric acid cannot come from hydrolysis of butyl butyrate. Hence, this supports the first reaction pathway (Scheme 4.3) for the production of the carboxylic acid salt. However, in the presence of a base, hydrolysis would be favoured and thus making both pathways operative.

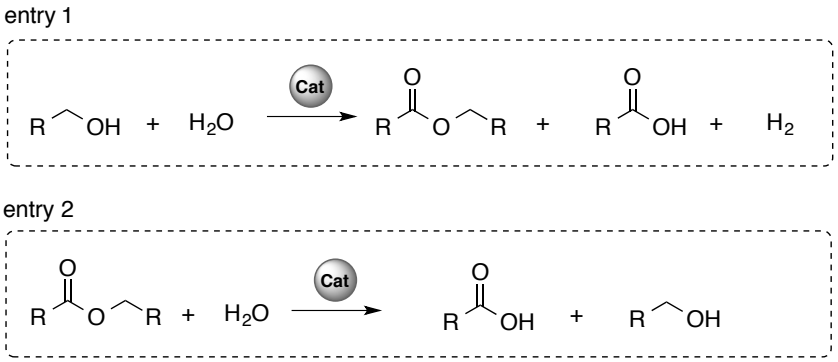

Scheme 4.4 *Two reactions under base-free conditions.*

Table 4.9 *Catalytic testing results for two reactions under base-free conditions.*

entry	cata.	yield (%)		
		butyl butyrate	butyric acid	butanol
1‡	**6a**	0.46	0.49	-
2†		-	0.058	-

‡reaction conditions: Ru / 1-butanol: 1 mol %; *n* (1-butanol): 54.6 mmol; *n* (water): 111 mmol; base-free; 3 h reflux under argon.

† reaction conditions: Ru / butyl butyrate: 2 mol %; *n* (butyl butyrate): 5.46 mmol; *n* (water): 22.2 mmol; base-free; 3 h reflux under argon.

4.7 Selective deuteration of alcohols

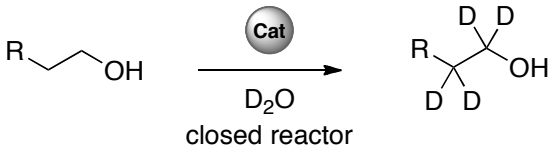

Fig. 4.9 *Selective deuteration of alcohol.*

As aliphatic ruthenium PNP pincer complexes proved to be more efficient than aromatic ruthenium PNN pincer complexes for the dehydrogenation of alcohol to carboxylic acid salt we turned our attention to the selective deuteration of alcohols, known to be catalysed by the same ruthenium PNN pincer complexes developed by Milstein[2].

4.7.1 Optimization of reaction conditions

Deuteration of 1-butanol was used as a test reaction with complexes **5a** and **6a** under different sets of reaction conditions (Table 4.10)

Table 4.10 *Deuteration of 1-butanol using catalysts **5a** and **6a**‡.*

entry	cata.	base (mol %)	time (h)	deuteration yield (%) α; β
1	/	NaOH (20)	0.5	0; 0
2	**5a**	NaOH (2)	0.5	72.1; 7.3
3		NaOH (5)	0.5	92.9; 17.6
4		NaOH (10)	0.5	95.3; 36.9
5		NaOH (20)	0.5	95.3; 38.3
6		NaOH (40)	0.5	74.1; 4.1
7		NaOH (80)	0.5	82.2; 4.4
8	**6a**	NaOH (10)	0.5	89.5; 39.1
9		/	0.5	1.0; 0.4
10		/	4	1.75; 0.1
11†		/	12	64.1; 0.0
12†		/	24	90.8; 2.7

‡reaction conditions: cata. / 1-butanol: 2000 ppm; *n* (1-butanol): 3 mmol, *n* (D_2O): 133 mmol; applied temperature: 120 °C; closed system; under air.

†cata. / 1-butanol: 1 mol %.

No deuteration was observed without a catalyst in the system (Table 4.10, entry 1). Influence of the sodium hydroxide amount was investigated using catalyst **5a**. With 5 to 20 mol % of sodium hydroxide, a yield higher than 90 % was obtained for

deuteration at the α position while level of deuteration of the β position ranged from 18 to 38 % (Table 4.10, entries 3-5). Unexpectedly, futher increase of NaOH concentration led to a decrease of the deuteration yield at both positions (Table 4.10, entries 6-7).

Using catalyst **6a**, with 10 mol % NaOH led to similar activity than catalyst **5a** albeit with a lower selectivity for the α position (Table 4.10, entries 4 vs. 8). Since we showed that catalyst **6a** catalyses the dehydrogenative coupling of alcohol under base-free condition (Fig. 3.11), deuteration in the absence of base was tested with this catalyst (Table 4.10, entries 9-12). Using 2000 ppm catalyst under base-free conditions, even after 4 h of reaction time, almost no deuteration was observed (Table 4.10, entries 9 and 10). Increasing catalyst loading to 1 mol % allowed obtaining 64.1 % deuteration selectively at the α position and 90.8 % after 24 h albeit with some deuteration of the β position (2.7 %) (Table 4.10, entries 11 and 12).

Compared with Milstein's catalyst (see Chapter 1, section 1.6), aliphatic PNP pincer ruthenium complexes **5a** and **6a** show much higher activities for the deuteration of alcohols. Using Milstein's catalyst with 20 mol % NaOH, under same reaction conditions, 24 h of reaction time is required while similar yields are obtained after 0.5 h with catalyst **5a** and **6a** with 10 mol % NaOH. Under base-free conditions, using 10 % of Milstein's catalyst **B** 80 % deuteration is obtained while with 10 times less catalyst, 90.8 % deuteration at the α position is obtained with complex **6a**, albeit with ~ 3% of β position deuteration. Based on these results, the following reaction conditions were chosen for testing of other catalysts: 10 mol % NaOH, 2000 ppm catalyst, 120 ^{o}C, 0.5 h, under air.

4.7.2 Screening of isolated catalysts

Eleven ruthenium pincer complexes were tested for the deuteration of 1-butanol (Table 4.11 and Fig. 4.10).

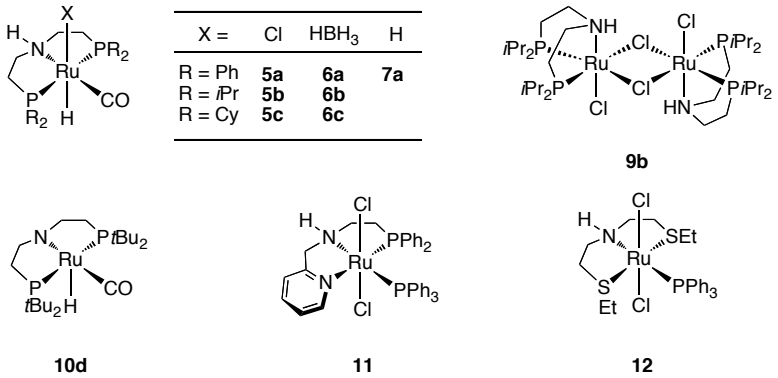

Fig. 4.10 *Structures of the ruthenium complexes used for the deuteration of 1-butanol.*

Table 4.11 *Screening of isolated catalysts*[‡].

entry	cata.	deuteration (% yield) α; β
1	**5a**	95.3; 36.9
2	**5b**	89.0; 25.5
3	**5c**	92.5; 4.6
4	**6a**	89.5; 39.1
5	**6b**	80.4; 38.0
6	**6c**	94.2; 4.9
7	**7a**	95.8; 29.6
8	**9b**	67.4; 25.6
9	**10d**	0; 0
10	**11**	20.5; 11.2
11	**12**	13.5; 17.1

[‡]reaction conditions: Ru / 1-butanol: 2000 ppm; NaOH / 1-butanol: 10 mol %; *n* (1-butanol): 3 mmol; *n* (D_2O): 133 mmol; applied temperature: 120 ^oC; closed system; 0.5 h under air.

All the tested catalysts except the unsaturated amido ruthenium complex **10d** were active for the deuteriation of 1-butanol (Table 4.11)

For carbonyl ruthenium PNP pincer complexes, no significant difference in yield and selectivity were observed upon substitution of the chloride ligand by borohydride (compare results for **5a-c** with **6a-c**, Table 4.11, entries 1-3 vs. 4-6). However for these catalysts, complexes having cyclohexyl substituents **5c** and **6c** were found to be the most selective for deuteration at the α position (Table 4.11 entries 3 and 6). Schneider's dimer **9b** showed lower activity and selectivity than the carbonyl ruthenium PNP pincer complexes (Table 4.11, entry 8). Triphenylphosphino ruthenium complexes having PNN or SNS ligand showed very little activity and poor selectivity for deuteration of the α position (Table 4.11, entries 10 and 11).

Unexpectedly, the triphenylphosphino complex **12** having SNS ligand was slightly more selective for the β position (α/β = 13.5/17.1). This may indicate that a different reaction mechanism is operative with this complex.

It should be noted that for some sensitive complexes, such as **7a**, under the deuteration conditions (air, non-purified butanol, heavy water), oxidation might occur. However this has no influence for a high catalytic activity (entry 7 in Table 4.11).

4.7.3 Screening of *in situ* formed catalysts

Four ruthenium precursors and three PNP ligands were used to generate a set of *in situ* formed catalysts that were used for the deuteration of 1-butanol (Fig. 4.11).

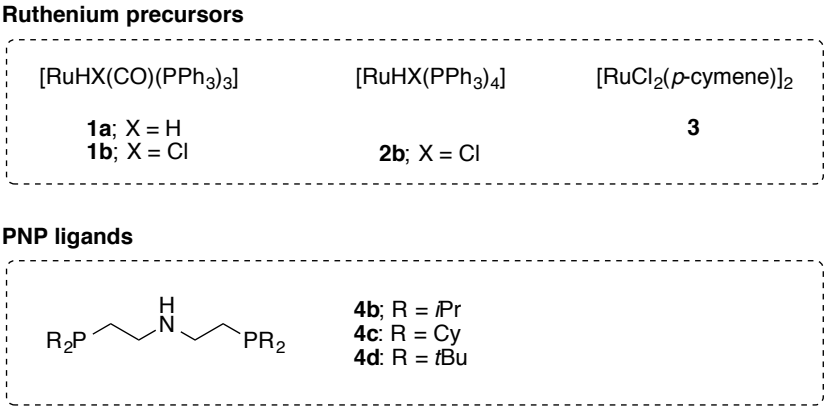

Fig. 4.11 *Structures of in situ formed catalysts.*

Table 4.12 *Deuteration of 1-butanol using in situ formed catalysts*[‡].

entry	cata.	PNP ligand	time	deuteration (% yield) α; β
1		/		0; 0
2	**1a**	**4b**	0.5 h	82.8; 11.5
3		**4c**		82.0; 2.3
4		**4d**		0; 0
5	**1a**	**4b**		95.2; 11.9
6		**4c**		91.9; 5.1
7		/		0; 0
8	**1b**	**4b**		96.2; 10.7
9		**4c**		96.3; 13.4
10		/	1 h	0; 0
11	**2b**	**4b**		78.7; 21.6
12		**4c**		85.7; 21.5
13		/		0; 0
14	**3**	**4b**		90.2; 36.8
15		**4c**		93.1; 12.0

[‡]reaction conditions: Ru / 1-butanol: 2000 ppm; NaOH / 1-butanol: 10 mol %; *n* (1-butanol): 3 mmol; *n* (D_2O): 133 mmol; applied temperature: 120 ^oC; closed system; under air.

No conversion was observed by using sole complex **1a**, **1b**, **2b** or **3** (Table 4.12, entries 1, 7, 10 and 13). For **1a**, yields higher than 90 % at α position can be observed with the presence of **4b** or **4c** after 1 h (Table 4.12, entries 5 and 6); while catalyst **1a/4d** showed no activity, which may be due to steric hindrance (Table 4.12, entry 4). Interestingly, as observed for isolated complexes, higher selectivities to the α postion were obtained when ligand **4c,** having cyclohexyl substituents, was used (Table 4.12, entries 3 and 6).

Besides **1a**, the other tested ruthenium precursors **1b**, **2b** or **3** also gave active catalysts when used together with PNP ligands **4b** or **4c**. Hydridochloro ruthenium complex **1b** showed similar activity than the dihydrido ruthenium complex **1a (**Table 4.12**,** entries 4 vs. 8 and 6 vs. 9). The tetraphoshine complex **2b** used with either ligand **4b** or **4c** gave less active and less selective catalysts (Table 4.12, entries 11 and 12). For ruthenium dimer **3**, active catalysts were obtained with both ligands **4b** and **4c** leading again to the formation of a more selective catalyst (Table 4.12, entries 14 and 15).

4.7.4 Other substrates

In addition to 1-butanol, the deuteration of several primary, secondary and functionalized alcohols was investigated using catalyst **5a** (Table 4.13).

Table 4.13 *Deuteration of alcohol catalysed by **5a**.*

entry	substrate	reaction conditions‡	deuteration (% yield) α; β
1	ethanol	20 mol % NaOH, 12h	76.9; 85.0
2		20 mol % NaOH, 24h	93.6; 91.8
3	1-pentanol	0.5 h	92.6; 1.2
4	2-methyl-1-butanol		86.7; 0.6
5	2-ethyl-1-hexanol		62.9; 0
6	dimethylaminoethanol	0.5 h	12.6; 19.0
7		5 h	52.0; 64.1
8		20 mol% NaOH, 6 h	60.3; 77.1
9	2-propanol	0.5 h	33.2; 58.7
10		2 h	46.3; 70.9
11	cyclohexanol	0.5 h	74.9; 83.2
12		1 h	60.7; 88.9

‡reaction conditions: catalyst: **5a**; Ru / alcohol: 2000 ppm; NaOH / 1-butanol: 10 mol %; *n* (alcohol): 3 mmol; *n* (D_2O): 133 mmol; applied temperature: 120 ^oC; closed system; under air.

With prolonged reaction time, ethanol could be deuterated at both α and β position with yields higher than 90 % (Table 4.13, entry 2). This is particularly interesting if the desired product is ethanol-d_6.

For branched primary alcohols, 2-methyl-1-butanol and 2-ethyl-1-hexanol, yields lower than for linear alcohols were obtained presumably due to increased steric hindrance (in Table 4.13, entries 3, 4 and 5).

β-aminoalcohol such as dimethylaminoethanol, and secondary alcohols such as 2-propanol and cyclohexanol could also be deuterated using catalyst **5a** but without selectivity for the α position (Table 4.13, entries 6 to 12).

4.8 Conclusions

Two types of ruthenium-based catalysts, *in situ* formed and isolated catalysts were used for two reaction types: acceptorless dehydrogenation of alcohols to

corresponding acid salts and selective deuteration of alcohols. Both *in situ* formed and isolated catalysts were screened for both reactions.

Regarding the acceptorless dehydrogenation of alcohols to corresponding acid salts, several reaction parameters were carefully studied using 1-butanol as model substrate, including catalyst concentration, water amount and reaction time. Moreover, isolated catalyst stability to air was studied. Using toluene as a catalyst immobilizing phase, catalyst and product could be separated and the catalyst recycled up to four times.

Studies on *in situ* formed catalysts showed that the use of a PNP ligand was crucial to ensure catalytic activity. Carbonyl tris-triphenylphosphine ruthenium complexes were found to lead to the more active catalysts. Ligand structure had little influence on the activity of the obtained complexes except for very bulky PNP ligand which almost completely suppressed catalyst activity.

For isolated catalysts, it was observed that substitution of the carbonyl ligand by a trimethylphosphine had a detrimental effect on the catalytic activity.

Compared with the reported state-of-the-art catalyst, both *in situ* formed and isolated catalysts showed a 10 times high TOF for this reaction.

Catalyst concentration was found to strongly affect catalytic performance. On one hand, lower catalyst loading led to higher turnover frequency, while on the other hand, higher catalyst loading allowed to obtain high yields in shorter reaction time.

Catalyst **5a** was shown to be stable under air and could be used with non-purified butanol keeping its high activity.

Catalyst recycling is usually complicated for most homogeneous catalytic systems. However, by using toluene as “catalyst-immobilizing phase”, the catalyst could be used for 5 consecutive runs without showing any sign of deactivation.

Regarding the deuteration of alcohols, borohydride ruthenium PNP pincer complexes could be used under base-free conditions, although higher catalyst loading and longer reaction time were required compared with basic condition.

Much higher activities can be observed for both *in situ* formed and isolated catalysts compared with reported state-of-the-art catalyst.

Besides 1-butanol, other substrates can also be used, such as ethanol, 1-pentanol, 2-methyl-1-butanol and 2-ethyl-1-hexanol, dimethylaminoethanol, 2-propanol and cyclohexanol. Deuteration yields higher than 90 % can be observed for ethanol at both α and β positions, which is particularly interesting if the desired product is ethanol-d_6.

4.9 References

[1] E. Balaraman, E. Khaskin, G. Leitus, D. Milstein, *Nat. Chem.* **2013**, *5*, 122-125.

[2] E. Khaskin, D. Milstein, *ACS Catal.* **2013**, 448-452.

Chapter 5 Conclusions and perspectives

With the need for a transition from fossil to renewable carbon feedstock for the production of chemicals, the catalytic transformation of (bio-)alcohols has gained a considerable importance in recent years. Among the different catalytic technolgies, the acceptorless dehydrogenation of alcohols constitutes an attractive methodology for their transformation into high value added products. This transformation allows converting the alcohols into reactive aldehydes or ketones with simultaneous production of molecular hydrogen, a co-product valuable in itself. Moreover, depending on the reaction conditions, the produced aldehyde can be further transformed *in situ* into a large variety of products such as esters, carboxylic acids, amides, amines, acetals, *etc*. Catalysts for this transformation have been known for more than 30 years. However efficient systems for the transformation of primary alcohols, among which ethanol and butanol that can be obtained from biomass fermentation, are still lacking. Nowaday, the most efficient organometallic complexes rely on cooperation between the metal center and the ligand to catalyse these dehydrogenation reactions. Among these catalysts, aromatic and aliphatic ruthenium pincer complexes show unprecedented activity and selectivity for dehydrogenation, dehydrogenative coupling and hydrogen borrowing transformation of alcohols. However, the transformation of primary alcohols, especially the ones presenting a short aliphatic chain, still suffers from low reaction rate, poor productivity and usually requires the use of an additional base.

In this context we have studied the use of ruthenium PNP complexes for the transformation of alcohols, focusing on butanol and ethanol. Both *in situ* prepared catalysts and well-defined ruthenium aliphatic PNP pincer complexes were investigated for the dehydrogenative coupling of primary alcohols to esters, the dehydrogenation of alcohols to carboxylic acid salts and the selective deuteration of alcohols. For these transformations, we focused on developing catalytic systems that

were at the same time very active, selective, productive and robust. To fulfill these requirements the catalyst structure was systematically varied and the reaction conditions were thoroughly investigated and optimised.

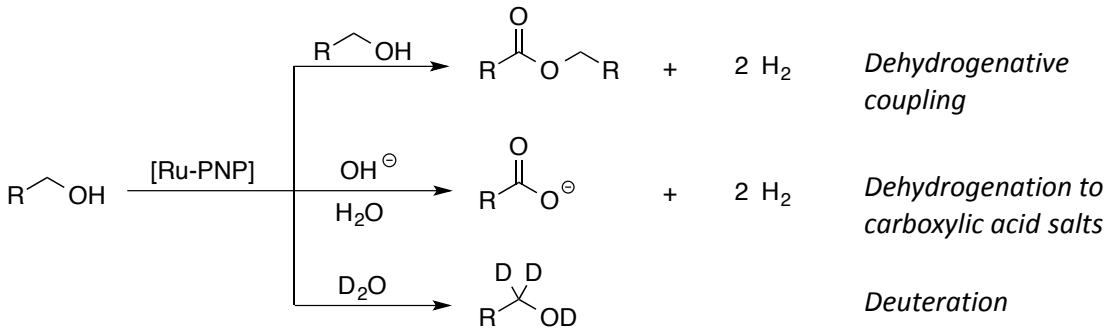

Scheme 5.1 *The three reactions catalysed by Ru-PNP studied in this thesis.*

5.1 Acceptorless dehydrogenative coupling of primary alcohols

Acceptorless dehydrogenative coupling of primary alcohols is an environmentally friendly and atom-efficient route to produce symmetrical esters. Application of this transformation is particularely attractive for the production of ethyl acetate from bio-ethanol and for the production of fatty esters, used in skin care applications, from fatty alcohols. Compared with the traditional esterification reaction using an acid and an alcohol, the evolved hydrogen can shift the reaction equilibrium to completion and thus overcome thermodynamic limitations.

Aromatic and aliphatic pincer ruthenium complexes have recently been reported as being very efficient catalysts for this transformation. However, the described systems, although very active, did not allow obtaining high yields in the desired products. Other systems required relatively high reaction temperature, circumventing their use for the transformation of lower alcohols such as ethanol under neat conditions. Finally, most of the described complexes require the addition of a base to ensure activity and this leads to a decrease of the reaction selectivity.

We investigated the use of *in situ* formed aliphatic ruthenium PNP pincer complexes for the dehydrogenative coupling of alcohol using 1-butanol as a model substrate. With dihydride ruthenium precursor together with aliphatic PNP ligands

with moderate steric hindrance, very active and productive catalysts were formed under reaction conditions leading to butyl butyrate with yield higher than 90 % under base-free conditions. The transformation was found to be extremely selective with unreacted 1-butanol being the only compound detected beside the desired ester product. Moreover the catalysts were found to be highly active with initial turnover frequencies ranging from 2000 h^{-1} to 2500 h^{-1}. Studies on the influence of the catalyst concentration showed that reaction rate is dependent on the catalyst concentration but with an order apparently lower than one. As a consequence, turnover frequency increased with lower catalyst loading. Therefore, with 20 ppm of catalyst, an initial turnover frequency of 3800 h^{-1} was observed and a total turnover number of 27000 was reached after 9 h of reaction. However, with such a low loading, the catalyst lost most of its activity before full conversion of the substrate was reached. In addition to 1-butanol other linear and branched alcohols > C_5 were efficiently transformed into the corresponding esters using these *in situ* formed catalysts.

In addition to *in situ* formed catalysts, well-defined complexes were also investigated. Several structurally related carbonyl ruthenium aliphatic PNP pincer complexes were used for the dehydrogenative coupling of 1-butanol. Under base-free conditions, hydridoborohydride complexes were found to be very active while hydridochloro complexes showed no activity at all. However, using sodium ethoxide as a base, the latter complexes showed similar activity to their hydridoborohydride conterpart albeit with lower selectivity due to the promotion of side reactions induced by the presence of the base. Both catalysts types proved to be very active with initial turnover frequency ranging from 2500 h^{-1} to 2800 h^{-1} allowing reaching ester yields higher than 95 %. The nature of the substituent at the phosphorus atom of the ligand did not seem to have a significant influence on the catalyst activity. Similar with *in situ* formed catalysts, for the isolated catalysts, the reaction rate was found to be proportional to the catalyst concentration again with an order apparently lower than one. This could result from “reservoir effects”, where higher dilution favours the

dissociation of catalyst aggregates to single defined active catalyst species. However, no evidence for catalyst aggregation could be observed. Alternatively, such dependance of the reaction rate with catalyst concentration may result from limitation of the reaction rate by the diffusion of the produced hydrogen out of the liquid phase. As a consequence, turnover frequency as high has 8000 h^{-1} was measured with a catalyst loading of 20 ppm but decrease to 2000 h^{-1} when loading was increase to 500 ppm. At low catalyst loading, a total turnover number of 38000 was reached after 8 h of reaction evidencing the robustness of the complex. In addition, hydridoborohydride complexes proved to be stable towards water and oxygen allowing to use non-degassed nor dried substrates.

In addition to 1-butanol other linear and branched alcohols > C_5 were efficiently transformed into the corresponding esters using hydridoborohydride complexes. Remarkably, ethanol could also be efficiently, selectively and fully tranformed into ethyl acetate at low temperature using these complexes under neat and base-free conditions. A yield higher than 90 % to ethyl acetate was observed after 24 h of reaction time with 500 ppm catalyst loading. To the best of our knowledge, this represents the first exemple of efficient dehydrogenative coupling of ethanol under neat and base-free conditions.

The excellent selectivity toward esters constitutes one of the advantages of the developed catalytic system. However, in some cases, aldehydes might be more desirable products. Using a large excess of acetone, it was found that aldehydes could be obtained as major product from primary alcohol dehydrogenation using hydridoborohydride ruthenium PNP pincer complexes. In this reaction, acetone acts as a “hydrogen accepting solvent” that suppress the hemiacetal formation and avoid the hydrogenation of the produced aldehyde. These results supports the fact that aldehyde is an intermediate in the dehydrogenative coupling of alcohols toward esters.

Hydridoborohydride carbonyl ruthenium PNP pincer complexes prove to be very efficient catalysts for the base-free dehydrogenative coupling of primary alcohols. Their excellent performances, together with the attractiveness of the transformation makes this system a good candidate for the industrial production of bulk and speciality chemicals such as ethyl acetate and fatty esters. Two patents have been filed regarding these applications. However, to target industrial application a better understanding of the reaction mechanism, reaction kinetic, catalyst stability and deactivation route would be highly desirable. Further studies aiming at understanding the rate dependance on catalyst concentration are currently underway. Wider variation of the catalyst structure, especially the replacement of the carbonyl moiety and the replacement of the PNP ligand by other non-innocent pincer ligands would allow developping more active catalysts. In addition, analog complexes, using iron instead of ruthenium as metal center could decrease the catalysts cost and hence further improve the overall attractiveness of the process.

5.2 Acceptorless dehydrogenation of primary alcohols to corresponding acid salts

Dehydrogenation of primary alcohols to carboxylic acid salts constitutes a new and promising oxidation methodology. It avoids overoxidation side reaction, produces valuable hydrogen as co-product and can be run under mild conditions using water as solvent and oxygen source. For this transformation, an aromatic PNN pincer ruthenium complex is the only reported catalyst. It allows obtaining high yields in carboxylic acid salts but at relatively low reaction rate and proved to be sensitive towards oxygen.

We investigated the use of *in situ* formed aliphatic ruthenium PNP pincer complexes for the dehydrogenation of alcohol to carboxylic acid salts using 1-butanol as a model substrate. Several ruthenium precursors together with aliphatic PNP ligands with moderate steric hindrance gave very active and productive catalysts under reaction conditions leading to butyric acid salt with yield ranging from 55 to 82 %. The transformation was found to be extremely selective with unreacted

1-butanol being the only compound detected beside the desired butyric acid salt. Compared with the other tested ruthenium precursors, carbonyl tristriphenylphosphine ruthenium complexes were found to give the more active catalysts.

Several structurally related ruthenium aliphatic PNP pincer complexes were used for the dehydrogenation of 1-butanol to butyric acid salts. All the investigated complexes showed similar elevated activity with the exception of dichlorotrimethylphosphino ruthenium PNP pincer complex. Both *in situ* formed and isolated catalysts were 10 times more active with TOF ranging from 250 h^{-1} to 280 h^{-1} against 23.3 h^{-1} for Milstein's aromatic ruthenium PNN complex.

Investigation of the reaction conditions showed that the water amount had a prononced effect on the reaction performances. An optimum water content was observed leading to highly productive system but reason for this behaviour is unclear. Similarly to dehydrogenative coupling, the reaction rate was found to be proportional to the catalyst concentration, here again, with an order apparently lower than one. As previously discussed, this may arise from a "reservoir effect" or a diffusion-controlled reaction. Compared with the state-of-the-art catalyst for this transformation, the aliphatic ruthenium PNP pincer complex were found to be 10 times more active allowing reaching similar product yields with reaction time 6 times shorter and half catalyst loading. Moreover, the catalyst could be used and handled under air without loss of its activity.

Taking advantage of the difference in solubility between the catalyst and the reaction product, a catalyst recycling procedure was developed using toluene as a "catalyst-immobilizing phase". This allowed using the catalyst for 5 consecutive runs without noticeable catalyst deactivation.

The developed catalytic system was also used for the hydrolysis of esters to carboxylic acid salts. This allows obtaining yields higher than 50 % into carboxylates as usually obtained with non-catalysed ester hydrolysis.

Aliphatic ruthenium PNP pincer complexes proved to be very efficient catalysts for the dehydrogenation of primary alcohols to carboxylic acid salts. However, the major drawback of such methodology is the requirement for stoichiometric amount of base. A more attractive system would be the direct production of carboxylic acid under base-free conditions. Further studies in this direction would be highly desirable.

5.3 Selective deuteration of alcohols

Deuterated alcohols are high value added compounds finding niche application in the study of biological mechanism. Their production relies today on inefficient and costly reactions making their preparation using cheap deuterium source desirable. Recently, it was shown that aromatic PNN pincer ruthenium complexes catalyse the deuteration of alcohol in closed systems using D_2O as deuterium source.

We investigated the use of both isolated and *in situ* formed aliphatic ruthenium PNP pincer complex for the deuteration of 1-butanol in a closed system.

Among the different catalysts, carbonyl ruthenium PNP pincer complexes, *in situ* formed or isolated, proved to be the most active, surpassing the state-of-the-art catalyst. Interestingly, the reaction could be performed in the absence of base with hydridoborohydride complexes allowing obtaining a high selectivity for deuteration of the alcohol α position, albeit with lower activity. Moreover this also evidences the robustness of these complexes, still active for hydrogen activation after 24 h at 120 ^{o}C in the presence of water and air.

Besides 1-butanol, other primary, secondary and functionalized alcohols could be deuterated using similar reaction conditions. Deuteration yields higher than 90 % can be observed for ethanol at both α and β positions, which is particularly interesting if the desired product is ethanol-d_6.

Appendices

1. List of figures

2. List of schemes

3. List of tables

Abstract

Catalyseurs à base de ruthénium pour la transformation des bio-alcools

Résumé: La déshydrogénation d'alcools pour former des esters ou des acides est une voie prometteuse pour la valorisation des bioalcools permettant de produire simultanément de l'hydrogène. De plus, la deutération sélective de ces alcools par de l'eau lourde constitue aussi une nouvelle réaction d'intérêt.

Dans la présente thèse, deux types de complexes ruthénium PNP (formés in-situ et isolés) ont été utilisés pour les réactions mentionnées ci-dessus. Pour les trois réactions les catalyseurs présentent une activité élevée, une excellente sélectivité ainsi qu'une bonne stabilité. Pour le couplage déshydrogénant des alcools des TOFs de plus de 8000 h^{-1} peuvent être obtenus avec une sélectivité supérieure à 99 %. Ainsi, pour la première fois l'acétate d'éthyle a pu être obtenu à partir d'éthanol en l'absence de base et de solvant. En présence de catalyseurs similaires, les alcools primaires peuvent être déshydrogènés en sels d'acides carboxyliques et le catalyseur recyclé à l'aide d'un système biphasique. Enfin ces complexes catalysent également la deutération sélective des alcools.

Mots Clés: ruthénium, bio-alcools, déshydrogénation, ligands PNP

Ruthenium catalysed transformation of bio-alcohols

Abstract: Acceptorless dehydrogenation of alcohols to corresponding esters or acids are environmentally friendly and atom-economic transformations for the valorisation of bio-alcohols, producing hydrogen as a valuable co-product. Selective deuteration of alcohols using heavy water as deuterium source is also a novel and interesting reaction.

In the present thesis, two types of ruthenium-PNP pincer catalysts (*in situ* formed and isolated) are used for above-mentioned reactions. For all three reactions, the catalysts show high activity, selectivity and stability. For the dehydrogenative coupling of primary alcohols, turnover frequency up to 8000 h^{-1} can be obtained with selectivity higher than 99 %. For the first time, ethyl acetate could be efficiently produced from ethanol under neat and neutral conditions. With similar catalysts, primary alcohol could be efficiently dehydrogenated to carboxylic acid salt and the catalyst could be recycled using a biphasic system. Finally these complexes also catalysed the deuteration of alcohols.

Keywords: ruthenium, bio-alcohols, dehydrogenation, PNP ligands